REGULATION OF IMMUNE RESPONSES BY *RasGEF1B* CIRCULAR RNA

NG WEI LUN

THESIS SUBMITTED IN FULFILMENT OF THE REQUIREMENTS FOR THE DEGREE OF DOCTOR OF PHILOSOPHY

INSTITUTE OF BIOLOGICAL SCIENCES
FACULTY OF SCIENCE
UNIVERSITY OF MALAYA
KUALA LUMPUR

2017

UNIVERSITY OF MALAYA

ORIGINAL LITERARY WORK DECLARATION

Name of Candidate: NG WEI LUN

Matric No: SHC130089

Name of Degree: DOCTOR OF PHILOSOPHY

Title of Project Paper/Research Report/Dissertation/Thesis ("this Work"):

REGULATION OF IMMUNE RESPONSES BY *RasGEF1B* CIRCULAR RNA

Field of Study: GENETICS AND MOLECULAR BIOLOGY

I do solemnly and sincerely declare that:

(1) I am the sole author/writer of this Work;
(2) This Work is original;
(3) Any use of any work in which copyright exists was done by way of fair dealing and for permitted purposes and any excerpt or extract from, or reference to or reproduction of any copyright work has been disclosed expressly and sufficiently and the title of the Work and its authorship have been acknowledged in this Work;
(4) I do not have any actual knowledge nor do I ought reasonably to know that the making of this work constitutes an infringement of any copyright work;
(5) I hereby assign all and every rights in the copyright to this Work to the University of Malaya ("UM"), who henceforth shall be owner of the copyright in this Work and that any reproduction or use in any form or by any means whatsoever is prohibited without the written consent of UM having been first had and obtained;
(6) I am fully aware that if in the course of making this Work I have infringed any copyright whether intentionally or otherwise, I may be subject to legal action or any other action as may be determined by UM.

Candidate's Signature Date:

Subscribed and solemnly declared before,

Witness's Signature Date:

Name: LIM YAT YUEN

Designation: SENIOR LECTURER

REGULATION OF IMMUNE RESPONSES BY *RasGEF1B* CIRCULAR RNA

ABSTRACT

Circular RNAs (circRNAs) constitute a large class of RNA species formed by the back-splicing of co-linear exons, often within protein-coding transcripts. Despite much progress in the field, it remains elusive whether the majority of circRNAs are merely aberrant splicing by-products with unknown functions, or their production is spatially and temporally regulated to carry out specific biological functions. To date, the majority of circRNAs have been cataloged in resting cells. Here, this research identifies a LPS-inducible circRNA: *mcircRasGEF1B*, which is predominantly localized in cytoplasm, shows cell-type specific expression, and has a human homolog with similar properties, *hcircRasGEF1B*. The functional experiments show that knockdown of the expression of *mcircRasGEF1B* reduces LPS-induced *ICAM-1* expression. Additionally, this study demonstrates that *mcircRasGEF1B* regulates the stability of mature *ICAM-1* mRNAs. To gain broader insights of *mcircRasGEF1B* function during cellular response to LPS stimulation, targeted *mcircRasGEF1B* depletion with high-throughput transcriptomic analysis is combined. The results show that knockdown of *mcircRasGEF1B* results in altered expression of a wide array of genes. Pathway analysis reveals an overall enrichment of genes involved in cell cycle progression, mitotic division, active metabolism, and of particular interest, NF-κB, LPS signaling pathways and macrophage activation. These findings expand the inventory of functionally characterized circRNAs with a novel RNA species that may play a critical role in fine-tuning immune responses during macrophage activation and protecting cells against microbial infection.

REGULASI TINDAK BALAS IMUN OLEH RNA BULAT *RasGEF1B*

ABSTRAK

RNA bulat (circRNAs) merupakan salah satu spesis RNA yang dibentuk melalui sambat balik ekson linear di dalam transkrip yang mengekodkan protein yang berfungsi. Walaupun bidang RNA mencapai banyak kemajuan, ia masih sukar difahami sama ada majoriti RNA bulat adalah hasil produk sambilan sambatan dengan fungsi yang tidak diketahui, ataupun pembentukan mereka adalah dikawal dari segi masa dan ruang, untuk menjalankan fungsi biologi yang tertentu. Setakat ini, majoriti RNA bulat telah dikatalogkan di dalam sel rehat. Penyelidikan ini berjaya mengenal pasti RNA bulat yang boleh diaruh oleh LPS iaitu *mcircRasGEF1B*, yang mana kebanyakannya terdapat dalam sitoplasma, menunjukkan ekspresi gen yang spesifik kepada sel tertentu, dan turut mempunyai suatu homolog manusia dengan sifat-sifat yang serupa iaitu *hcircRasGEF1B*. Selain itu, eksperimen fungsian turut menunjukkan bahawa pengurangan ekspresi *mcircRasGEF1B* turut mengurangkan transkrip *ICAM-1* yang diaruh oleh LPS. Penyelidikan ini juga telah membuktikan bahawa *mcircRasGEF1B* mengawal kestabilan mRNA *ICAM-1* yang matang. Untuk mendapatkan pandangan yang lebih luas tentang fungsi *mcircRasGEF1B* semasa tindak balas selular atas rangsangan LPS, pengurangan *mcircRasGEF1B* dengan pemprosesan tinggi analisis transcriptomic telah digabungkan. Keputusan eksperimen menunjukkan bahawa pengurangan *mcircRasGEF1B* menyebabkan pengubahan ekspresi dalam banyak gen. Analisis fungsi biologi mendedahkan pengayaan gen yang terlibat dalam perkembangan kitaran sel, pembahagian mitosis, metabolisme aktif, dan terutamanya, isyarat NF-κB, LPS dan pengaktifan makrophaj. Penemuan ini mengembangkan inventori RNA bulat yang telah dicirikan dari segi fungsi, di mana RNA bulat mungkin memainkan peranan yang amat penting dalam menala halus tindak balas imun serta untuk melindungi sel-sel daripada jangkitan mikrob.

ACKNOWLEDGEMENTS

First, I would like to thank my mentor Dr. Ea Chee Kwee, for providing me a chance to embark on a career in science. His outstanding scientific advice, discussion, and motivation are very applicable throughout my scientific journey. He sets a good example of a great scientist and challenges us to think, troubleshoot, and develop ideas. I can honestly say that I would not be in the position I am now without his guidance.

I would also like to thank my mentor, Dr. Lim Yat Yuen for his constant support, advice, and scientific discussion throughout the journey. He provides a platform for a great working environment to help me stay focus in my experiments.

My deep gratitude goes to all the Epigenetics lab members, Kok Siong, Wan Ying, Ming Cheang, Taznim, and Sheng Wei for their friendship, support and company. I would like to acknowledge a few people in the United States, Dr. Brian R. Calvi, Dr. Bingqing Zhang, and Dr. Kalen R. Dionne, for introducing me to the research world.

Last but not least, I would like to thank my friends and family for their unconditional trust, patience, and encouragement during my study. I am blessed my parents have faith on me throughout all these years.

TABLE OF CONTENTS

LIST OF FIGURES

LIST OF TABLES

LIST OF SYMBOLS AND ABBREVIATIONS

ADAR : adenosine deaminase acting on RNA

ASO : antisense oligo

AGO : argonaute

BAFF : B-cell activating factor

BLC : B-lymphocyte chemoattractant

CD40L : CD40 ligand

CCL5 : chemokine (C-C motif) ligand 5

CircRNA : circular RNA

ENCODE : encyclopedia of DNA elements

eRNA : enhancer RNA

ELC : Epstein-Barr virus-induced molecule 1 ligand CC chemokine

ETV6 : ETS variant 6

IKK : IκB kinase

IRAK1 : IL-1 receptor-associated kinase-1

IRAK4 : IL-1 receptor-associated kinase-4

IκB : inhibitor of NF-κB

ICAM1 : intercellular adhesion molecule 1

IFNβ : interferon-beta

IP10 : interferon gamma-induced protein 10

IRF3 : interferon regulatory factor 3

IL-1β : interleukin-1 beta

IL1R : interleukin-1 receptor

IL6 : interleukin-6

LILRB3 : leukocyte immunoglobulin like receptor B3

LPS : lipopolysaccharide

lncRNA : long non-coding RNA

LT-β : lymphotoxin-beta

miRNA : micro RNA

MyD88 : myeloid differentiation primary response gene 88

NEMO : NF-κB essential modulator

NIK : NF-κB-inducing kinase

NLR : NOD-like receptor

NF-κB : nuclear factor kappa B

PAMP : pathogen associated molecular patterns

PLCL2 : phospholipase C like 2

piRNA : piwi-interacting RNA

PCR : polymerase chain reaction

RACE : rapid amplification of cDNA ends

RASGEF1B : RasGEF Domain Family Member 1B

RNaseR : ribonuclease R

rRNA : ribosomal RNA

RBP : RNA binding protein

SLC : secondary lymphoid tissue chemokine

shRNA : short hairpin RNA

siRNA : small-interfering RNA

snoRNA : small nucleolar RNA

TAB1 : TAK1-binding protein 1

TAB2 : TAK1-binding protein 2

TBK1 : TANK-binding kinase 1

TRIF : TIR domain-containing adaptor protein inducing IFNβ

TIR : Toll/IL-1 receptor

TLR : toll-like receptor

tRNA : transfer RNA

TAK1 : transforming-growth-factor-beta-activated kinase 1

TNFα : tumor necrosis factor alpha

A20 : tumor necrosis factor, alpha-induced protein 3

TNFR : tumor necrosis factor receptor

TRAF2 : tumor-necrosis-factor-receptor-associated factor 2

TRAF3 : tumor-necrosis-factor-receptor-associated factor 3

TRAF6	: tumor-necrosis-factor-receptor-associated factor 6
E1	: ubiquitin-activating enzyme
E2	: ubiquitin-conjugating enzyme
UBC13	: ubiquitin-conjugating enzyme 13
UBE2D2	: ubiquitin conjugating enzyme E2 D2
E3	: ubiquitin ligase

LIST OF APPENDICES

CHAPTER 1: INTRODUCTION

Circular RNAs (circRNAs) are a special class of endogenous non-coding RNAs formed by the back-splicing of linear transcripts into a covalently closed circular molecule. Although some circRNAs were initially identified decades ago, they were long considered to be mere alternative splicing by-products of little biological importance (Nigro et al., 1991). The advancement of high-throughput sequencing technologies reveals thousands of loci in the human, mouse, and other genomes produce circRNAs in a cell-type specific manner. Some of these circRNAs are in fact functional (Hansen et al., 2013; Jeck et al., 2013; Memczak et al., 2013; Salzman et al., 2013). The functions of circRNAs appear to be mostly manifested via post-transcriptional regulatory mechanism, notably as miRNA sponges (Memczak et al., 2013). Despite the progress made so far, the number of functionally characterized circRNAs remains very low. Thousands of cytoplasmic circRNAs have been identified, with most of them having less than three binding sites for a particular miRNA, which undermine their regulatory potency as miRNA sponges. Furthermore, most ENCODE experiments have been carried out in cell lines under unperturbed conditions, leaving circRNAs expressed in many important biological contexts largely unexplored. One of them is the transcriptomic response of immune cells following exposure to inflammatory stimuli. Understanding the potential regulatory role of circRNAs in immune responses is critical for the complete understanding of their regulation and is thus of significant relevance to a number of therapeutic contexts, including cancer, heart disease and autoimmunity.

In this study, mouse macrophages, RAW264.7 was used to identify circRNAs in response to LPS stimulation. With the customized computational pipeline, the candidate circRNAs were first shortlisted and verified as *bona fide* circRNAs. Further characterization was performed to assess the cell type specificity, conservation, subcellular localization, and translatability of the selected circRNA. With the observed

inhibitory effect of circRNAs on LPS response genes in TLR4 pathway, the molecular mechanism was dissected by investigating the upstream signaling of NF-κB pathway and measuring the stability of mature mRNA.

The study objectives are:

- To extract candidate circRNAs in respond to inflammatory stimuli (LPS)
- To verify and characterize LPS-responsive circRNA
- To elucidate the function of circRNA in regulating immune response
- To determine the transcriptome-wide effects of circRNA in response to LPS treatment

CHAPTER 2: LITERATURE REVIEW

2.1 Overview of circular RNAs (circRNAs)

The central dogma of molecular biology provides a framework for the flow of genetic information. Despite the general notion that DNA is transcribed into RNA and RNA is translated into protein, only a small fraction of the human genome (1.5%) accounts for protein coding sequence, with the rest of the genome being associated with non-coding RNA molecules (Lander et al., 2001). Thus, the majority of RNA is not translated. These classes of non-coding RNAs are produced from endogenous transcripts with diverse physiological roles and functions. Besides the classical non-coding RNAs that exist in the form of ribosomal RNA (rRNA) and transfer RNA (tRNA), other non-coding RNAs, including microRNAs (miRNA), long non-coding RNAs (lncRNAs), piwi-interacting RNAs (piRNAs), small interfering RNAs (siRNAs), enhancer RNAs (eRNAs), and small nucleolar RNAs (snoRNAs), have also been implicated in mediating core cellular functions. (Gomes et al., 2013; Iwasaki et al., 2015; Lam et al., 2014; Morris & Mattick, 2014; Tollervey & Kiss, 1997). A long ignored member that recently gains attention in the growing list of non-coding RNA family is circular RNAs (circRNAs).

Though the discovery of circRNAs was demonstrated for at least more than 20 years ago (Nigro et al., 1991), circRNAs were ignored as artifacts of RNA splicing due to several reasons. Firstly, reports suggest that the process of exon shuffling and generation of circRNAs are not supported because they are produced from back-splicing, which defy the central dogma of mRNA production via linear exons splicing (Figure 2.1). Secondly, our knowledge on circRNAs remains limited as the detection of circular transcripts through traditional RNA analysis is challenging. Unlike other small RNAs and miRNAs, circRNAs are hardly separated from other RNA species by size or

electrophoresis. Conventional molecular biology tools that require amplification or fragmentation strategy will destroy circRNAs. For instance, circRNAs have no free ends. Molecular assays that employ polyadenylated RNA or rapid amplification of cDNA ends (RACE) enrichment will exclude circRNAs from the downstream analysis (Jeck & Sharpless, 2014). Thirdly, circRNAs with back-spliced reads are out-of-order on exons arrangement. Standard bioinformatics tools filter out such sequences as unmapped reads. Though these complications obscure the detection of circRNAs from other gene products, researchers have developed multiple strategies to overcome these pitfalls through new bioinformatics algorithms, exonuclease-enriched sample preparation, and rRNA depleted high-throughput sequencing. As a result, circRNAs are currently being revived as one of the most actively researched non-coding RNAs (Figure 2.2).

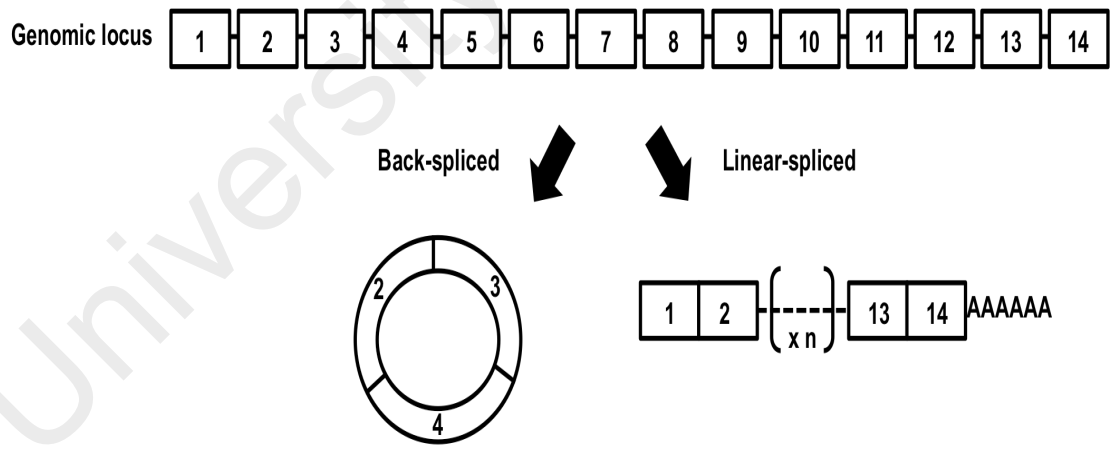

Figure 2.1: Splicing products of exons within a genomic locus. Schematic depiction of the exon structure of a linear transcript (right) and a back-spliced circular transcript (left).

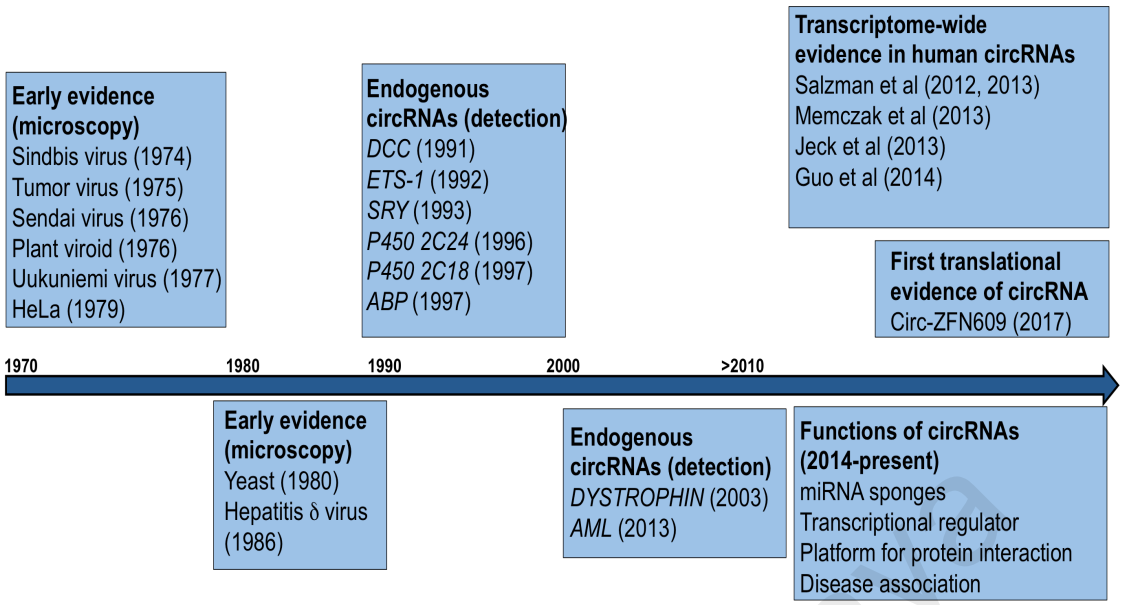

Figure 2.2: Timeline of the discovery of circRNAs. The major findings made from 1970s to present. The 1970-1980s mark the early observation of circRNAs through electron microscopy. The onset of 1990s represents a time period for detection and characterization of individual endogenous circRNAs in cells. Post 2010s era indicates large-scale detection with high-throughput technologies and functional elucidation of circRNAs.

2.2 The development of circRNAs as functional non-coding RNAs

2.2.1 Early evidence of circRNAs

Early studies of circRNAs stemmed from the electron microscopic studies of viral genetic materials, including Sindbis virus (Hsu et al., 1974), tumor virus (Kung et al., 1975), Sendai virus (Kolakofsky, 1976), Uukuniemi virus (Hewlett et al., 1977), and Hepatitis δ virus (Kos et al., 1986), provided the initial evidence for the existence of circRNAs under denatured conditions. It was also suggested that these viral genome were circular molecules maintained by base-paring between complementary sequences at the 3' and 5' ends of linear molecules (Hewlett et al., 1977; Kolakofsky, 1976). Besides, a class of plant pathogen with uncoated RNA molecules, known as viroid, was also found to harbor covalently closed single stranded RNA molecules (Sanger et al., 1976). Following the discoveries of viral genome circRNAs, the quest to identify circRNAs in eukaryotic cells were first confirmed in the cytoplasm of HeLa cells (Hsu & Coca-Prados, 1979), and the yeast mitochondrial RNA (Arnberg et al., 1980). However, microscopy approach could not distinguish circRNAs from RNA lariats. For example, previous report on yeast circular mitochondrial RNA (Arnberg et al., 1980) was later proven to be RNA lariats (Vanderveen et al., 1986).

It took more than a decade before the first evidence of endogenous circRNAs was shown in *DCC* transcript (28 exons) in human cells (Nigro et al., 1991). This finding described an abnormally spliced transcript with 5' upstream exons were shuffled to 3' downstream exons using canonical splice sites. The authors reported four scrambled exons isolated from cytoplasmic RNAs that were less abundant (one thousandth of linear products), non-polyadenylated, and found in both human and rodent cells. However, the authors did not observe complementarity between the intron sequences adjacent to the exons in this study, which could be responsible for the

splicing event. In addition, the authors speculated that trans-splicing might contribute to the occurrence of scramble exons, yet the hypothesis remained untested.

The second report on circRNAs partially answered the splicing event. The author showed that known *ETS-1* shuffled exons occurred in proximal to large introns (Cocquerelle et al., 1992). In addition, they also hypothesized that mis-splicing mechanism was mainly an intramolecular process. The authors observed mis-spliced RNA species in low molecular weight (fractions 2 to 4) in poly A-RNA fractions, arguing that multimeric structure did not exist. Furthermore, it was unlikely that intermolecular splicing occured between two different *ETS-1* transcripts because amplification of the back-spliced RNA could not be isolated in high molecular weight RNA fractions. The authors further provided evidence that *ETS-1* transcript was an exonic circRNAs, localized in the cytoplasm, was stable under actinomycin D treatment, and utilized canonical splice sites (Cocquerelle et al., 1993).

The subsequent work on mammalian sex determining gene, *SRY*, revealed the production of exonic circRNAs from the *SRY* locus in mouse testis (Capel et al., 1993). Two pieces of evidence provided support for *SRY* circularization. First, the 5' RACE experiment failed to identify a start site. Second, RNase H cleavage assay with different oligos yielded expected products based on circular *SRY* (Capel et al., 1993).

Similar evidence on circRNAs was then continually being reported in different human and rat tissues, such as Cytochrome C *P-450 2C24* (rat kidney and liver) (Zaphiropoulos, 1996), *P-450 2C18* (epidermis) (Zaphiropoulos, 1997), *ABP* (rat testis) (Zaphiropoulos, 1997), *Dystrophin* (brain and skeletal muscle) (Gualandi et al., 2003), and *AML1* (bone marrow and blood) (Xu et al., 2013). Each discovery began with the examination of scrambled exons and observation of back-spliced PCR products. Moreover, in each case, these circRNAs were reduced in oligo dT primed RT-PCR

samples (Lasda & Parker, 2014). However, the circular transcripts identified were generally less abundant than the linear products from the parental genes. Therefore, circRNAs were considered as rare events with unclear biological functions before the advent of genome-wide sequencing technologies.

2.2.2 Transcriptome-wide profiling technology in circRNAs discoveries

The development of genome-wide transcriptome technology has enabled in-depth characterization of circRNAs in terms of identification, abundance, and putative functions. This includes longer read lengths, better algorithms and ribosomal RNA (rRNA)-depleted non-polyadenylated RNA sequencing.

The first genomic approach on circRNAs was carried out with rRNA depletion (Ribozero or RiboMinus) strategy. Independent mapping of pair-end reads from opposite cDNA ends revealed thousands of exon junctions with opposite order on the same gene during gene annotation in multiple cell lines and tissues. The authors relied on existing gene annotation to construct candidate circRNAs from pre-existing gene models, and did not shortlist circRNAs from unannotated genes (Salzman et al., 2012). Validation of several candidates using qPCR revealed that these transcripts were predominantly RNase R resistant and non-polyadenylated (Salzman et al., 2012).

As an extension of this genome-wide method, Memczak et al. (2013) identified back-spliced sequence from rRNA-depleted reads from human, mouse, and nematode cells. Instead of relying on candidate gene approach, the authors mapped the reads to genomic locations *de novo*. The unmapped reads were then remapped to the two ends of a single gene separately to identify back-spliced sequence from individual reads. This method provided a better resolution of splice sequence AG/GT in a genomic context. The authors showed that many candidate circRNAs were resistant to RNase R, and were highly stable. The authors concluded that these back-spliced circRNAs were abundant,

stable, conserved, and both tissue- and developmental-specific. Although this method enabled identification of unannotated splice sites, it is less sensitive compared to the candidate approach.

Further refinement of the sequencing approach was described in mammalian cells by enriching for exonic circRNA with RNase R treatment (CircleSeq) (Jeck et al., 2013). Since RNase R digestion is a hallmark experiment for the validation of circRNAs (Suzuki et al., 2006), the authors compared RNA-seq libraries with and without RNase R treatment. This method used MapSplice algorithm on the basis of two features (Jeck & Sharpless, 2014) : 1) back-spliced reads were identified as segmented reads; 2) Reads from RNase R-treated circRNAs should be at least 8- to 16-fold enriched than mock-treated control. The author then generated 3 circle sets: low, medium, and high stringency to classify the candidates. Though this method conferred a deeper coverage and stringency of circRNAs and RNA lariats, more RNA inputs were required for the enrichment procedure before RNA sequencing.

To further expand the identification and characterization of mammalian circRNAs, Guo et al. (2014) developed a "dual alignment" pipeline to identify circRNAs and calculated the relative abundance on a large set of non-poly A enriched ENCODE data. The authors showed that most circRNAs spanned less than five exons, and most of them were expressed in selected cell types with low abundance. In comparison with previous circRNAs catalog, the author reasoned that most annotated circRNAs were present in only one catalog were due to difference in cell types and computational methods. For example, Guo et al. (2014) required circRNAs fraction ≥ 10, Jeck et al. (2013) required enrichment of circRNA in RNase R samples and 2Mb read fusions, while Memczek et al. (2013) required minimum two junction reads per circRNA. While raising doubts on the biological functions of most mammalian circRNAs, this finding provided a new framework for circRNA investigations.

Apart from mammalian cells, numerous genome-wide studies on circRNAs were carried out for various purposes in different organisms, as described in archaea (Danan et al., 2012), rice (Lu et al., 2015), amoeba (Boesler et al., 2011), human malaria parasite (Broadbent et al., 2015), human cell-free saliva (Bahn et al., 2015), human and mouse pre-implantation embryos (Dang et al., 2016; Fan et al., 2015). These analyses found strong evidence for thousands of circRNAs in various domains of life, suggesting that circRNAs may be prevalent with important biological roles.

2.3 General properties of circRNAs

There are several key properties of circRNAs. First, circRNAs are stable. Most of the circRNAs possess half-life over 48 hours (Jeck et al., 2013), compared to an average 10 hours in linear mRNAs (Schwanhausser et al., 2011). Moreover, transcriptional block with actinomycin D shows that circRNAs are highly stable after 24 hours, exceeding the stability of house keeping gene, *GAPDH* (Memczak et al., 2013). Though circRNAs are highly unstable in serum with half-life less than 15 seconds (Jeck & Sharpless, 2014), exosome-contained circRNAs are found to be stable in serum at room temperature up to 24 hours (Li et al., 2015b). Compare to free circRNAs in serum that are susceptible to RNA endonucleases, the higher stability of exosome-circRNAs might be due to the protection of exosomes or protein partners (Li et al., 2015b).

Second, circRNAs are abundant among different species. Bioinformatics analysis on human transcriptome study shows evidence of exon scrambling events in more than several hundreds of genes, of which the scrambled isoforms are expressed at comparable levels to canonical linear isoforms (Salzman et al., 2012). Analysis of human (HeLa and H9) cells shows 2748 transcript isoforms, while *Drosophila* shows 800 scrambled exon spliced junctions (Salzman et al., 2013; Salzman et al., 2012). In addition, a more systematic study reveals approximately 2000 human, 1900 mouse, and

700 nematodes circRNAs (Memczak et al., 2013). Moreover, a biochemical-based approach with high-throughput RNA-seq from rRNA-depleted, RNase R digested RNA pools reveals more than 25,000 distinct back-spliced RNA species in human fibroblast (Jeck et al., 2013). A more detailed calculation on circRNAs abundance in human tissues shows that one gene produces multiple circRNAs. For instance, a total of 5,955 host genes yield 20,530 circRNAs (Zheng et al., 2016), and diversity of Alu pairing competition leads to alternative circularization from the same gene (Zhang et al., 2014). Apart from that, human body fluids also contain circRNAs. For instance, more than 400 (cell-free saliva) (Bahn et al., 2015), 1000 (serum exosomes) (Li et al., 2015b), and 4000 circRNAs (peripheral whole blood) (Memczak et al., 2015) have been identified. However, an expanded report on ENCODE data shows that 7,112 human circRNAs found constitutes of 10% of the transcripts accumulated from their loci, with most of the circRNAs are of low abundance. Though some of the expression of circRNAs is low, there are exceptions. For example, 90% of the *Sry* transcripts in adult mouse testis exist in circular form (Capel et al., 1993). Additionally, *Fmn* gene generates around 70 to 80% of scrambled transcripts (Chao et al., 1998). In short, one of the challenges is that traditional methods in RNA detection that requires free 5' or 3' terminal may underestimate the abundance of circRNAs.

Third, circRNAs are predominantly localized in the cytoplasm. The electron micrograph from circRNAs extracted from the cytoplasm of HeLa cells provides the first indication of the cytoplasmic localization of circRNAs (Hsu & Coca-Prados, 1979). The examination of circRNAs using different methods, such as subcellular fractionation and *in situ* hybridization, has reached similar conclusion (Cocquerelle et al., 1993; Jeck et al., 2013; Memczak et al., 2013; Nigro et al., 1991; Salzman et al., 2012; Zheng et al., 2016).

Fourth, circRNAs are evolutionary conserved and cell-type specific. Early studies showed that there is a substantial conservation of circRNAs in mammals (Jeck et al., 2013; Legnini et al., 2017; Memczak et al., 2013). For example, 69 circRNAs in murine testis are orthologous to the precise genomic sequence in human circRNAs (Jeck et al., 2013). In another study, 40% of the highly expressed human circRNAs overlap with mouse circRNAs, in which the genomic location in human is overlapped with syntenic region in mouse (Legnini et al., 2017). At the molecular level, it has been shown that DNA that encodes circRNAs is more conserved than DNA of flanking exons (Rybak-Wolf et al., 2015). On the other hand, reports show that the relative abundance of circRNAs varies across tissues. For instance, there is relatively higher abundance of circRNAs in neuronal tissues compared to heart, liver, testis, and lung (You et al., 2015), consistent with other reports that demonstrated that hundreds of circRNAs are expressed at > 10 folds higher than host linear transcripts, especially in the brain (Ashwal-Fluss et al., 2014; Rybak-Wolf et al., 2015; Veno et al., 2015; Westholm et al., 2014). Another computational report identified distinct circular-splice junctions (d.c.j) across different cell lines, including leukemia cell K562 (16,559 d.c.j), fetal lung fibroblast cell AG04450 (11,590 d.c.j), and foreskin fibroblast BJ (7,771 d.c.j).

2.4 Biogenesis of circRNAs

There are three mechanisms that have been proposed to generate circRNAs, which are the direct back-splice, the lariat intermediate, and the RNA binding protein (RBP) factors models.

2.4.1 Direct back-splice model

Direct back-splicing model refers to the event where downstream splice donor is paired with unspliced upstream splice acceptor. The branch point located upstream of the circularized exon attacks a downstream splice donor, generating a Y-shaped intermediate. Next, the 3' end of the exon attacks its own 5' end; ultimately produce a circRNA (Figure 2.3A).

To facilitate the production of circRNAs, sequence specific elements, such as flanking introns with inverted or ALU repeats, are required. Various sizes of flanking introns contain inverted repeat sequences that base-pair and bring the splice sites in close proximity to process circRNAs production via 5' to 3' splicing (Ivanov et al., 2015; Liang & Wilusz, 2014; Zhang et al., 2014). For example, *SRY* gene contains exons flanked by inverted repeats of more than 15 kb surrounding the mouse *SRY* exons that circularize (Capel et al., 1993). Additional experiment shows that a minimum of 400 complementary nucleotides base-pairing is necessary for *SRY* circularization (Dubin et al., 1995). Liang and coworker mutagenizes circRNAs expression vectors and concludes that miniature introns with less than 100 nucleotides containing splice sites with 30 to 40 nucleotides inverted repeats are sufficient for circularization (Liang & Wilusz, 2014). Collectively, analysis on sequence requirements using mini-genes from natural circRNAs and genome-wide computational sequence analysis suggest that complementary sequence circRNAs production is associated with ALU repeats (Ivanov et al., 2015; Jeck et al., 2013; Zhang et al., 2014).

2.4.2 Lariat intermediate model

Lariat intermediate arises from internal splicing with lariats containing skipped exons are produced as a result of exon skipping (Figure 2.3B). For example, exon-skipping events are consistent with circRNAs production from cytochrome *P450 2C24* gene (Zaphiropoulos, 1996). Furthermore, simple eukaryote genomes are almost devoid of repeat sequences. In yeast, it has been shown that lariat structures containing exons are a common intermediate before the production of circRNAs (Barrett et al., 2015).

2.4.3 RNA-binding protein (RBP) factors model

Both intron pairing and lariat precursor models could not sufficiently explain how a single abundant transcript can generate cell- and tissue-specific circRNAs (Jeck & Sharpless, 2014; Salzman et al., 2013). Alternative splicing is known to play key roles of transcriptional controls in development and physiological responses. Thus, tightly regulated alternative splicing event in circRNAs production prompts the likelihood of the involvement of RBPs (Figure 2.3C).

RBPs bind to the flanking introns and the interaction between RBPs bring the splice donor and acceptor into close proximity, thereby generating circRNA (Ashwal-Fluss et al., 2014). For example, the splicing factor muscleblind (MBL) regulates the production of its own *circMBL* from its second exon in both flies and humans. Flanking introns bracketing circularized exon of MBL contain conserved MBL binding sites and modulation of MBL levels affects *circMBL* biogenesis (Ashwal-Fluss et al., 2014). In addition, Quaking (QKI), which belongs to the STAR family of KH domain-containing RBPs, promotes circRNA biogenesis during epithelial and mesenchymal transition (Conn et al., 2015). QKI binds to intronic QKI binding motifs and insertion of such motifs into linear RNA is sufficient to induce *de novo* circRNAs formation (Conn et al., 2015). Lastly, adenosine deaminase acting on RNA (ADAR), a highly conserved RNA-

editing enzyme, has been implicated in circRNA biogenesis as well. In the absence of ADAR1 and ADAR2, the expression of circRNAs is upregulated independently of the linear host mRNA expression (Ivanov et al., 2015). It is likely that ADAR blocks the base-pairing between intron inverted repeats, thereby preventing circRNAs formation.

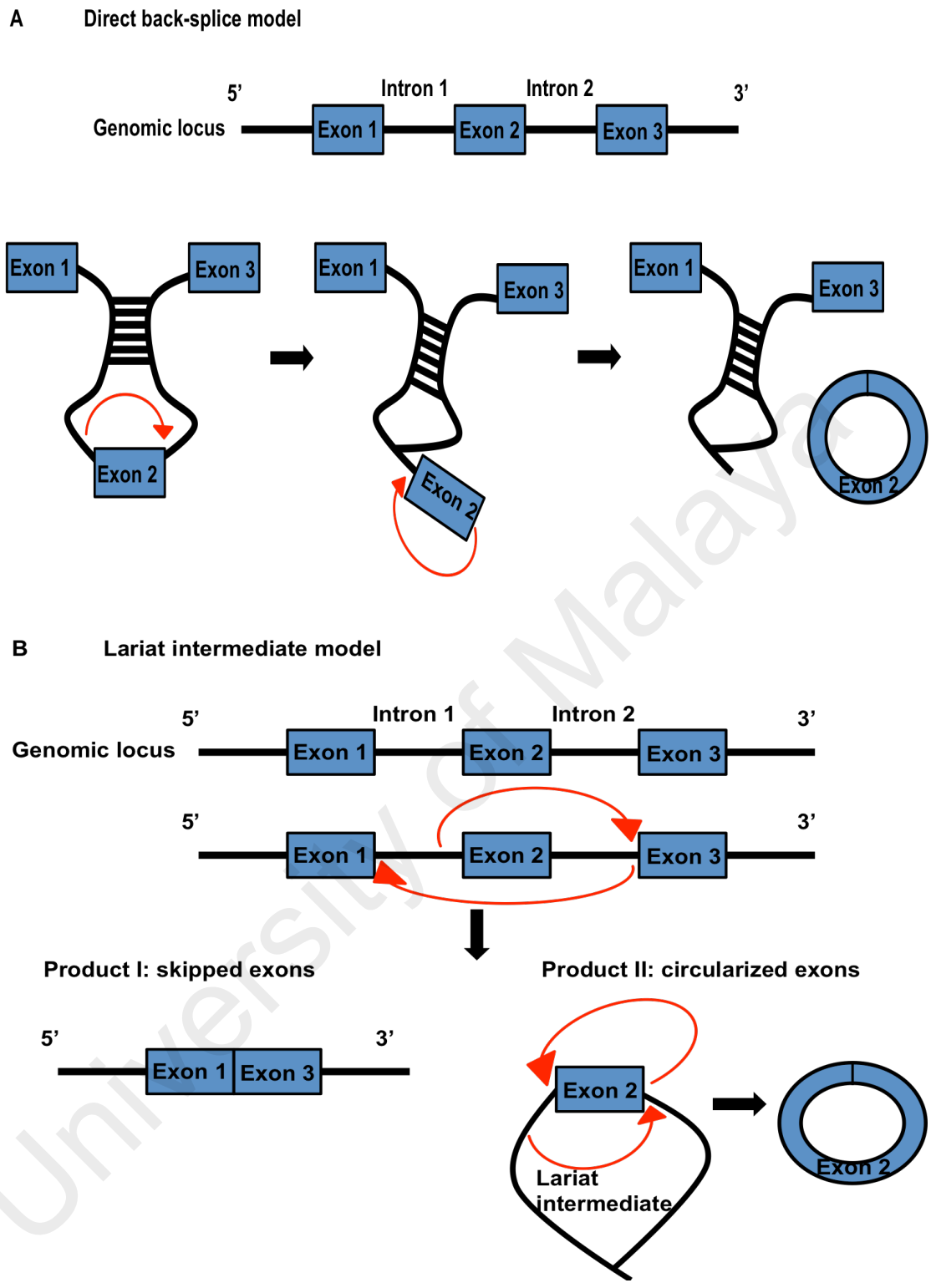

Figure 2.3: Models of circRNA biogenesis**.** (A) Direct back-splice model requires ALU repeats complementation or intronic reverse complement motifs to bring the donor-acceptor together, forming a circularized exon. Exon skipping is not required in this model; (B) Lariat intermediate model requires exon skipping during canonical linear splicing to generate a lariat structure containing circularized exons. (C) RBP factors model involves additional proteins to promote circularization, such as QKI, ADAR, and MBL.

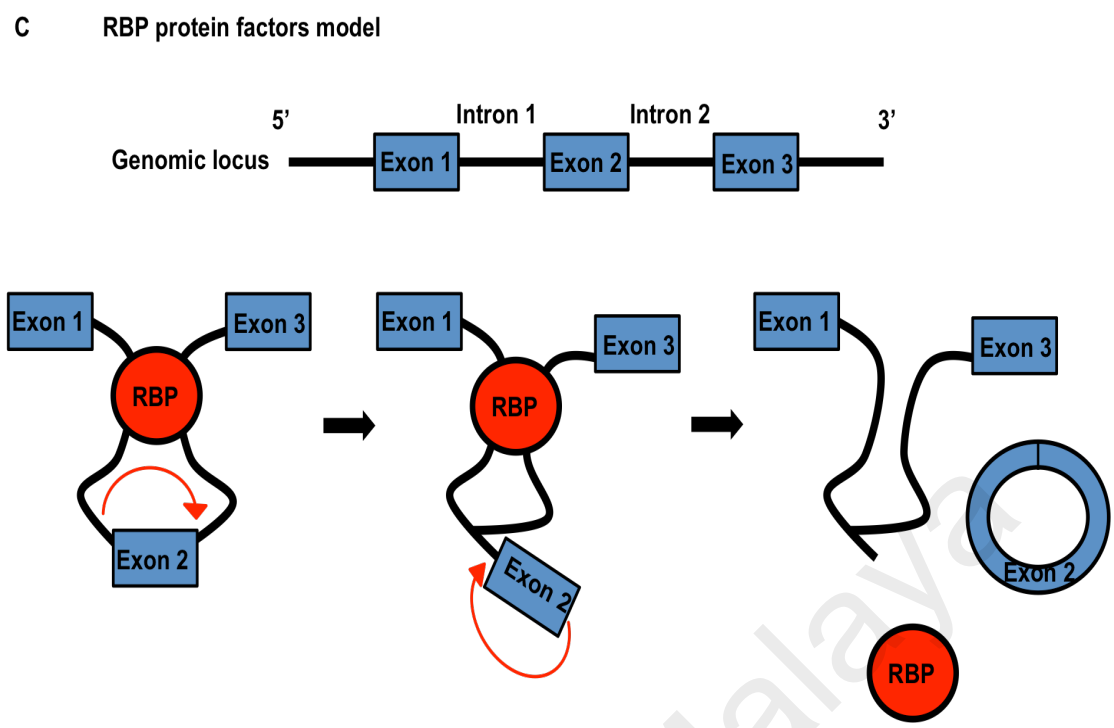

Figure 2.3, continued

2.5 Validation tools for circRNAs

Divergent primer is used to amplify away from the genomic context, but converges when back-spliced sequences bring outer sequence back together. However, this method could not rule out tandem DNA duplication and trans-splicing, in which both can generate apparent back-splice junction on the same gene. Hence, alternative additional tools to assess back-splice sequence are needed.

Enzymatic methods further strengthen the circularity of a molecule. The treatment with RNase R exonuclease (3' to 5' exonuclease activity), and tobacco acid phosphatase (5' to 3' exonuclease activity) degrades linear RNA while preserving circRNA. Comparison between mock and enzyme treatment reveals an enrichment of circRNAs species relative to linear transcripts.

A standard or virtual northern blot can be used to assess circRNAs (Jeck et al., 2013). CircRNAs migrate slower relative to linear RNA products. Gel electrophoresis can be used to show circular topology of circRNAs. In 2D gel electrophoresis, movement of circRNAs is retarded through highly cross-linked than lesser cross-linked gels (Tabak et al., 1988), forming a distinct arc shaped movement, compared to a smooth migration by linear RNAs (Jeck & Sharpless, 2014; Matsumoto et al., 1990).

2.6 Functions of circRNAs

2.6.1 MicroRNA sponge

Accumulating evidence has demonstrated the functional roles of circRNAs in different cellular physiologies (Figure 2.4A). CircRNAs have been shown to function as microRNA (miRNA) sponges. CircRNAs sequester miRNAs via base-pairing, thus keeping miRNAs away from their mRNA targets. The first miRNA sponging activity from CDR1-as circRNAs is proven both *in vitro* and *in vivo* (Hansen et al., 2013; Memczak et al., 2013). Both studies show that CDR1-as is densely bound by AGO and harbors 63 seed regions for miR-7. *In vitro* assay shows that CDR1-as binds to miR-7 (Hansen et al., 2013). Over-expression of CDR1-as reduces the transcriptional repression activity of miR-7, thereby enhances the expression of miR-7 target genes. *In vivo* analysis in zebrafish demonstrates the role of CDR1-as in regulating the activity of miR-7 that is crucial for brain development (Memczak et al., 2013). Over-expression of CDR1-as mimics the phenotypes of knocking down of miR-7 with morpholinos, in which the size of the mid-brain reduces in zebrafish embryo. These findings provide the first functional role of circRNAs as a developmental regulator. Similarly, *SRY* circRNA harbors 16 seed sequences for miR-138, binds to AGO2, and reduces gene repression activity of miR-138 (Hansen et al., 2013). Though no functional role is described, this study supports the hypothesis that some circRNAs are miRNA sponges.

Following the description of circRNAs as miRNA sponges, numerous circRNAs have been implicated to bind disease-related miRNAs, suggesting the involvement of circRNAs in disease development. For instance, *circ-ITCH* sponges miR-7, miR-17, and miR-214 in esophageal squamous cell carcinoma (Li et al., 2015a), *circ-HRCR* sponges miR-223 in heart dystrophy (Wang et al., 2016a), *circ_0005105* sponges miR-26a in chondrocyte extracellular matrix (Wu et al., 2017), *circ-000203* sponges miR-

26b-5p in cardiac fibroblast (Tang et al., 2017), and *circ-ZNF609* sponges miR-150-5p in Hirschsprung's disease (Peng et al., 2017) .

Nonetheless, genome-wide analysis reveals that miRNA sponging could not be widely applied across all circRNAs (Guo et al., 2014; Jeck et al., 2013; Memczak et al., 2013; You et al., 2015). For example, very few of circRNAs harbor more than 10 seed regions for a single miRNA (Jeck et al., 2013). Thus, there is constant exploration in understanding the other functional roles of circRNAs.

2.6.2 Transcriptional regulators

Besides serving as miRNA sponges, there are reports showing that circRNAs function as transcriptional regulators (Figure 2.4B). CircRNAs generated from *Fmn* are essential for limb development. Deletion of back-splice acceptor in the murine shows normal limb development but incomplete penetrant renal agenesis. The authors postulated that "mRNA trap" functions of circRNAs via sequestering transcriptional start site, resulted in a non-coding transcript with reduced Formin protein expression (Chao et al., 1998). In addition, a special subclass of circRNAs, exon-intron circRNAs (ElciRNAs), associates with RNA polymerase II in human cell. These nuclear localized ElciRNAs interact with U1 snRNP and Pol II transcription complex at the promoter of their parental genes and regulate the expression of their parental genes (Li et al., 2015c). Hence, some circRNAs function as transcriptional regulators that modulate their parental gene expression.

2.6.3 Platforms for protein interaction

Previous finding reveals that non-coding RNA control gene expression at both the transcription and post-transcriptional levels via physical interaction with RNA binding proteins or other non-coding RNAs (Turner et al., 2014). CircRNAs might have similar roles in protein interactions to mediate cellular functions (Figure 2.4C). For example, circRNAs are associated with AGO2 and RNA Pol II (Jeck et al., 2013; Memczak et al., 2013). In addition, similar scenario is also found in *circ-Mbl*, which competes for binding to Mbl protein for the linear splicing (Ashwal-Fluss et al., 2014). Besides, circFoxo3 forms a ternary complex with CDK2 and p21, and blocks cell cycle progression by arresting CDK2 functions (Du et al., 2016).

2.6.4 Translational ability of circRNAs

Several lines of evidence show that introduction of internal ribosome entry site (IRES) and reading frames result in translation of engineered circRNAs *in vitro* (Abe et al., 2015; Chen & Sarnow, 1995; Kramer et al., 2015; Wang & Wang, 2015). Thus, it raises the possibility that endogenous circRNAs derived from protein coding DNA sequence, for example, those with ATG translational start site, could be translated into functional proteins (Figure 2.4D). Though polysome profiling shows that majority of the circRNAs provides no evidence for translation (Guo et al., 2014; Jeck et al., 2013), the first endogenous translational evidence of protein coding circRNA in eukaryotes is indicated in *circ-ZNF609*. The authors demonstrated that *circ-ZNF609* contains a start codon and with an in frame stop codon created upon circularization. This circRNA controls myoblast proliferation, is associated with heavy polysomes, and translated through splicing dependent, cap-independent mechanism (Legnini et al., 2017).

2.6.5 Disease association

It has been shown that some circRNAs are associated with human diseases. The INK4/ARF locus at chromosome 9p21 is one of the most frequently altered regions in human cancers. Besides encoding for cyclin dependent kinase inhibitors $p15^{INK4b}$, and $p16^{INK4}$, there is a new large antisense non-coding RNA, *ANRIL*, which is mapped to the same locus. Importantly, the expression of a circular variant of ANRIL, *circ-ANRIL*, affects *ANRIL* splicing and correlates with human atherosclerosis (Burd et al., 2010). In addition, *has_circ_0001649* was downregulated in hepatocellular carcinoma tissues, and its expression was shown to correlate with tumor size and tumor embolus (Qin et al., 2016). A comparison using circRNA microarray data from T cells isolated from both adults and elderly shows that circRNA 100783 is involved in chronic CD28 associated CD8 (+) T cell aging, and could serve as a new biomarker (Wang et al., 2015). Moreover, a RNA microarray correlation study of circRNAs expression in peripheral blood of coronary artery disease (CAD) in 12 CAD patients and 12 control individuals suggests that peripheral blood circRNA, *has_circ_0124644*, can be used as a diagnostic biomarker for CAD (Zhao et al., 2017).

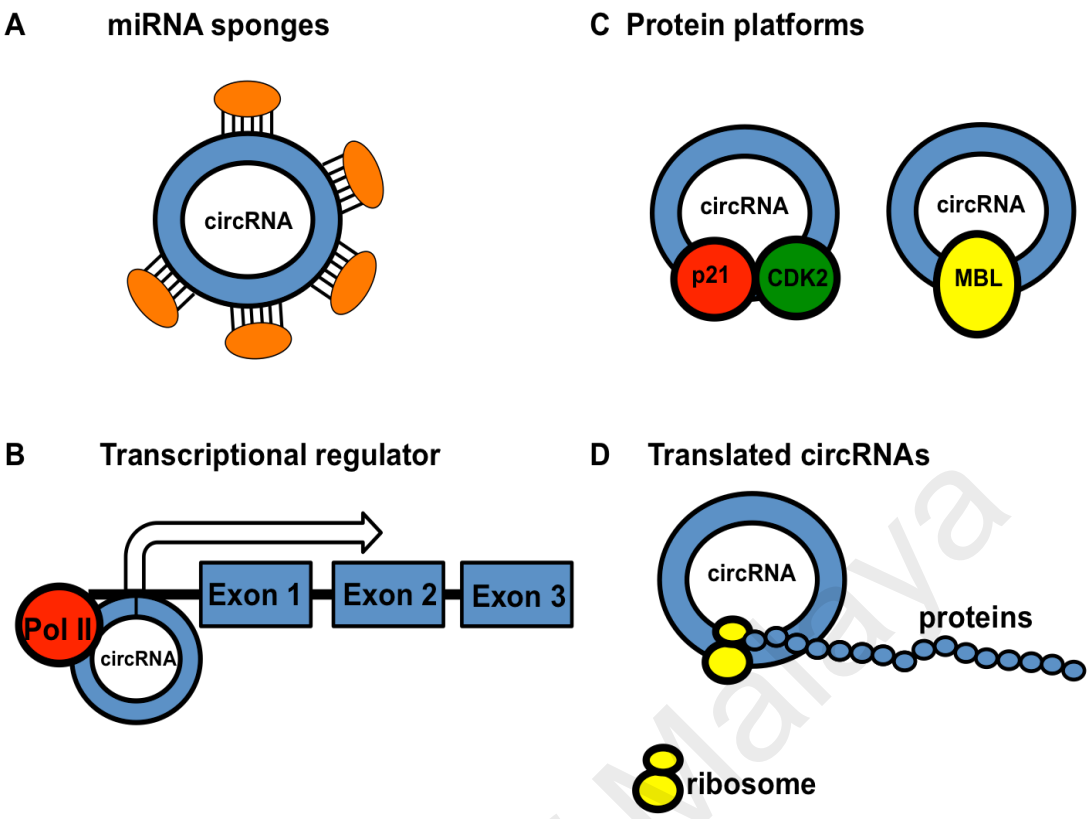

Figure 2.4: Potential functions of circRNAs. (A) CircRNA harbors miRNAs binding sites and serves as miRNA sponges, which indirectly controls gene expression; (B) Stable circRNAs function as transcriptional regulator by binding to RNA polymerase II; (C) CircRNAs act as protein platforms. RBP (MBL) binds to circRNA to compete with linear alternative splicing; Cell cycle proteins bind to circRNAs to strengthen p21/CDK2 interaction, blocking cell cycle progression; (D) CircRNA that contains ORF and in-frame stop codon is translated into proteins in splicing-dependent, cap-independent manner.

2.7 Databases of circRNAs

A growing number of over thousands of circRNAs have been identified by different groups. Hence, the compilation of circRNAs databases and resources is necessary for better navigation. Existing databases include circBase (Glazar et al., 2014), CircNet (Liu et al., 2016), Circ2Traits (Ghosal et al., 2013), circPedia (Zhang et al., 2016), circRNABase (Li et al., 2014b), circInteractome (Dudekula et al., 2016), and plant-specific PlantcircBase (Chu et al., 2017) (Table 2.1).

Table 2.1: List of available circRNA databases

Database Name	Types of cells	Highlights
CircBase	*H. sapiens* (hg19) *M.musculus* (mm9) *C.elegans* (ce6) *L. chalumnae* (latCha1) *L. menadoensis* (latCha1) *D.melanogaster* (dm3)	One of the earliest and comprehensive databases. Custom python scripts can be downloaded
CircNet	464 RNA-seq samples without PolyA selection from 26 different human tissue samples	Provides a total of 212,950 circRNAs Provides a total of 34,000 circRNAs with junction sites >3, as highly expressed circRNAs. Provides circRNA expression profiles across 26 different human tissues Predicts circRNA-miRNA interactions and regulatory networks Provides genomic annotation of circRNAs using integrated genome browser
Circ2Traits	Data sources taken from 1953 predicted human circRNAs (Memczak et al., 2013), and miR2Disease (174 different human disease) (Jiang et al., 2009)	Measures the likelihood of a circRNA and disease association, calculated using hypergeomtric test, $p < 0.01$ Visualizes circRNA-miRNA-mRNA-lncRNA interactome network for individual disease Information about disease associated SNP in circRNA loci
CircPedia	31 human 26 mouse 30 fly 12 worm	Integrative database to annotate alternative back-splicing in circRNAs across different cell lines with circRNA characterization pipeline CIRCexplorer2

Table 2.1, continued

circRNABase	*H. sapiens* (hg19) *M.musculus* (mm9)	Predicts miRNA-circRNA interactions by overlapping circRNA sequence with CLIP-seq peaks from miRNA targets
circInteractome	109 datasets of RNA binding proteins (RBP) and circRNAs for RNA binding sites (Glazar et al., 2014).	Searches RBP binding to a circRNA and sequences upstream or downstream of circRNAs Identifies RBPs binding to circRNA junctions Identifies miRNAs targeting circRNAs Designs divergent primers and siRNAs specific for circRNAs
PlantcircBase	*Arabidopsis thalina* (TAIR10) *Hordeum vulgare* (ASM32608v1.26) *Oryza sativa* (RGAPv7) *Solanum lycopersicum* (SL2.40.25) *Zea mays* (AGPv3.22)	Predicts circRNAs as miRNA sponges. Provides plant circRNAs with related information (sequence, host genes, expression, experimental validation)

2.8 Overview of NF-κB signaling pathway

Cells respond to external stimuli such as microbial infections, inflammatory cytokines, physiological stresses and viral infections, through transmission of signals from cell surface or cytosolic receptors to the nucleus. In mammals, Nuclear Factor Kappa-B (NF-κB) represents one of the best-studied signaling pathways with tightly controlled regulatory mechanism in response to stresses. There are five members of NF-κB family: RelA (p65), RelB, and c-Rel, and precursor proteins NF-κB1 (p105/p50), and NF-κB2 (p100/p52) (Gilmore, 2006). All NF-κB proteins share a Rel homology domain, which allows them to bind as dimers to κB sites at the promoters or enhancers to activate or repress transcription of hundreds of genes (Hayden & Ghosh, 2004).

There are two main NF-κB activation pathways in cells: canonical and non-canonical pathways (Figure 2.5). The canonical pathway is activated mainly by physiological NF-κB stimuli, such as tumor necrosis factor receptor (TNFR), interleukin 1 beta (IL-1β), and pathogen associated molecular patterns (PAMPs). In resting cells, NF-κB dimers are bound to inhibitory IκBα proteins and sequestered as an inactive form in the cytoplasm (Ghosh et al., 1998). The initiation of IκB protein degradation is mediated through the upstream IκB kinase complex containing two catalytic subunits IKKα and IKKβ, and a regulatory subunit, IKKγ or NEMO. Activation of the IKK complex phosphorylates IκBα at two conserved serines (S32 and S36) in the N-terminal regulatory domain of IκB. In canonical pathway, it is IKKβ subunit that catalyzes the phosphorylation (Brown et al., 1995; Chen et al., 1995; DiDonato et al., 1996). Once phosphorylated, IκBα is rapidly polyubiquitinated. Ubiquitination of IκBα involves E2 of the UBC4/5 family (Alkalay et al., 1995; Chen et al., 1995; Chen et al., 1996) and the E3 ligase Skp1-Cul1-F-box ligase containing the F-box protein βTrCP (SCF-βTrCP) (Jiang & Struhl, 1998; Margottin et al., 1998;

Spencer et al., 1999; Winston et al., 1999; Yaron et al., 1998). Subsequently, IκBα is degraded by 26S proteasome, which allows NF-κB to translocate into the nucleus and activate a wide array of genes (Hayden & Ghosh, 2004). In contrast, the noncanonical pathway is induced primarily by TNF family cytokines, including CD40L, BAFF, and LT-β, that lead to the activation of NIK. Activated NIK mediates the phosphorylation of IKKα, instead of IKKβ and IKKγ. Phosphorylated IKKα then phosphorylates p100 at the C-terminus. Finally, processing of p100 to mature p52 by ubiquitin-proteasome dependent mechanism generates the active p52-RelB heterodimer. The complex then translocate into nucleus to turn on the transcription of the target genes (Hayden & Ghosh, 2004).

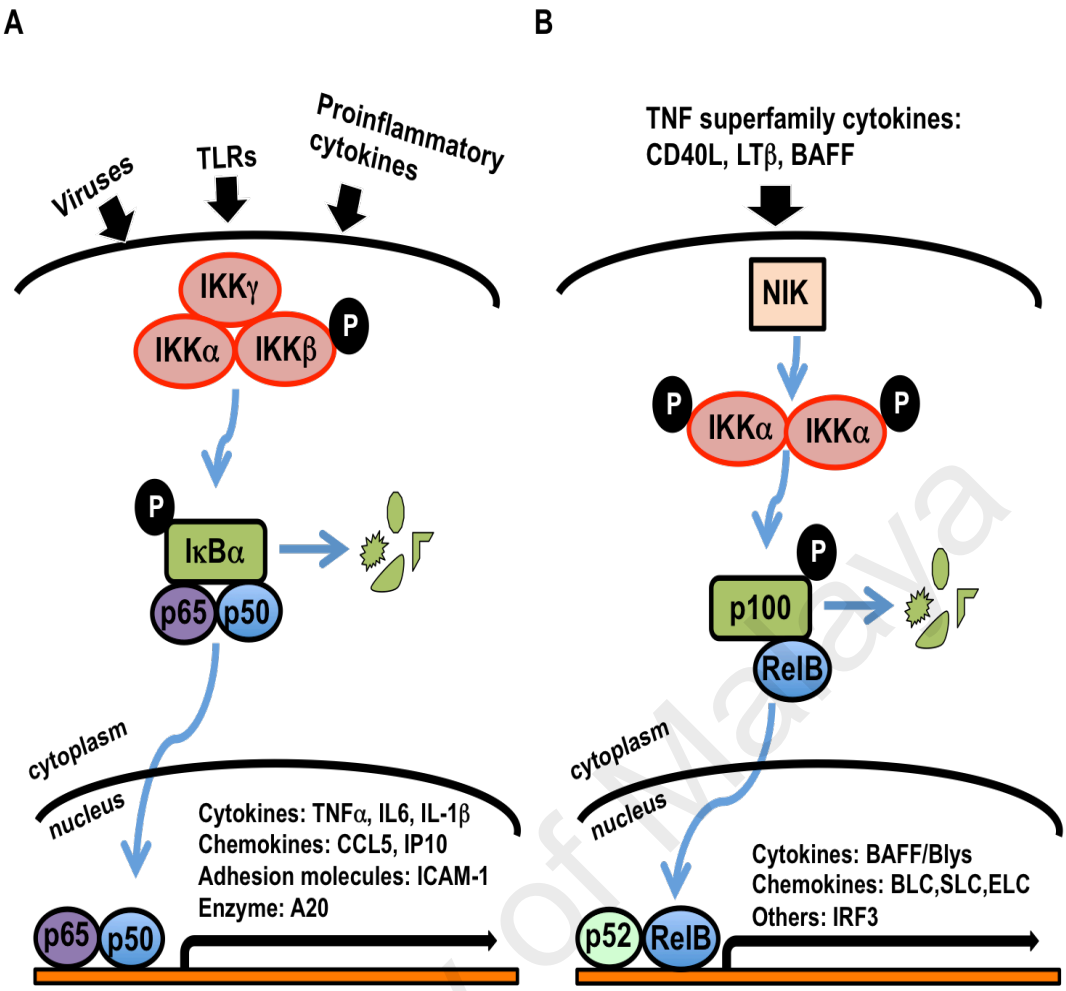

Figure 2.5: The canonical and noncanonical NF-κB signaling pathway. (A) In the canonical NF-κB pathway, NF-κB is sequestered in the cytoplasm through its association with IκBα. Upon stimulation by viruses, proinflammatory cytokines, or toll-like receptors, IKKβ phosphorylates IκBα, resulting in the degradation of IκBα via the ubiquitin-proteasome system. Freed NF-κB then translocate into the nucleus to activate target genes. (B) In the noncanonical NF-κB pathway, stimulation by TNF superfamily members (CD40L, LTβR, BAFF/Blys) activates NIK. NIK mediates IKKα phosphorylation, which in turn phosphorylates p100. The processing of p100 to mature form p52 results in the formation of p52/RelB heterodimer. Translocation of p52/RelB into the nucleus activates genes related to the development of the secondary lymphoid organs. (TLRs, toll-like receptors; IKK, IκB kinase; TNFα, tumor necrosis factor alpha; IL-1β, interleukin-1 beta; CCL5, chemokine (C-C motif) ligand 5; IP10, interferon gamma-induced protein 10; ICAM1, intercellular adhesion molecule 1; A20, tumor necrosis factor, alpha-induced protein 3; CD40L, CD40 ligand; LT-β, lymphotoxin-β; BAFF, B-cell activating factor; NIK, NF-κB-inducing kinase; BLC, B-lymphocyte chemoattractant; SLC, secondary lymphoid tissue chemokine; ELC, Epstein-Barr virus-induced molecule 1 ligand CC chemokine; IRF3, interferon regulatory factor 3).

2.9 Toll-like Receptors (TLRs)

Toll-like receptors (TLR) play an essential role in the innate immune response via recognition of PAMPs (Figure 2.5). The Toll protein was first discovered in *Drosophila* and shown to be required for the establishment of dorsal-ventral pattern during embryogenesis (Anderson et al., 1985). It was then demonstrated that Toll-mutant flies were highly susceptible to fungal infection (Lemaitre et al., 1996). This finding soon led to the identification of the first human Toll homolog, also known as Toll-like receptor 4 (TLR4) (Medzhitov & Horng, 2009). Detailed study on TLR4 shows that it induces genes involved in immune responses and cells or mice with mutation in TLR4 gene are hyporesponsive to lipopolysaccharide (LPS) (Poltorak et al., 1998). To date, there are 10 and 13 TLR family members in human and mouse, respectively. The cytoplasmic portion of all the TLRs exhibits high similarity to Toll/IL-1 receptor (TIR) domain, while extracellular region showed unrelated structures. This suggests that they recognize specific patterns of microbial components. Genetic analysis reveals that, among the TLRs, nucleic acid sensing TLRs (TLR3, 7, 8, and 9) localizes within the endosome while the other TLRs locates at the plasma membrane. Each TLR has been characterized to specifically recognize specific components of pathogens, for instance, TLR1/2 (triacylated lipoprotein), TLR3 (double-stranded RNA), TLR4 (lipopolysaccharide/LPS), TLR5 (bacteria flagellin), TLR6/TLR2 (diacyl lipopeptides), TLR7 (imidazoquinoline, single stranded RNA), TLR8 (single stranded RNA), and TLR9 (umethylated CpG DNA) (Takeda & Akira, 2004) (Figure 2.6). Importantly, these TLRs trigger the production of proinflammatory cytokines and maturation of antigen presenting cells in the immune system to fight off microbial infections (Akira et al., 2006).

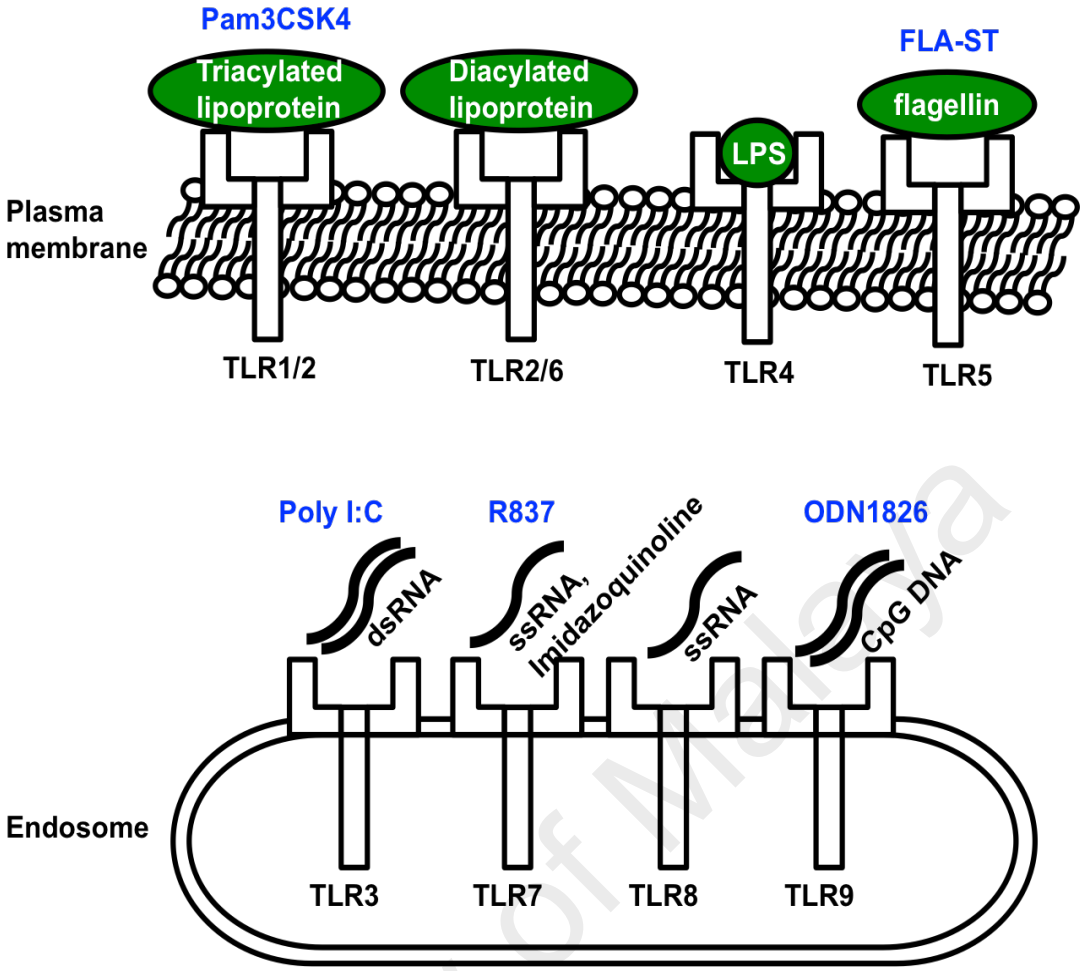

Figure 2.6: TLRs and ligands. TLR1, 2, 4, 5, and 6 localize to the plasma membrane, while TLR3, 7, 8, and 9 resides in endosome. TLR2 is crucial in recognizing microbial lipopeptides. TLR2 associates with TLR1 and TLR6 to discriminate the difference between triacyl- and diacyl- lipopeptides. TLR4 senses bacterial endotoxin LPS whereas TLR5 senses bacterial flagellin. TLR3 is a dsRNA receptor. TLR7 and TLR8 sense ssRNA, while TLR9 is a CpG DNA receptor. Agonist Pam3CSK4, FLA-ST, Poly I:C, R837, and ODN1826 are ligands for TLR1/2, TLR5, TLR3, TLR7, and TLR9 respectively.

2.10 LPS/TLR4/NF-κB signaling pathway

LPS is a structural component on the outer membrane of gram-negative bacteria. It consists of three core elements: Lipid A, core oligosaccharide, and an O side chain (Raetz & Whitfield, 2002). Lipid A is the key PAMP of LPS, which results in TLR4/LPS pathway activation (Beutler, 2000). Upon LPS stimulation, there are two LPS activation pathways: myeloid differentiation primary response gene 88 (MyD88)-dependent (Figure 2.7A) and TIR domain-containing adaptor protein inducing IFNβ (TRIF)-dependent pathways (Figure 2.7B). In the MyD88-dependent pathway (Figure 2.7A), MyD88 recruits IL-1 receptor-associated kinase-4 (IRAK-4). IRAK-4 then induces the phosphorylation of IRAK-1. Phosphorylated IRAK-1 recruits tumor-necrosis-factor-receptor-associated factor 6 (TRAF6) to the receptor complex. TRAF6 in conjunction with ubiquitin-conjugating enzyme 13 (UBC13), and ubiquitin-conjugating enzyme E2 variant 1 (UEV1A) promotes the recruitment and activation of transforming-growth-factor-beta-activated kinase 1 (TAK1) complex in an ubiquitination dependent manner. TAK1 then phosphorylates IKK complex, which ultimately phosphorylates IκB. The free NF-κB then translocate to the nucleus to induce immune-related genes (Akira & Takeda, 2004).

In the TRIF-dependent pathway (Figure 2.7B), TRIF recruits TRAF3. TRAF3 facilitates the activation of TBK1, and IκB kinase-ε (IKKε) (Hacker et al., 2006; Oganesyan et al., 2006), which in turn phosphorylates interferon regulatory factor 3 (IRF3) at the C-terminal region. This phosphorylation allows IRF3 to form a homodimer, which translocates into the nucleus and induces target gene expression (Kawai & Akira, 2007).

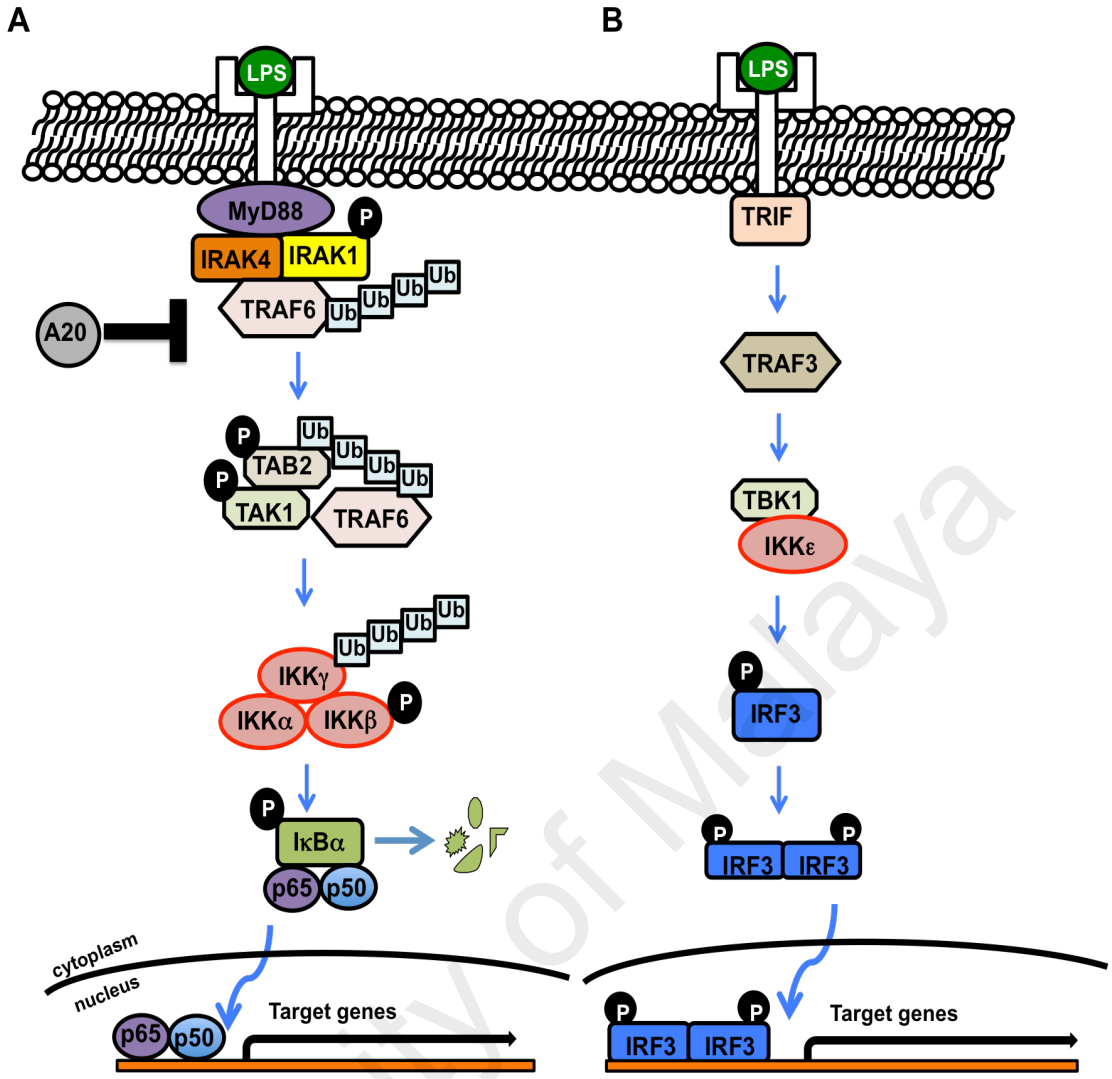

Figure 2.7: The TLR4/LPS signaling pathway. (A) TLR4-mediated MyD88- dependent NF-κB signaling pathway. MyD88 binds to TLR4 through the cytoplasmic TIR domains of TLRs. After LPS stimulation, IRAK-4, IRAK-1, and TRAF6 are recruited to form a complex. IRAK-4 phosphorylates IRAK-1. Phosphorylated IRAK-1 and TRAF6 dissociates from the complex. TRAF6 interacts with TAK1, TAB1, and TAB2. Activated TAK1 phosphorylates IKK complex (IKKα, IKKβ, and IKKγ/NEMO), and finally induces NF-κB translocation to activate target genes. (B) TLR4-mediated TRIF-dependent signaling pathway. TRIF recruits TRAF3, then interacts with TBK1, IKKε. These kinases phosphorylates IRF3. Phosphorylated IRF3 dimerizes and translocates into nucleus to activate target genes.

CHAPTER 3: MATERIALS AND METHODS

3.1 Antibodies

Antibodies against HSP90 (sc-8262), IRF3 (sc-15991), p65 (sc-372), IκBα (sc-203), α-tubulin (sc-8035), SNF2H (sc-13054 X), and ICAM-1 (sc-1511) were purchased from Santa Cruz Biotechnology, USA.

3.2 TLR agonists

LPS and actinomycin D were purchased from Sigma Aldrich, USA. PAM3CSK4, ODN1826, and FLA-ST were purchased from InvivoGen, USA. R837 and IKK inhibitor were purchased from Merck, USA. Doxycycline was bought from Fisher Scientific, USA, and poly I:C was purchased from Tocris Bioscience, USA.

3.3 Cell lines and culture conditions

RAW264.7, MEF, HEK293T and THP-1 cells were purchased from ATCC. RAW264.7 and THP-1 cells were cultured in Rosewell Park Memorial Institute medium (RPMI) while HEK293T and MEF cells were cultured in Dulbecco's Modified Eagle's Medium (DMEM). Both media were supplemented with 10% fetal bovine serum (FBS), penicillin G (100 μg/ml), and streptomycin (100 μg/ml). Cells were maintained at 37^{o}C with 5% CO_2 in a humidified incubator.

3.4 Plasmids

An shRNA targeting the exon junction of *mcircRasGEF1B* containing 11 bases of exon 4 and 14 bases of exon 2 was subcloned into a PLKO-Tet-Puro vector purchased from Addgene. The plasmid was subsequently verified by automated DNA sequencing. The shRNA sequences were as described in Table 3.1.

Table 3.1: shRNA sequences used in qPCR analysis

shRNA oligo	**Sequences**
shRNA *mcircRasGEF1B* top	CCGG*GTGGCGAGGAGGAAAGTATGCCTCA*CTC GAG*TGAGGCATACTTTCCTCCTCGCCAC*TTTTT
shRNA *mcircRasGEF1B* bottom	AATTAAAAA*GTGGCGAGGAGGAAAGTATGCCT CA*CTCGAG*TGAGGCATACTTTCCTCCTCGCCAC*

Italics: exons of mcircRasGEF1B

3.5 ASO transfections

ASOs were synthesized by IDT technologies, and 20 nM of ASOs were transfected into RAW264.7 cells with the X-tremeGENE HP DNA (Roche) according to the manufacturer's protocol. On day one, 400k cells were seeded and transfected at the same time. To maximize knockdown efficiency, ASO transfection was repeated 24 hours after the initial transfection. The ASOs sequences were listed in Table 3.2.

Table 3.2: ASO sequences used in qPCR analysis

List of ASOs	**Sequences**
Control ASO	5' mC*mC*mA*mG*mU*mG*G*C*G*A*G*G*A*G *G*A*A*A*mG*mU*mA*mU*mG*mC 3'
mcircRasGEF1B ASO I	5' mG*mC*mA*mU*mA*mC*T*T*T*C*C*T*C*C* T*C*G*C*mC*mA*mC*mU*mG*mG 3'
mcircRasGEF1B ASO II	5' mC*mU*mU*mU*mC*mC*T*C*C*T*C*G*C*C* A*C*T*G*mG*mC*mC*mA*mU*mC 3'

"*": phosphorothioate; "m": 2' O-methyl

3.6 Identification of circular splice junctions

Except where explicitly stated otherwise, all RNA-seq analyses were carried out using custom-written python scripts. Total RNA-seq sequencing reads of each subcellular fraction from LPS-stimulated macrophages were downloaded from GEO series GSE32916 (Bhatt et al., 2012). The sequences of all possible circular splice junctions within the same gene based on annotated exons (the ENSEMBL63 annotation and the mm9 version of the mouse genome were used) were compiled, retaining *RL*15 bp on each side of the junctions (equivalent to requiring at minimal length of 15 bp for spliced alignment overhangs) where *RL* is the read length. The circular junction sequences were then combined with the sequences of the full-length annotated transcripts and a Bowtie index was created, which was used to align reads that do not map to the whole genome sequence (Langmead et al., 2009). Candidate circular RNAs were then identified based on reads mapping to circular junctions.

3.7 Quantitative RT-PCR

On day one, RAW264.7 cells were seeded and transfected with 20 nM of control and ASO. After the initial transfection, ASO transfection was repeated 24 hours later. The cells were incubated for one more day. On day four, cells were treated with LPS for 2 hours and harvested for RNA extraction. Total RNA was isolated with the Thermo Scientific GeneJET RNA Purification Kit. Complementary DNAs were synthesized using M-MuLV reverse transcriptase (New England BioLabs, USA), and Random Hexamers (Invitrogen, USA). Quantitative PCR was performed with 2X SYBR Green PCR Master mix (Thermo Scientific, USA) and run on a Bio-Rad Connect Real-Time PCR System. The relative expression levels of linear mRNAs using a SYBR Green assay were normalized to housekeeping gene *L32*. The qPCR parameter for SYBR Green is 95 ^{o}C for 3 minutes, followed by 40 cycles of both 95 ^{o}C for 2 seconds, and 60

^{o}C for 20 seconds. Expression levels of circular RNA were measured using gene specific divergent primers using a Taqman assay. The relative expression levels of circular versus linear isoforms were normalized to housekeeping gene *GAPDH*. The qPCR parameter for Taqman is 50 ^{o}C for 2 minutes, 95 ^{o}C for 20 seconds, followed by 3 steps of 40 cycles at 95 ^{o}C for 3 seconds, 59.3 ^{o}C for 20 seconds, and 72 ^{o}C for 30 seconds. The sequences of the primers used are listed in Table 3.3.

Table 3.3: Primer sequences used in qPCR analysis

List of primers	**Sequences**
mL32/5'	AACCCAGAGGCATTGACAAC
mL32/3'	ATTGTGGACCAGGAACTTGC
mICAM-1/5'	TTCACACTGAATGCCAGCTC
mICAM-1/3'	GTCTGCTGAGACCCCTCTTG
mCcl-5/5'	GCTGCTTTGCCTACCTCTCC
mCcl-5/3'	TCGAGTGACAAACACGACTGC
mTNFα/5'	CTACTCCCAGGTTCTCTTCAA
mTNFα/3'	GCAGAGAGGAGGTTGACTTTC
mU6/5'	CTCGCTTCGGCAGCACATATAC
mU6/3'	GGAACGCTTCACGAATTTGCGTG
pre-*ICAM-1*/5'	CAGATCCTGGAGACGCAGAG
pre-*ICAM-1*/3'	CATTGGGGTCAGTCAGGTCT
mature *ICAM-1*/5'	CACGCTACCTCTGCTCCTG
mature *ICAM-1*/3'	AAGGCTTCTCTGGGATGGAT
hL32/5'	AGCTCCCAAAAATAGACGCAC
hL32/3'	TTCATAGCAGTAGGCACAAAGG
hIL-1β/5'	ACAGATGAAGTGCTCCTTCCA
hIL-1β/3'	GTCGGAGATTCGTAGCTGGAT
mcircRasGEF1B/5'	GTATGACTTCCGGGACGAGA
mcircRasGEF1B/3'	TGTTGGATAAGGGCTTCCAG
mlinearRasGEF1B/3'	GATGTCCCGCTGTATGGAC
mcircPlcl2/5'	CTTGCCGTGTCTCCTCGATT
mcircPlcl2/3'	CGTCCAGCAGAAAATACCGA
mcircUbe2d2/5'	TTGTGTGATCCCAATCCAGA
mcircUbe2d2/3'	TCTAGCCTGCCAATGAAACA
mcircEtv6/5'	TGTTCACACAGTGCCTCGAGC
mcircEtv6/3'	GGGCGTGTATGAAATTCGTT
mcircLilrb3/5'	AGGGGAACCTGGATGCAGAA
mcircLilrb3/3'	GCTGGGTGTCCAGTAGTGTC
Taqman *hcircRasGEF1B*/5'	TCGGGATGAAAGAATGATGAGA
Taqman *hcircRasGEF1B*/3'	AAAGGGAGGAGTCTGAGGCATAC
Taqman *hcircRasGEF1B* probe	CAGTGGCGAAGAGGA
Taqman *mcircRasGEF1B*/5'	CCGGGACGAGAGAATGATGA
Taqman *mcircRasGEF1B*/3'	GGACTGGTAGAGGTTTCGGTTG
Taqman *mcircRasGEF1B* probe	CAGTGGCGAGGAGGA

3.8 RNase R exonuclease assay

Total RNA was purified with Thermo Scientific GeneJET RNA Purification Kit. Exonuclease digestion experiment was carried out by incubating 35 μg of purified total RNA with or without 15 U of RNase R (Epicentre Biotechnologies) at 37 ^{o}C for 30 minutes. The mock- and RNase R- treated RNA were subsequently purified with the Thermo Scientific GeneJET RNA Purification Kit.

3.9 Subcellular fractionation analysis

RAW264.7 cells were resuspended in a homogenization buffer (10 mM HEPES, 10 mM KCl, 10 mM EDTA, 10 mM EGTA, 1 mM DTT, 1 mM $MgCl_2$, 0.5% NP-40, and 5% glycerol). Cells were incubated on ice for 20 minutes and then centrifuged at 4 ^{o}C at 500g for 10 minutes. Supernatants were collected as cytoplasmic fractions while the pellets were washed 3 times with the homogenization buffer. Total RNA from both cytoplasmic and nuclear fractions were purified with the Thermo Scientific GeneJET RNA purification kit. Arbitrary unit was calculated based on the equation:

Cytoplasm fraction: [1/(input/total RNA)], Cytoplasm+/Nucleus/Nucleus+: [2^($Ct_{cytoplasm}$-$Ct_{cytoplasm+/nucleus/nucleus+}$)/(input/total RNA)].

3.10 Polysome analysis

Twenty million RAW264.7 cells were seeded and treated with LPS for 2 hours. The cells were then treated with 200 μM cycloheximide for 10 minutes to stabilize polysome complexes. The cells were lysed with a hypotonic lysis buffer (10 mM Tris, pH 7.5; 1.5 mM $MgCl_2$; 10 mM KCl; 0.5 mM DTT; 0.5 mM PMSF; 1X Protease Inhibitor) containing 0.1% NP40. The cells were incubated on ice for 30 minutes and centrifuged at 800g at 4 ^{o}C for 10 minutes. The supernatants were collected as cytoplasmic extracts. Cytoplasmic supernatant was loaded onto a continuous sucrose gradients 10% to 50% in 400 mM KOAc (pH 7.5), 25 mM HEPES, 15 mM $Mg(OAc)_2$,

200 μM cycloheximide and 50 units/mL RNase Inhibitor (NEB). Sucrose gradients were centrifuged at 4 ^{o}C at 100,000g for 3 hours in a SW41 rotor. Equal volume of fractions was collected and total RNA was extracted. The identity of individual fractions was confirmed by loading equal volume of eluted RNA samples in an agarose gel with ethidium bromide staining to visualize the ribosomal RNAs. Free mRNAs and polysome fractions were pooled and reverse transcribed with equal input of RNA. The relative abundance of free mRNA and polysomes was determined with the equation: free mRNA: [1/(input/total RNA)], polysomes: [2^($Ct_{polysome}$-$Ct_{freemRNA}$)/(input/total RNA)] and presented as 100% stacked graph.

3.11 Immunoblot analysis

RAW264.7 cells were pretreated with ASOs (as described in section 3.5) before being treated with LPS (100 ng/ml) for 0, 6, 9, and 12 hours. The cells were lysed with hypotonic lysis buffer (10 mM Tris, pH 7.5; 1.5 mM $MgCl_2$; 10 mM KCl; 0.5 mM DTT; 0.5 mM PMSF; 1X Protease Inhibitor) containing 0.1% NP40. The cells were incubated on ice for 30 minutes and centrifuged at 800g at 4 ^{o}C for 10 minutes. The supernatants were collected as cytoplasmic extracts. The nuclear pellets were resuspended in nuclear lysis buffer (25 mM Tris, pH 7.5; 420 mM NaCl; 1.5 mM $MgCl_2$; 0.2 mM EDTA; 25% Glycerol; 0.5 mM DTT; 0.5 mM PMSF; 1X Protease Inhibitor). The nuclear extracts were collected by centrifugation at maximum speed at 4 ^{o}C for 10 minutes. Both cytoplasmic and nuclear extracts were quantified with Bradford assay and immunoblotted. Band intensity was quantified with the ImageLab (Biorad) software.

3.12 RNA extraction, library preparation, and sequencing

Total RNA was isolated with the Thermo Scientific GeneJET RNA Purification Kit. The RNA samples were checked for quality using Bio-Analyzer 2100 (Agilent Technologies, San Diego, CA, USA) and Qubit RNA assay kit (APPENDIX A). Total

RNA (1.5 μg) from each sample was used to prepare library using ScriptSeq Complete Kit (Epicentre Inc, Madison, WI, USA) according to manufacturer's protocol. The sequencing depth was assessed before data analysis (APPENDIX B)

3.13 RNA-seq data processing and analysis

Except where otherwise indicated, all analysis were carried out using custom-written Python scripts.

Paired-end (2x75bp) RNA-seq reads were aligned against the mm9 version of the mouse genome using TopHat2 (Kim et al., 2013) (version 2.0.8), run with Bowtie (Langmead et al., 2009) (version 0.12.9), and the Ensembl 66 annotation with the following parameters: --no-discordant --no-mixed --read-realign-edit-dist 0 --read-edit-dist 4 --read-mismatches 4 --min-segment-intron 10 --min-coverage-intron 10. Raw sequencing reads are available from the Gene Expression Omnibus under GEO accession number GSE99811.

Gene-level quantification in Fragments Per Kilobase per Million mapped fragments (FPKM) units was carried out using Cufflink (Trapnell et al., 2012) (version 2.0.2).

For differential expression analysis, sequencing counts at the gene level were obtained using HTSeq (Anders et al., 2015) (version 0.6.1p1). DESeq2 (Love et al., 2014) was then used to identify differential expressed genes between different conditions. One of the three replicates of unstimulated ASO II treated cells exhibited a globally discordant transcriptomic profile, and it was excluded accordingly from the differential expression analysis.

Statistically enriched functional categories of genes were identified using FuncAssociate 2.0 (Berriz et al., 2009).

3.14 Statistical tests

All of the statistical tests in this study were calculated using 2 tailed student's t-test (Microsoft Excel)

CHAPTER 4: RESULTS

4.1 Identification of *mcircRasGEF1B* as a LPS-inducible circRNA

As the first step to determine if any circRNAs might regulate the immune response, circRNA expressed upon LPS stimulation were catalogued using publicly available RNA-seq data from mouse macrophages with annotation-based pipeline (Bhatt et al., 2012). With the help of Dr. Marinov, a total of 1,916 circRNAs across different subcellular fractions and treatment conditions were successfully identified. From there, the predictions were validated by carrying out RT-PCR on 5 circRNA candidates of various sizes (APPENDIX C), including *mEtv6* (132 nucleotides), *mLilrb3* (1935 nucleotides), *mRasGEF1B* (2423 nucleotides), *mPlcl2* (4900 nucleotides), and *mUbe2d2* (7902 nucleotides).

To verify the 5 circRNA candidates, total RNA from mouse macrophages (RAW264.7) cells with or without LPS stimulation were harvested and the presence of circRNAs were measured with 2 approaches. First, circRNA specific PCR amplification was conducted using divergent primers and Sanger sequencing to identify the back-splice junction. Second, to rule out the possibility of trans-splicing and genomic rearrangement, RNase R, an exonuclease that degrades linear but not circularized RNA molecules was used. As a result, out of the 5 tested circRNA candidates, all of them showed back-spliced junction (Figure 4.1A-E), and 4 of them were resistant to RNase R (Figure 4.1A, B, D, E), while only 1 of them was inducible after LPS stimulation. Therefore, *mcircRasGEF1B* was identified as a LPS-inducible circRNA (Figure 4.1E), which was selected for further characterization in this study.

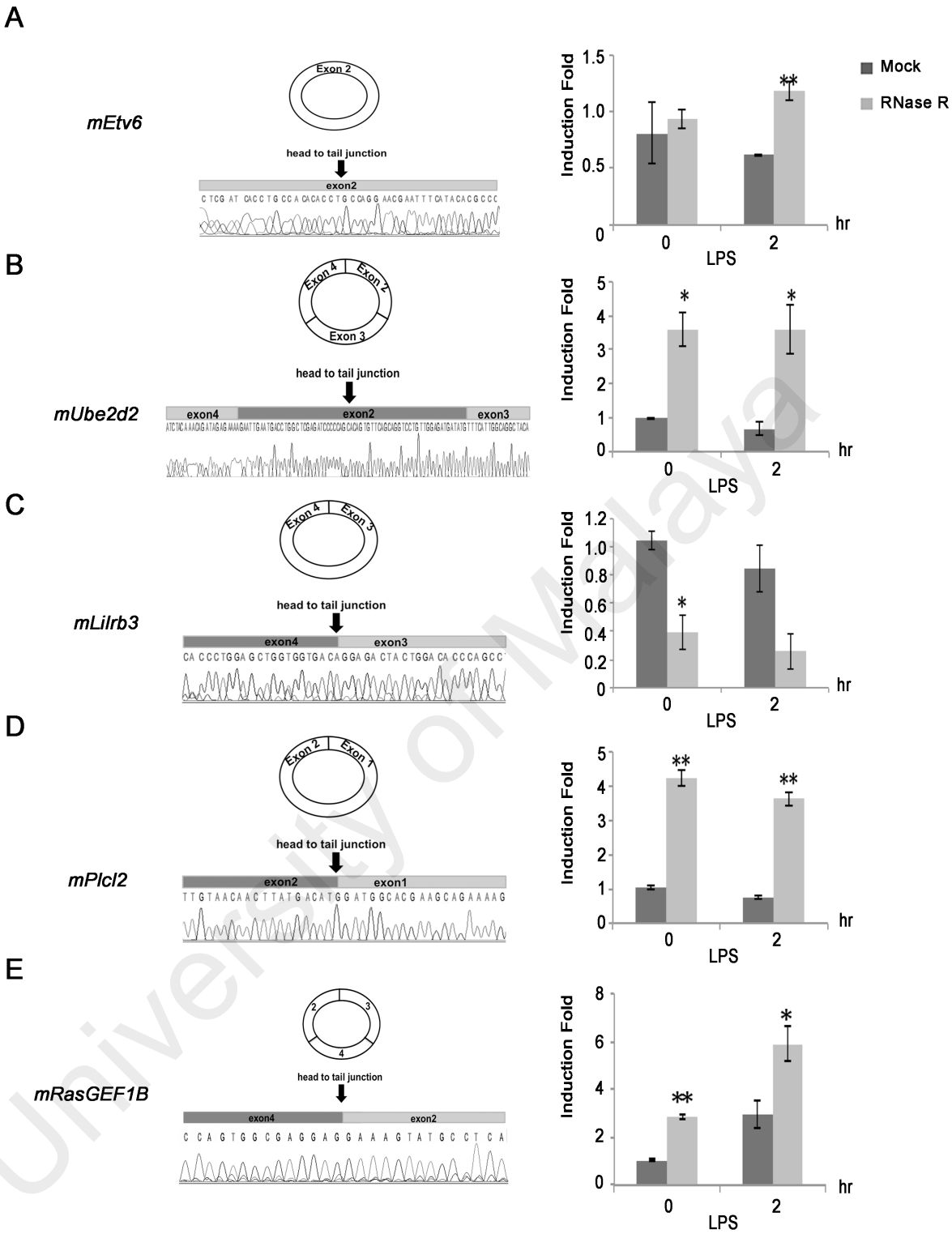

Figure 4.1: Identification of LPS-inducible circRNAs. Chromatograms of Sanger sequencing showing the sequence of the back-splice junction (left panels) and total RNA from RAW264.7 cells induced with or without LPS for 2 hours subjected to RNase R exonuclease assay (right panels) to confirm the circularity of (A) *mEtv6*; (B) *mUbe2d2*; (C) *mLilrb3*; (D) *mPlcl2*; and (E) *mRasGEF1B*. All experiments were carried out in duplicates. (*, $p < 0.05$; **, $p < 0.01$).

4.2 NF-κB dependent expression of LPS-inducible *mcircRasGEF1B*

After the identification of *mcircRasGEF1B* as a LPS-inducible circRNA, subsequent efforts were focused to study this specific RNA molecule. Mouse *RasGEF1B* contains 14 exons while *mcircRasGEF1B* is the result of exons 2 to 4 circularization (Figure 4.2A, APPENDIX C). To gain more detailed insight into the expression dynamics of *mcircRasGEF1B,* RAW264.7 cells were stimulated with LPS and its expression was measured at various time points (0, 1, 2, 6, 12, and 24 hours). *CCL5* is known as one of the robust LPS-responsive genes (Liu et al., 2005). Thus it was used as a positive control to check the LPS induction quality. Besides, mouse linear *RasGEF1B*, *mlinRasGEF1B,* was also shown to be induced by LPS (Andrade et al., 2010). In this experiment, similar to the *mlinRasGEF1B* parental gene, *mcircRasGEF1B* was induced as early as 1 hour post LPS stimulation. In addition, *mcircRasGEF1B* was stably expressed up to 12 hours after LPS treatment, while *mlinRasGEF1B* expression was reduced by 50% by that time (Figure 4.2B).

LPS stimulation activates NF-κB, which serves as the key transcription factor in the TLR4/LPS signaling pathway (Qin et al., 2005). To investigate if LPS-induced expression of *mcircRasGEF1B* is dependent on NF-κB, the NF-κB activation was blocked by treating RAW264.7 cells with IKK inhibitor VII at various concentrations prior to LPS stimulation. IKK inhibitor VII is a selective ATP competitive inhibitor of IKK complex, thereby inhibiting cellular IκBα degradation, and blocking NF-κB mediated gene expression (Waelchli et al., 2006). In the presence of 1.5 μM inhibitor, induction of *CCL5* was reduced by 90% while induction of *mcircRasGEF1B* was reduced by 42% (Figure 4.2C). Increasing IKK VII inhibitor concentration to 2.5 μM led to almost complete abolishment of LPS-induced expression of *mcircRasGEF1B*.

These results demonstrate that LPS induces the expression of *mlinRasGEF1B* and *mcircRasGEF1B* in an NF-κB-dependent manner.

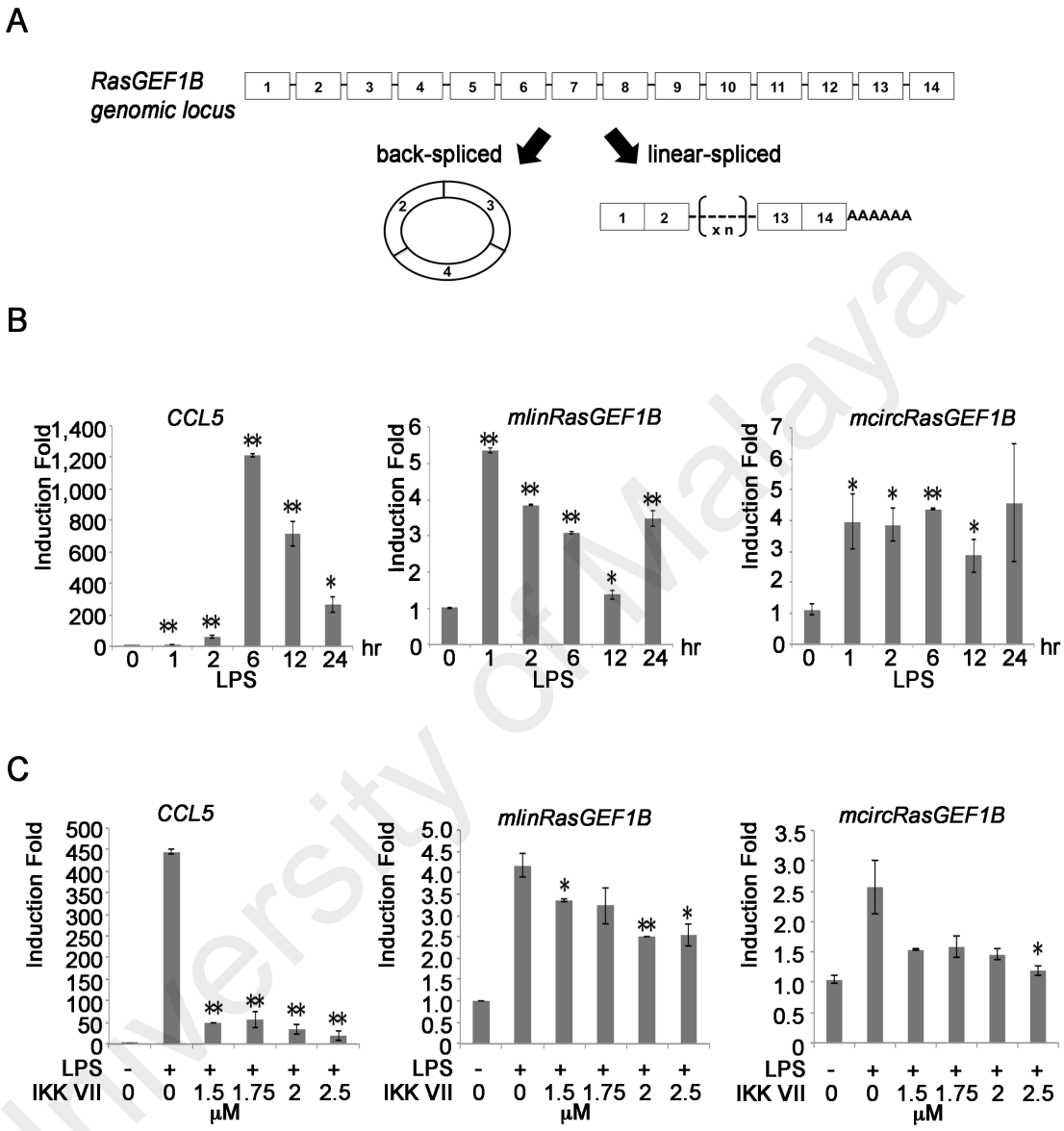

Figure 4.2: LPS-inducible and NF-κB dependent expression of *mcircRasGEF1B* in mouse macrophages. (A) Schematic depiction of the exon structure of linear *RasGEF1B* (right) and the back-splicing circular transcript (left). (B) RAW264.7 cells were treated with or without LPS for the indicated time periods. The expression levels of *CCL5*, *mlinRasGEF1B* and *mcircRasGEF1B* were measured by qRT-PCR. (C) RAW264.7 cells were pre-treated with the indicated doses of IKK VII for 1 hour before induction with or without LPS for 2 hours. The expression levels of *CCL5*, *mlinRasGEF1B* and *mcircRasGEF1B* were measured by qRT-PCR using RNA harvested after 2 hours of LPS treatment. All experiments were carried out in duplicates. (*, $p < 0.05$; **, $p < 0.01$).

4.3 TLR-mediated expression of *mcircRasGEF1B*

Previous study showed that the linear form of *RasGEF1B*, *mlinRasGEF1B* was strongly induced by poly I:C, and LPS (stimulating TLR3 and TLR4 respectively), while to a lesser extent by ODN CpG DNA and the synthetic triacylated lipopeptide Pam3CYS (stimulating TLR9 and TLR1/2 respectively) (Andrade et al., 2010). In addition, flagellin stimulates TLR5 while imiquimod (R837) can be used to specifically activate TLR7 (Hemmi et al., 2002). To test if *mcircRasGEF1B* was regulated by TLRs other than TLR4, RAW264.7 cells were treated with PAM3CSK4, ODN1826, LPS, FLA-ST (flagellin from *S. typhimurium*), poly I:C and R837. RAW264.7 cells responded to all of the stimulants except FLA-ST as evidenced by the induction of *TNFα* (Figure 4.3). Both *mlinRasGEF1B* and *mcircRasGEF1B* were robustly induced by LPS and ODN CpG DNA, and to a lesser extent by poly I:C and Pam3CSK4 (Figure 4.3). The results suggest that *mcircRasGEF1B* and *mlinRasGEF1B* expression is induced through several TLR pathways, including TLR4, TLR9, TLR3 and TLR1/TLR2.

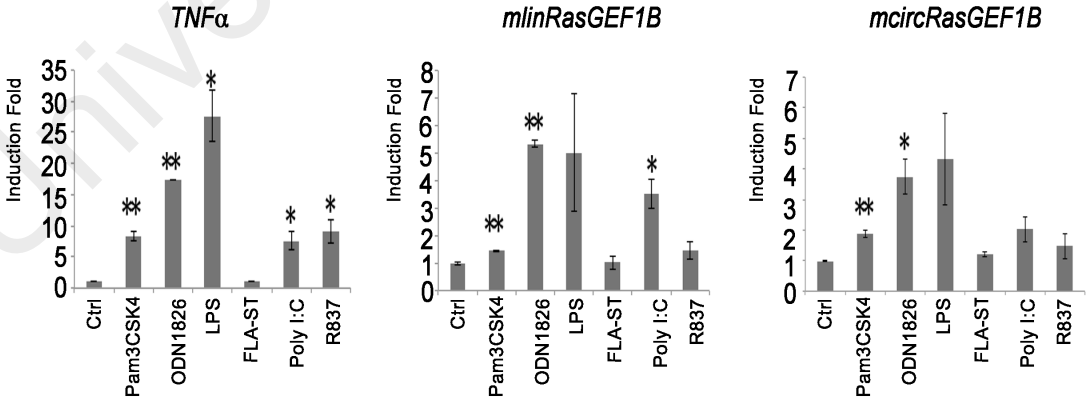

Figure 4.3: TLR-mediated *mcircRasGEF1B* expression. The indicated TLR ligands were used to treat RAW264.7 cells for 2 hours. The expression levels of *TNFα*, *mlinRasGEF1B*, and *mcircRasGEF1B* were measured by qRT-PCR using RNA harvested after 2 hours of ligands treatment. All experiments were carried out in duplicates. (*, $p < 0.05$; **, $p < 0.01$).

4.4 Cell-type specific expression of *mcircRasGEF1B*

An analysis of circRNA expression patterns among 15 expression cell lines by the ENCODE consortium highlighted that many circRNAs are cell-type specific (Salzman et al., 2013). To examine whether the induction of *mcircRasGEF1B* is cell-type specific, mouse embryonic fibroblast (MEF) cells were treated with LPS for various time points (0, 1, 2, 6, 12, and 24 hours), and the expression of *CCL5*, *mlinRasGEF1B*, and *mcircRasGEF1B* was measured. In this experiment, expression of *CCL5* was induced in response to LPS stimulation in MEF cells. However, LPS failed to induce either *mlinRasGEF1B* or *mcircRasGEF1B* in MEF cells. This result implies that LPS induces the expression of *circRasGEF1B* in a cell-type specific manner (Figure 4.4).

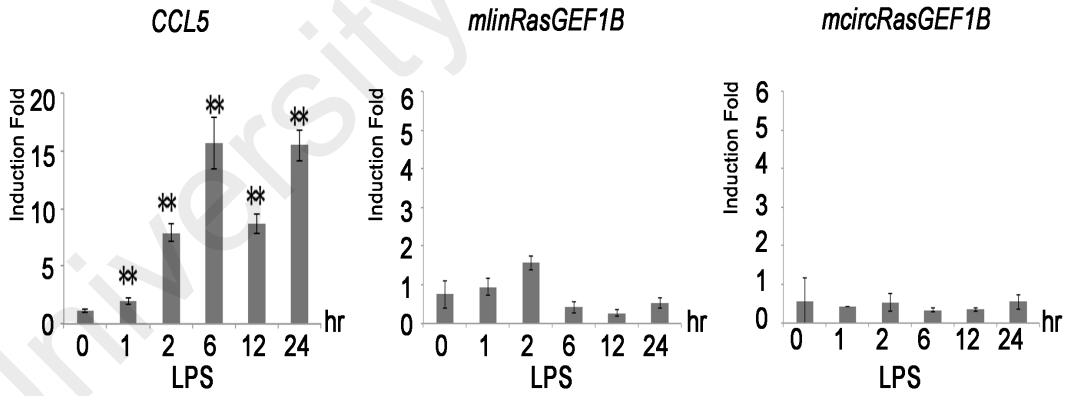

Figure 4.4: Cell-type specific *mcircRasGEF1B* expression. MEF cells were induced with or without LPS for the indicated time periods. The expression levels of *CCL5*, *mlinRasGEF1B*, and *mcircRasGEF1B* were measured by qRT-PCR. All experiments were carried out in duplicates. (*, $p < 0.05$; **, $p < 0.01$).

4.5 Evolutionary conserved expression of *circRasGEF1B*

Early evidence of conservation in circRNAs was demonstrated in several reports (Jeck et al., 2013; Legnini et al., 2017; Memczak et al., 2013). Additionally, it was also shown that DNA that encodes circRNAs is more conserved than DNA of flanking exons (Rybak-Wolf et al., 2015). To assess the conservation of *circRasGEF1B*, the sequences of human and mouse *RasGEF1B* were first aligned. Both mouse and human *RasGEF1B* contain 14 exons and exons 2 to 4 share high sequence homology with 86% identity (Figure 4.5A APPENDIX C). Divergent primers were then designed to detect and study the expression of *hcircRasGEF1B* in a human macrophage cell line, THP-1. The predicted *hcircRasGEF1B* is detected in these cells (Figure 4.5B). Similar to the observation in mouse, expression of *hcircRasGEF1B* in THP-1 cells is induced upon LPS stimulation. *IL1β* is a positive control for the quality of LPS induction (Figure 4.5C). Furthermore, the circularity of *hcircRasGEF1B* is confirmed using an RNase R treatment, to which it was resistant unlike the positive control *L32*, an abundant housekeeping ribosomal transcript and *hlinRasGEF1B* (Figure 4.5D). Taken together, this results show that *circRasGEF1B* is conserved between human and mouse.

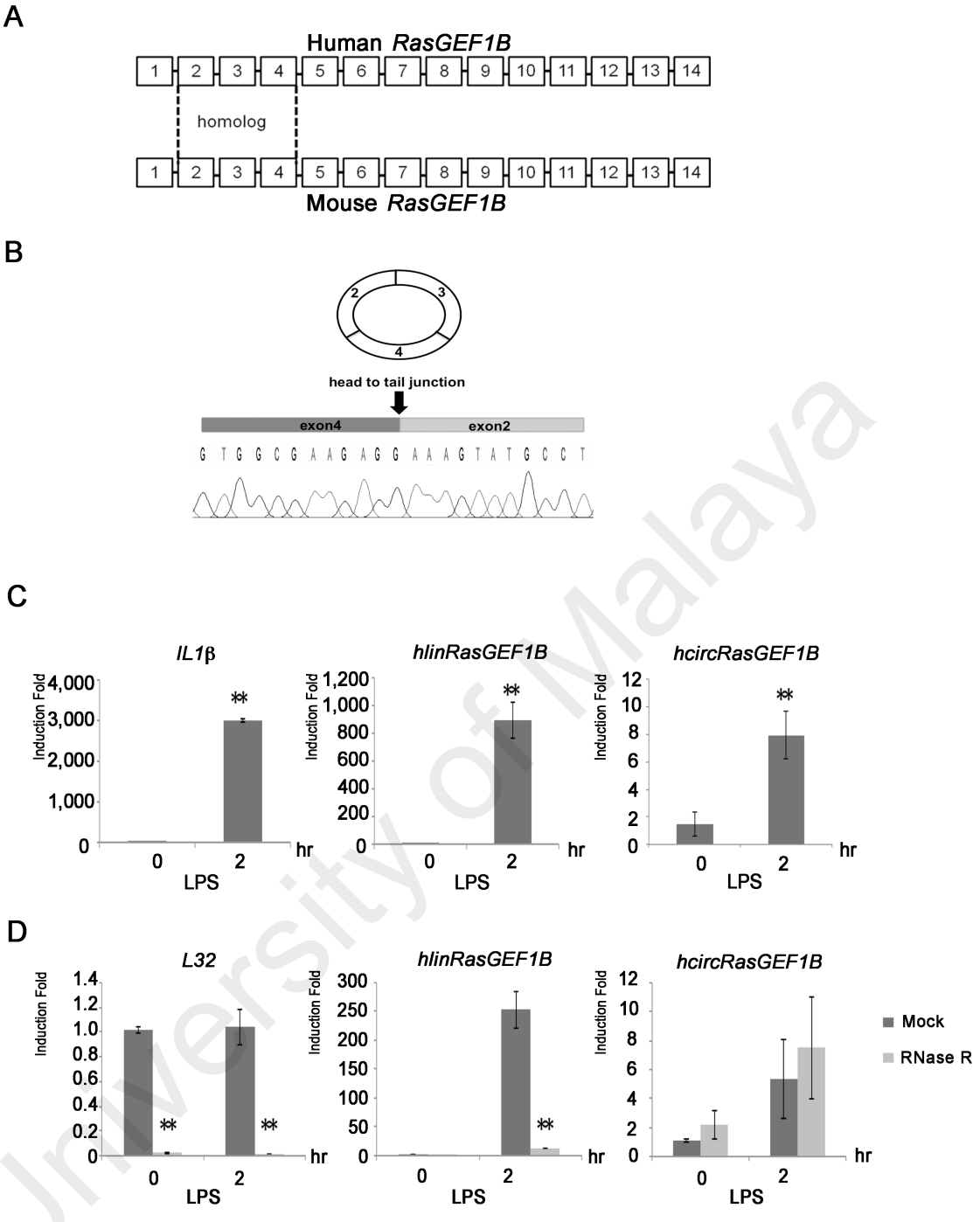

Figure 4.5: Evolutionary conserved expression of *circRasGEF1B*. (A) Schematic representation of human *RasGEF1B* (top) and mouse *RasGEF1B* (bottom); Sequence homology between conserved exons 2, 3, and 4 is highlighted (dashed lines). (B) A chromatogram of Sanger sequencing showing the sequence of the back-splicing junction of *hcircRasGEF1B* (exons 2 and 4). (C) Human THP-1 cells were induced with or without LPS for 2 hours. The expression levels of *IL1β, hlinRasGEF1B* and *hcircRasGEF1B* were measured by qRT-PCR. (D) THP-1 cells were induced with or without LPS for 2 hours and total RNA was subjected to RNase R treatment to confirm the circularity of *hcircRasGEF1B*. The levels of *L32*, *hlinRasGEF1B* and *hcircRasGEF1B* were measured by qRT-PCR. All experiments were carried out in duplicates. (*, $p < 0.05$; **, $p < 0.01$).

4.6 Localization and RNA translatability of *mcircRasGEF1B*

As a first step towards understanding the physiological role of *circRasGEF1B,* its subcellular localization was determined. To this end, RAW264.7 cells were treated with LPS for 2 hours and fractionated into nuclear and cytoplasmic fractions. The cytoplasmic *L32* and nuclear *U6* transcripts were used as controls for the purity of cytoplasmic and nuclear fractions, respectively. As expected, *L32* was predominantly enriched in the cytoplasmic fraction while *U6* was enriched in the nuclear fraction. Intriguingly, *mcircRasGEF1B* was predominantly localized to the cytoplasm similar to *mlinRasGEF1B* (Figure 4.6A). These results are consistent with previous reports showing that majorities of circRNAs are cytoplasmic (Jeck et al., 2013; Salzman et al., 2012), and suggest that *mcircRasGEF1B* might play a role in the post-transcriptional regulation of gene expression.

The *mcircRasGEF1B* arises from the circularization of exons 2, 3, and 4. The translational start site of *mlinRasGEF1B* resides in exon 2, which is part of *mcircRasGEF1B*. To test if *mcircRasGEF1B* is being translated into a functional protein, free- and polysome-bound mRNAs were isolated by sucrose gradient ultracentrifugation. An agarose gel was run to verify separation of 18S, 28S, and polysome fractions and earlier fractions (fractions 1-9) were pooled as free mRNAs while remaining fractions (fractions 10-23) as polysomes (Figure 4.6B). The relative quantity of linear transcripts (*mlinRasGEF1B, A20, TNFα, IP10, IκBα*, *ICAM-1* and *GAPDH*) and circular transcript (*mcircRasGEF1B*) were then measured by qRT-PCR. Linear products were enriched in the ribosome bound fraction for the genes assayed. Circular product, *mcircRasGEF1B,* however, was highly abundant in the free mRNA fraction (Figure 4.6C). This finding is in agreement with other reports that failed to identify polysome-bound circRNAs (Guo et al., 2014; Jeck et al., 2013; Salzman et al., 2012). Taken together, this result shows that cytoplasmic localized AUG-containing

mcircRasGEF1B did not bound to polysomes, and is not translated.

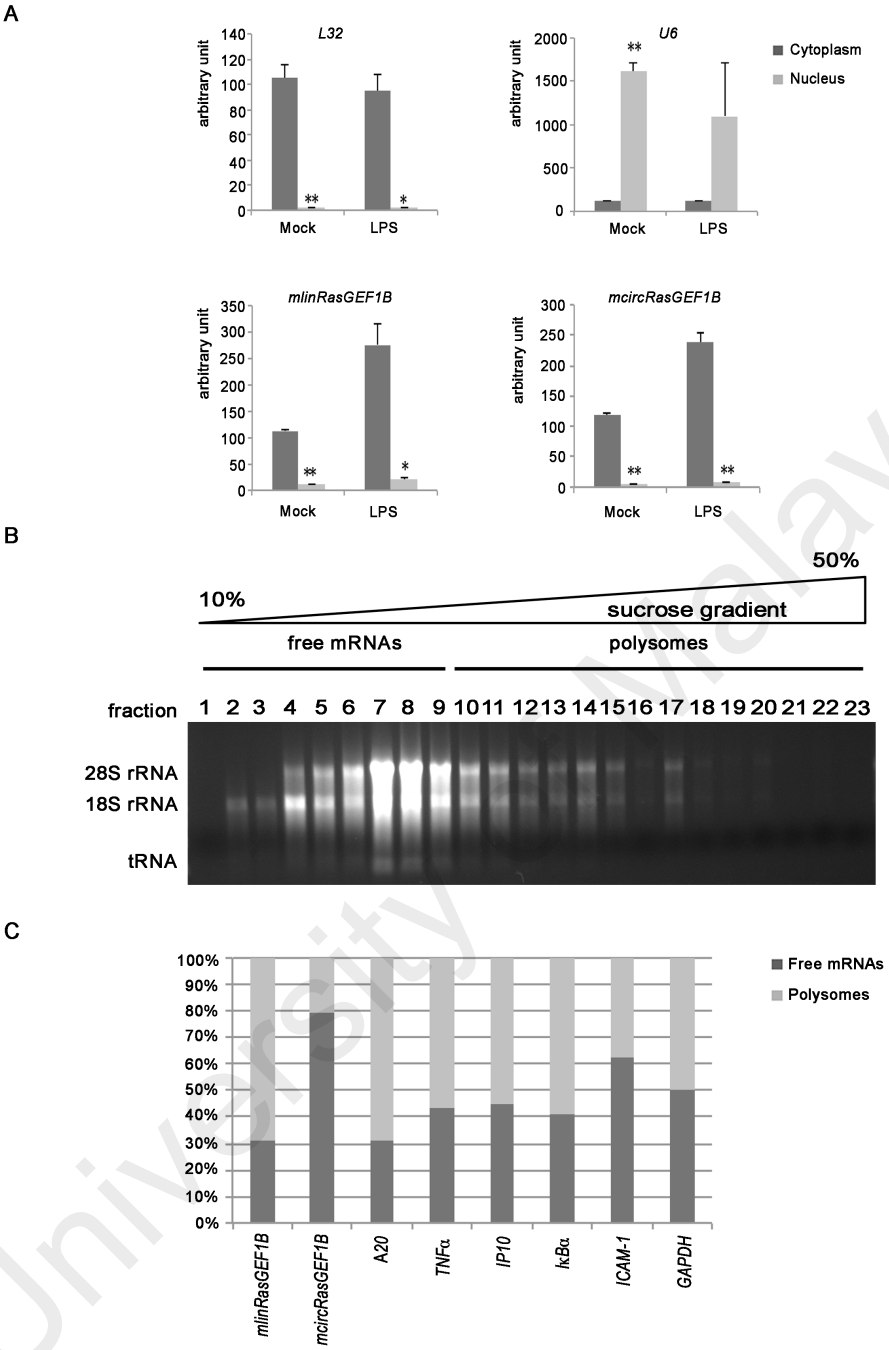

Figure 4.6: *mcircRasGEF1B* is predominantly located in cytoplasm and is not translated. (A) RAW264.7 cells were induced with or without LPS for 2 hours. Whole cell lysates were fractionated into cytoplasmic and nuclear fractions. The levels of *L32*, *U6*, *mlinRasGEF1B*, and *mcircRasGEF1B* in these fractions were measured by qRT-PCR. All experiments were carried out in duplicates. (*, $p < 0.05$; **, $p < 0.01$). (B) RAW 264.7 cells were induced with LPS for 2 hours and cytoplasmic supernatant was subjected to sucrose gradient centrifugation. Total RNA from each fraction was harvested and verified with agarose gel. (C) The levels of linear transcripts (*mlinRasGEF1B*, *A20*, *TNFα*, *IP10*, *IκBα*, *ICAM-1* and *GAPDH*), and circular transcript *mcircRasGEF1B*, in free mRNA and polysome-bound fractions were measured by qRT-PCR (n = 2).

4.7 Regulation of the expression of *ICAM-1* in the TLR4/LPS signaling pathway by *mcircRasGEF1B*

To test if *mcircRasGEF1B* plays a role in regulating the TLR4/LPS pathway, loss-of-function assay was employed. The expression of *mcircRasGEF1B* was knocked down using two RNase-H based antisense oligonucleotides (ASOs), ASO I, and II, of which both target the back-splice junction of *mcircRasGEF1B.* A sense-strand version of ASO I was used as a control ASO (Figure 4.7A). ASO I, and II specifically knocked down the expression of *mcircRasGEF1B* but had no or little effect on *mlinRasGEF1B* (Figure 4.7B). The effect of *mcircRasGEF1B* knockdown on LPS target genes was examined and it was found that it resulted in reduction of *ICAM-1* levels at 2 hours after LPS induction. LPS-induced *ICAM-1* expression was reduced by 27% in ASO I, and 39% in ASO II (Figure 4.7B). A more detailed time course using ASO I transfected cells revealed that LPS-induced *ICAM-1* expression was reduced by 27% and 30% at 2 hours and 6 hours respectively in the absence of *mcircRasGEF1B* (Figure 4.7C). To minimize the possibility that the effect observed with *mcircRasGEF1B* ASO-mediated silencing was caused by an ASO off-target effect, an inducible short hairpin RNA (shRNA) targeting the junction of exon 4 and exon 2 of *mcircRasGEF1B* (Figure 4.7D) was constructed. *McircRasGEF1B* was knocked down by treating stable RAW264.7 cells carrying the inducible shRNA transgene with doxycycline for 2 days prior to LPS induction. Treating the cells with doxycycline significantly reduced the expression of *mcircRasGEF1B* but not the linear *mlinRasGEF1B* (Figure 4.7E). Importantly, there was a 30% reduction of LPS-induced expression of *ICAM-1* in the absence of *mcircRasGEF1B,* which was consistent with the ASO mediated knockdown results (Figure 4.7E). To further confirm the effect of ICAM-1 at the protein level, western blot in *mcircRasGEF1B*-deficient cells was conducted. *McircRasGEF1B* was knocked down with ASO I, and ASO II, and treated with LPS for 6, 9, and 12 hours. The reduction of

ICAM-1 protein was detected across every time point, suggesting that *mcircRasGEF1B* effect was confirmed in both ICAM-1 mRNA and protein levels (Figure 4.7F). Taken together, these data indicate that *mcircRasGEF1B* positively regulates the expression of *ICAM-1* in the TLR4/LPS signaling pathway.

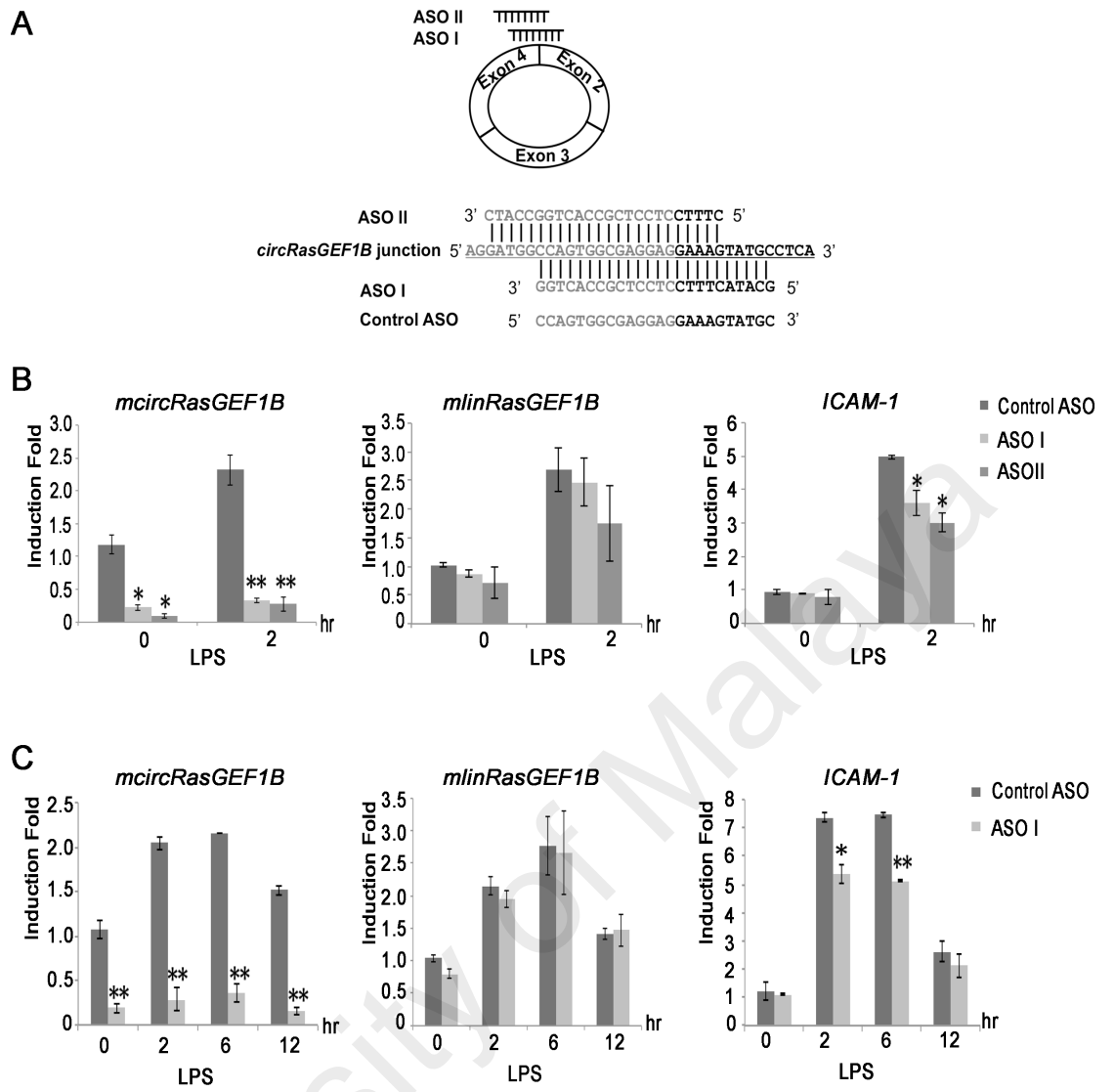

Figure 4.7: *mcircRasGEF1B* positively regulates the LPS-induced expression of *ICAM-1*. (A) ASO I and II targeting *mcircRasGEF1B* at the junction of exons 4 and 2. The control ASO is in the sense orientation but with the same coordinates as ASO I. (B) RAW264.7 cells were transfected with ASO I, ASO II, and control ASO, and induced with LPS for 2 hours. The expression levels of *ICAM-1*, *mlinRasGEF1B* and *mcircRasGEF1B* were measured by qRT-PCR. (C) RAW264.7 cells were knocked down with ASO I or control ASO and induced with LPS for the indicated time periods. The expression levels of *ICAM-1*, *mlinRasGEF1B*, and *mcircRasGEF1B* were measured by qRT-PCR. (D) Schematic depiction of the inducible shRNA construct targeting the back-splice junction of *mcircRasGEF1B*. (E) A stable RAW264.7 clone carrying the shRNA construct was induced with 2.5 μg of Doxycycline for 2 days before treatment with or without LPS. The expression levels of *ICAM-1*, *mlinRasGEF1B* and *mcircRasGEF1B* were measured by qRT-PCR. (*, $p < 0.05$; **, $p < 0.01$). Experiments were carried out in duplicates, n=2 (B, C) and triplicates, n=3 (E). (F) RAW264.7 cells were knocked down with control ASO, ASO I, and ASO II and then induced with or without LPS for the indicated time periods. Whole cell extracts were immunoblotted with the indicated antibodies. Intensity of bands was quantified using Image Lab (Biorad) software normalized to α-tubulin and shown in relative to 0 minute control ASO. (CA: control ASO, AI: ASO I, AII: ASO II). This is a representative data from 3 independent time course experiments.

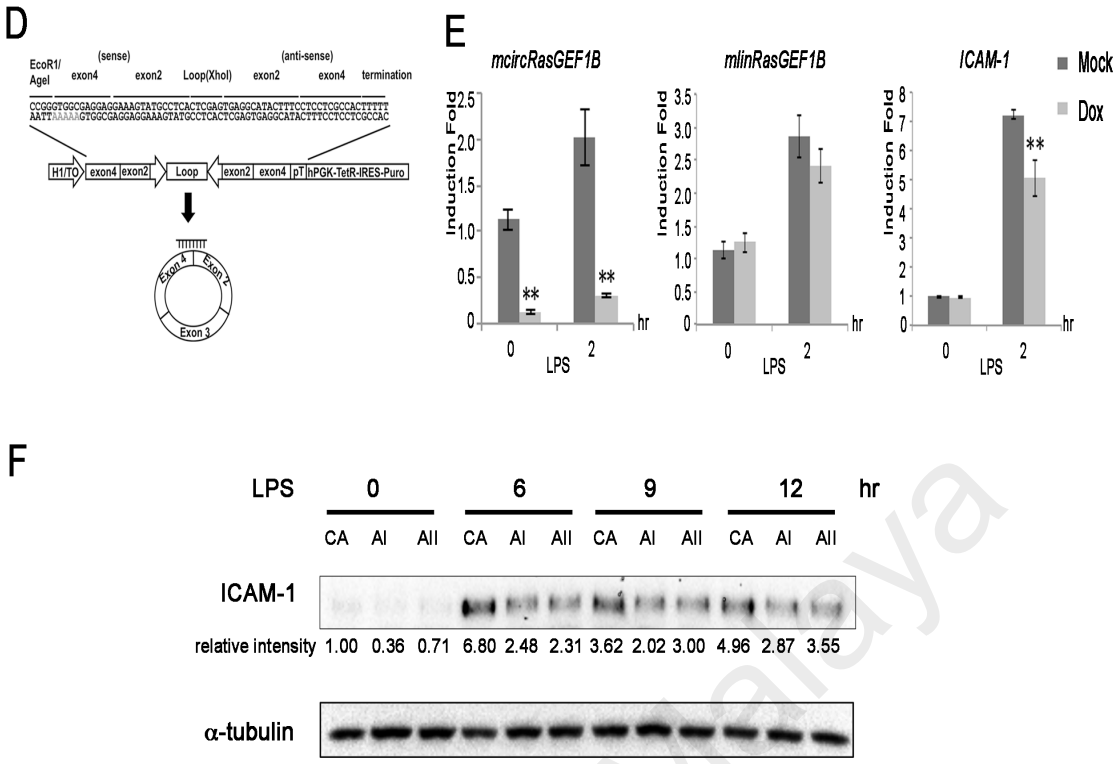

Figure 4.7, continued

4.8 Mechanism: The upstream signal transduction of TLR4/LPS pathway is unaffected by *mcircRasGEF1B*

In the knockdown assays, decreased mRNA levels of *ICAM-1* could be due to a variety of mechanisms. In this study, 2 possibilities were considered in which either *mcircRasGEF1B* reduces transcription of *ICAM-1* or it reduces stability of *ICAM-1* mRNA. The reduction of the transcription of *ICAM-1* could be due to blocking of the TLR4 signaling or direct inhibition of transcription by *mcircRasGEF1B*. First, the possibility of knockdown of the expression of *mcircRasGEF1B* affects the TLR4 signaling was tested. RAW264.7 cells were transfected with control or *mcircRasGEF1B*-specific ASO I, and cell lysates were fractionated into cytoplasmic and nuclear fractions. Since LPS induces the activation of NF-κB and IRF3, the IκBα degradation and the nuclear translocation of p65 and IRF3, of which are biochemical hallmarks of NF-κB and IRF3 activation respectively (Figure 2.7) were examined. It was found that *mcircRasGEF1B* knockdown led to no obvious differences in the degradation of IκBα, nuclear translocation of p65, or IRF3 activation (Figure 4.8). Thus, these results imply that *mcircRasGEF1B* does not regulate the upstream signal transduction of TLR4/LPS pathway.

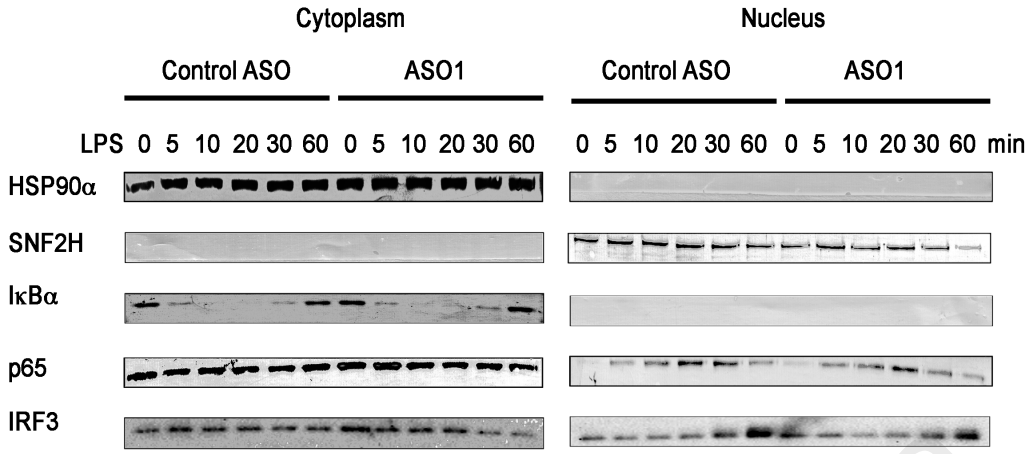

Figure 4.8: *mcircRasGEF1B* does not affect upstream signal transduction of TLR4/LPS pathway. RAW264.7 cells were knocked down with ASO I or control ASO, and then induced with or without LPS for the indicated time periods. Whole cell extracts were fractionated and the fractions were immunoblotted with the indicated antibodies.

4.9 Mechanism: Regulation of the stability of *ICAM-1* transcript by *mcircRasGEF1B*

Given that *mcircRasGEF1B* is enriched in the cytoplasm, it is unlikely that it directly regulates transcription in the nucleus. Therefore, whether *mcircRasGEF1B* affects the stability of *ICAM-1* transcripts was investigated. First, the stability of *ICAM-1* pre-mRNA and mature mRNA was assessed by quantitative RT-PCR measurements after blocking transcription with actinomycin D (ActD) for 1, 2, and 4 hours in the presence and absence of ASO I. mRNA stability after 2 hours of LPS induction was measured and normalized to that of the relatively stable *L32* mRNA. In agreement with other reports showing that circRNAs are more stable than linear RNAs (Jeck et al., 2013; Memczak et al., 2013), these assays revealed that *mcircRasGEF1B* is more stable than *mlinRasGEF1B* (Figure 4.9A). Furthermore, as observed before, ASO I specifically reduced the expression of *mcircRasGEF1B* but not *mlinRasGEF1B* (Figure 4.9A). Interestingly, in *mcircRasGEF1B*-deficient cells, there was a reduction of the levels of mature *ICAM-1* mRNA but not of its pre-mRNA (Figure 4.9B). More importantly, there was a small but reproducible decreases in the stability of mature *ICAM-1* mRNA (13% at 1 hour, 23% at 2 hours, and 12% at 4 hours post ActD treatment) in *mcircRasGEF1B*-depleted cells (Figure 4.9C). In addition, LPS-induced levels of *ICAM-1* pre-mRNA were similar between control and *mcircRasGEF1B*-depleted cells, suggesting that *mcircRasGEF1B* does not affect the transcription of *ICAM-1*. Taken together, the results suggest that *mcircRasGEF1B* controls LPS-induced *ICAM-1* expression through regulating the stability of its mature mRNA.

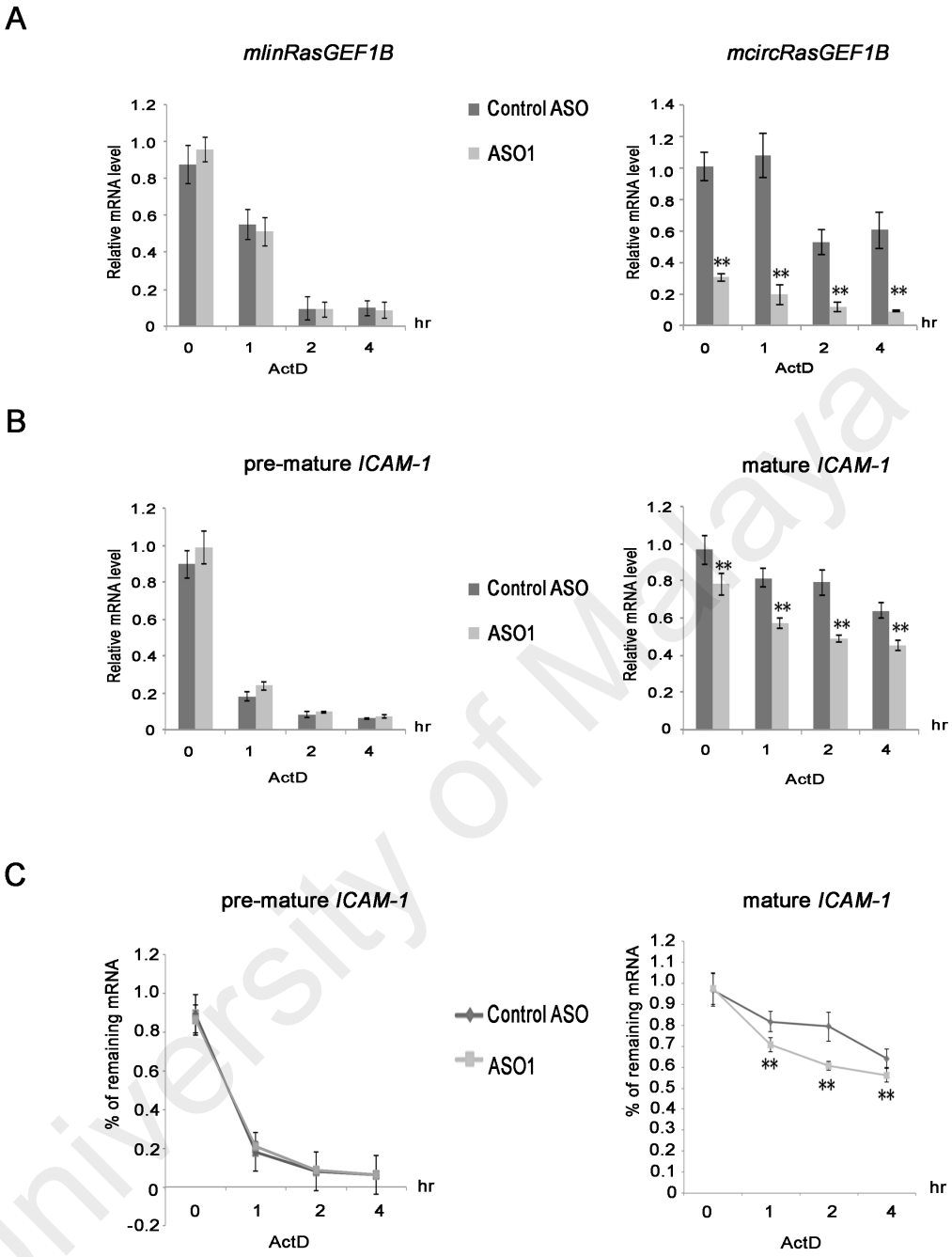

Figure 4.9: *mcircRasGEF1B* regulates the stability of *ICAM-1* mRNA. **(A)** RAW264.7 cells were transfected with ASO I or control ASO, and then treated with LPS for 2 hours followed by treatment with 1 μg/ml of ActD for the indicated time periods. The expression levels of *ICAM-1*, *mlinRasGEF1B* and *mcircRasGEF1B* were measured by qRT-PCR. **(B)** Relative levels of *ICAM-1* pre-mRNA and mature mRNA were measured relative to the levels of *L32*'s mRNA. **(C)** The stability of *ICAM-1* pre-mRNA and mature mRNA measured relative to *L32*. All experiments were carried out in quadruplicates, n=4. (*, $p < 0.05$; **, $p < 0.01$).

4.10 Mechanism: Model of action

A proposed model of action mediated by *circRasGEF1B* in TLR4/LPS pathway is shown in Figure 4.10. LPS stimulates TLR4-mediated NF-κB signaling, which leads to the transcription of proteins involved in antimicrobial responses, such as ICAM-1. *circRasGEF1B* stabilizes mature *ICAM-1* transcripts, leading to a stable expression of ICAM-1 protein and antimicrobial responses. In contrast, *circRasGEF1B* deficiency reduces stable mature *ICAM-1* transcripts and therefore its proteins. However, the molecular interactions of *circRasGEF1B* and *ICAM-1* mRNA remains to be elucidated.

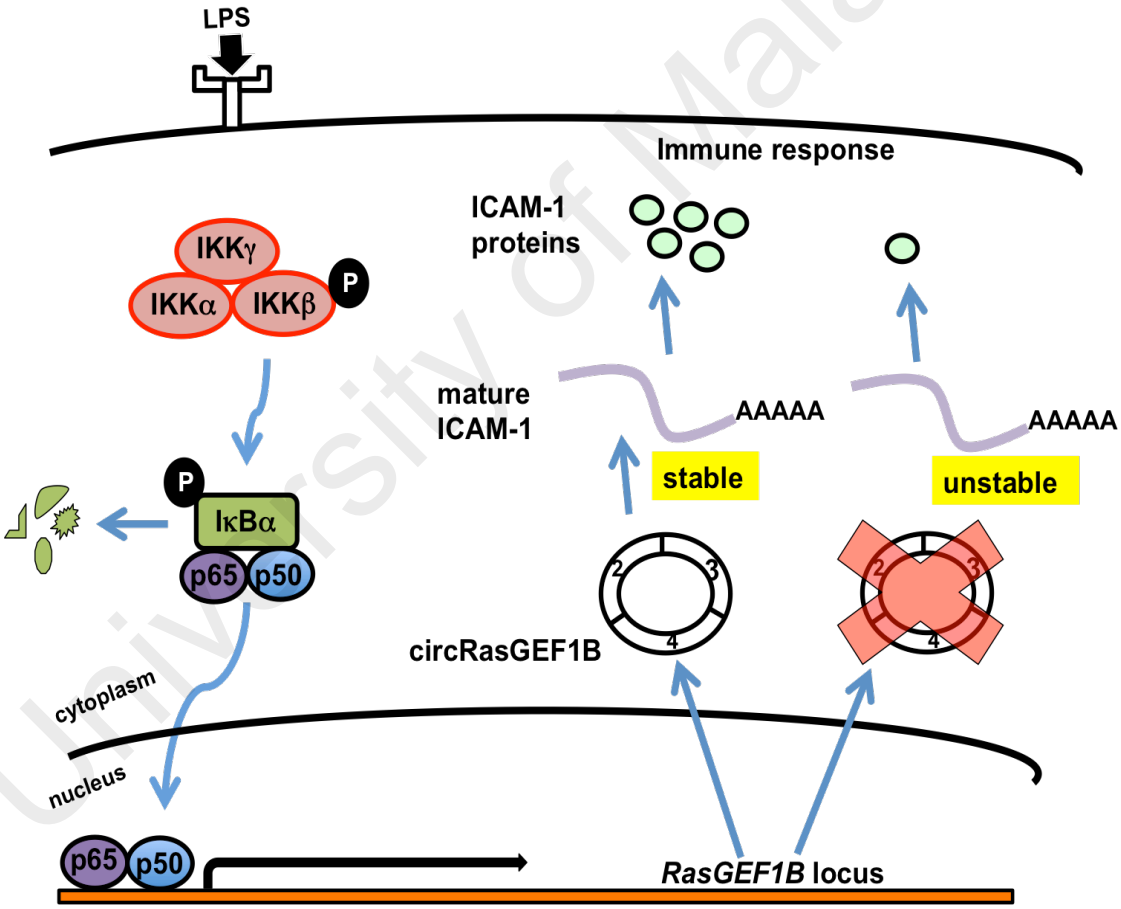

Figure 4.10: Model of action of *circRasGEF1B* increases the stability of ICAM-1 in TLR4/LPS pathway.

4.11 Transcriptome-wide characterization of LPS-induced genes in the presence or absence of *mcircRasGEF1B*

In this study, a model of mechanism of *mcircRasGEF1B* reduces the transcript and protein levels of LPS-induced ICAM-1 through destabilizing its mature mRNA products were described. However, the question of to what extend *mcircRasGEF1B* is an important regulator of the inflammatory network remains open. To address this question, the genome-wide gene expression dynamics upon activation of the TLR4/LPS pathway in control and *mcircRasGEF1B*-deficient backgrounds were characterized. To determine how knockdown of *mcircRasGEF1B* alters the transcriptomic profile of murine macrophage upon LPS stimulation, the expression of *mcircRasGEF1B* in RAW264.7 cells was knocked down using two different ASOs, ASO I, and II, both of them targeting the back-splice junction unique to *mcircRasGEF1B* (Figure 4.11A). A sense-strand version of ASO I was used as a control. Then, RNA-seq experiments were carried out after rRNA removal from the total RNA from 3 biological replicates of RAW264.7 cells of all 3 (Control, ASO I and ASO II) backgrounds, with and without LPS stimulation. Next, reads were mapped to the genome, gene levels were quantified, read counts per gene was extracted, and genes differentially expressed upon LPS stimulation in each background, and genes differentially expressed between control and *mcircRasGEF1B*-knockdown cells were identified with DESeq2 (Love et al., 2014) (Figure 4.11B). Robust knockdown efficiency, with ASO I reduces *mcircRasGEF1B* levels by 76%, and ASO II depletes *mcircRasGEF1B* by 85% (Figure 4.11C) was observed. In agreement with the previous findings, the reduction of *ICAM-1* expression in both ASO I and ASO II-treated cells was also observed (Figure 4.11D).

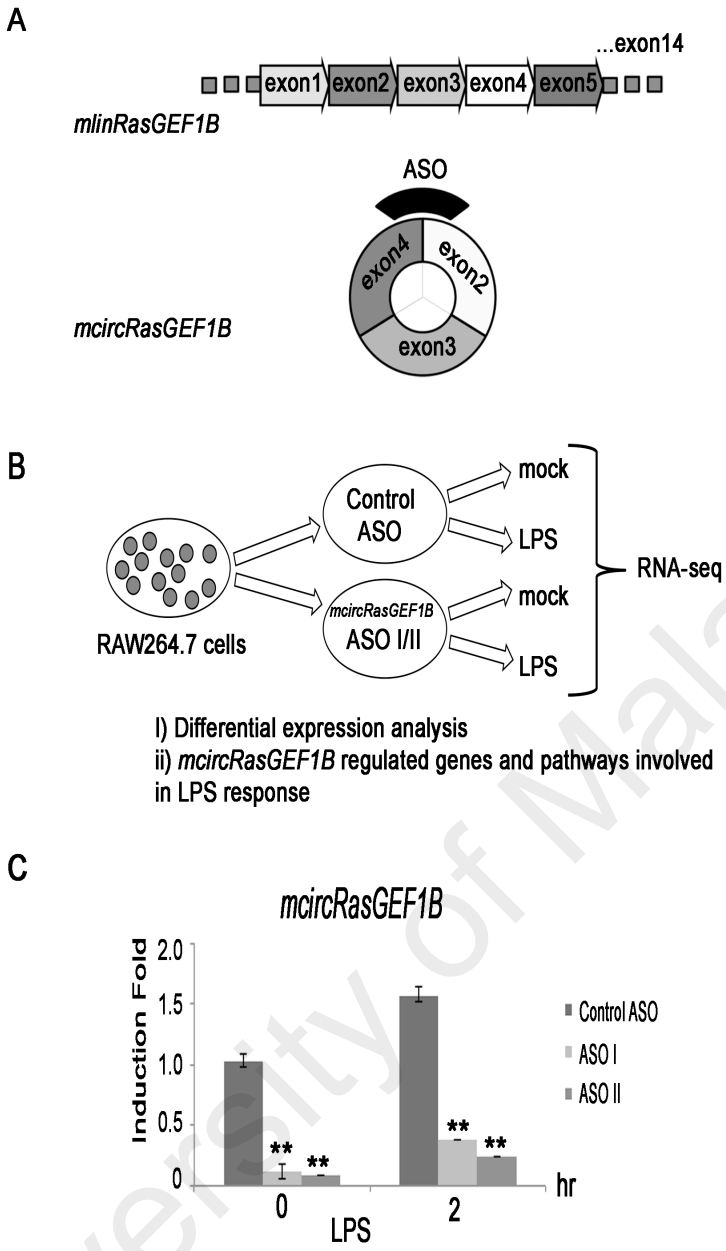

Figure 4.11: Transcriptome-wide characterization of LPS-induced genes in the presence or absence of *mcircRasGEF1B*. (A) *mcircRasGEF1B* is produced by the *RasGEF1B* locus in mouse though back-splicing. Antisense oligos (ASO) were designed specifically targeting the back-splice junction for the purpose of depleting *mcircRasGEF1B*. (B) RAW264.7 cells were treated with the *mcircRasGEF1B* targeting ASO I, and ASO II oligos as well as with a control oligo, then subjected to LPS treatment (n = 3). Gene expression changes were then characterized at the global level using RNA-seq, thus identifying the genes and pathways that appear to be regulated by *mcircRasGEF1B*. (C) RAW264.7 cells were transfected with ASO I, ASO II, and control ASO, and induced with LPS for 2 hours. The expression of *mcircRasGEF1B* was measured by qRT-PCR. (D) The expression level of *ICAM-1* in RNA-seq data (top); and qRT-PCR (bottom) was measured relative to *L32*. Error bars represent the variation range of triplicate experiments. (*, $p < 0.05$; **, $p < 0.01$). (FPKM: Fragments Per Kilobase of transcripts per Million mapped reads)

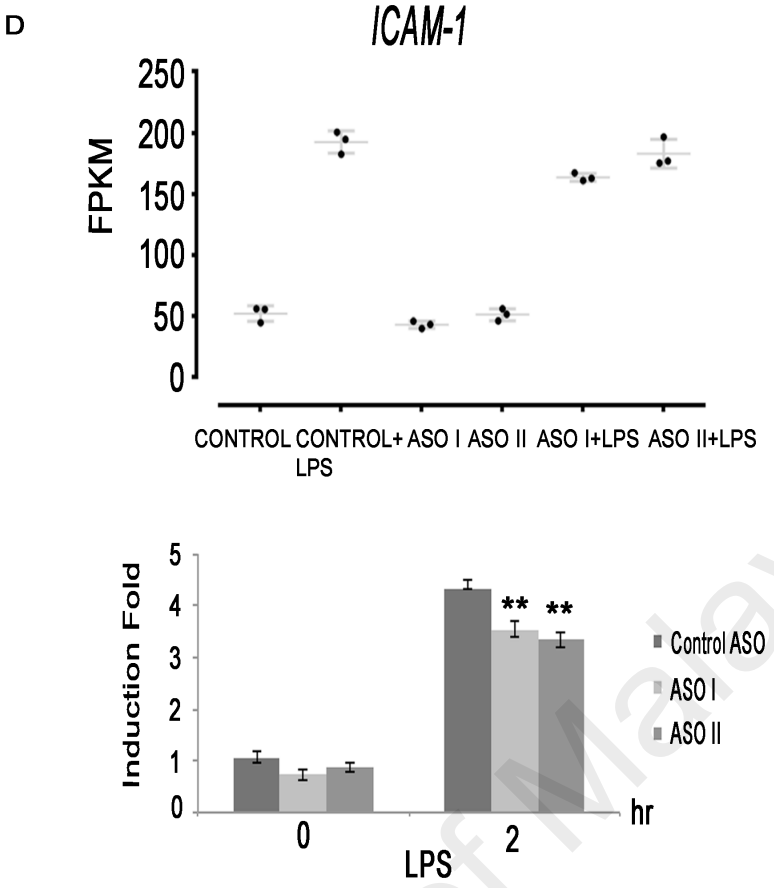

Figure 4.11, continued

4.12 Genome-wide expression changes upon *mcircRasGEF1B* depletion

To directly examine the role of *mcircRasGEF1B* in the cellular response to TLR4/LPS pathway activation, differentially expressed genes between ASO I-treated, ASO II-treated, and control cells upon LPS stimulation where compared. A total of 558 upregulated and 409 downregulated genes after LPS stimulation in ASO I-treated cells relative to control cells were observed (Figure 4.12A and C). The transcriptome profiles of ASO II-treated cells were considerably more different, with 1,916 upregulated and 1,870 downregulated genes (Figure 4.12B and C), again consistent with the higher efficiency of ASO II-mediated *mcircRasGEF1B* knockdown. Furthermore, the LPS-responsive genes between ASO I- and ASO-II-treated cells were compared, and it showed that 166 upregulated and 262 downregulated genes were common to both conditions (Figure 4.12D). These results show that perturbation of *mcircRasGEF1B* affects the transcriptional or post-transcriptional regulation of hundreds to thousands of genes in response to LPS stimulation.

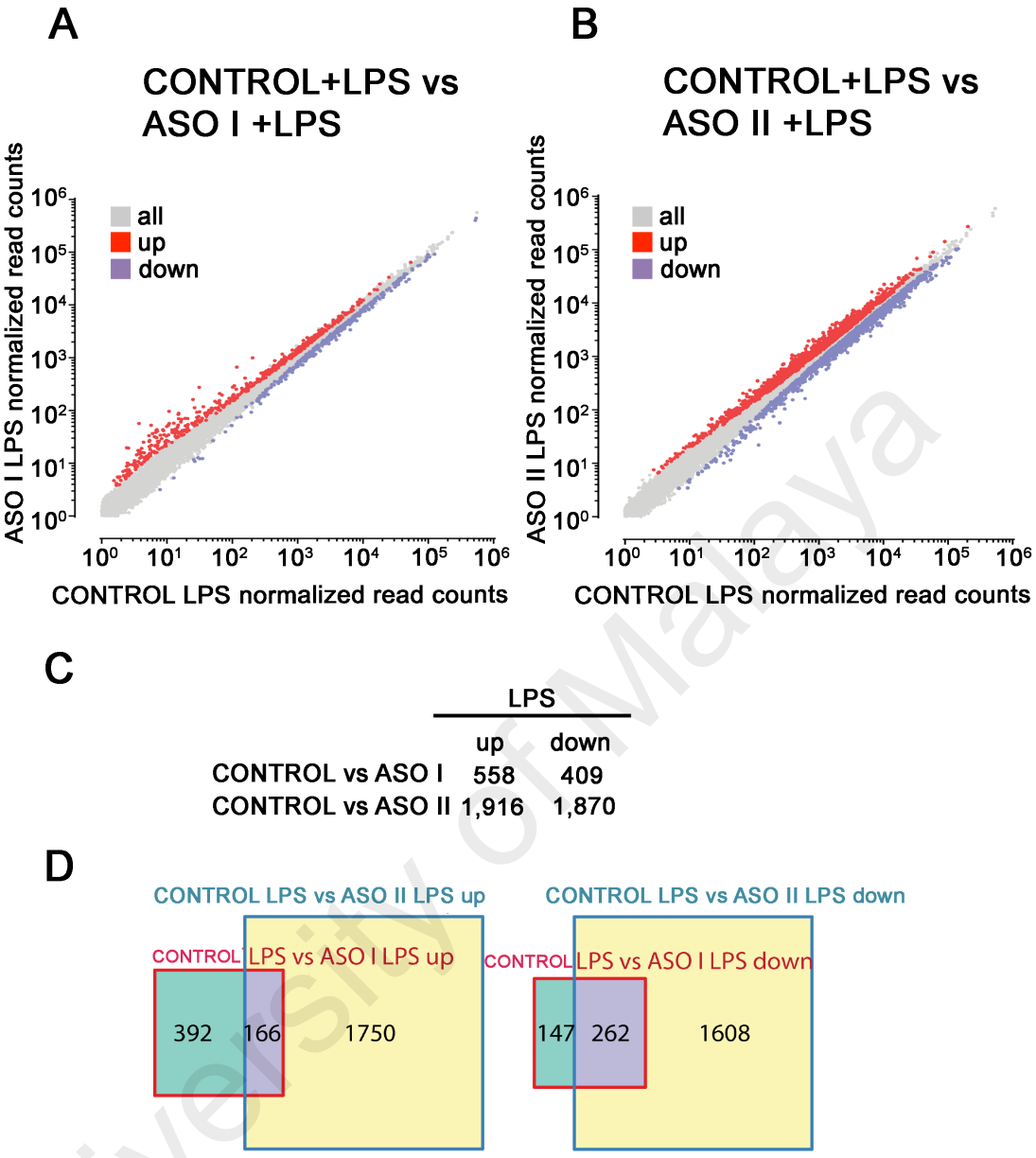

Figure 4.12: Gene expression changes upon *mcircRasGEF1B* depletion**.** (A and B) Scatter plots show gene expression changes in (A) LPS-stimulated ASO I-treated cells; (B) LPS-stimulated ASO II-treated cells; relative to LPS-stimulated control cells. (C) Number of differentially expressed genes in ASO I- and ASO II-treated, and LPS-stimulated cells; (D) Overlap between differentially expressed genes in ASO I- and ASO II- treated LPS-stimulated cells.

4.13 Genes affected by *mcircRasGEF1B* depletion are enriched for functional categories related to LPS response

The gene expression analysis revealed that perturbation of *mcircRasGEF1B* affected hundreds of genes after LPS stimulation. Next, in order to understand the biological roles of the genes misregulated upon *mcircRasGEF1B* depletion, significantly enriched ($p \leq 0.05$ after correcting for multiple hypothesis testing) gene ontology (GO) functional categories of genes in the sets of genes up- and downregulated relative to control in LPS-stimulated ASO-treated cells were identified (Figure 4.13). To do this, the genes up- and downregulated in the ASO II background were focused due to the higher magnitude of the effect of ASO II on the macrophage transcriptome profile (Figure 4.11C). The GO analysis revealed that genes upregulated in *mcircRasGEF1B* knockdown cells are enriched for categories involved in metabolic activity, autophagy, DNA replication and mitotic division, and immune response, specifically the regulation of IκB/NFκB signaling and the LPS response pathway. A number of coherent functional categories were revealed in the set of downregulated genes. This specifically included genes involved in chromatin remodeling, RNA splicing, cell adhesion, as well as mitochondrial respiratory function and macrophage activation. A more detailed examination of the lists of downregulated genes corroborated these global observations. For example, among the top downregulated genes was *IFNB1*, a member of the type I interferons, which play key roles in the defense against viral infections and in the innate immune responses to pathogens; production of *IFNB1* is dependent on the LPS-induced TRIF-dependent pathway (Toshchakov et al., 2002). The LPS-mediated activation of RAW264.7 cells is known to be associated with the regulation of cell cycle progression (Zhuang & Wogan, 1997), and the NF-κB and TLR4/LPS signaling pathways are the mechanism through which LPS response is mediated, thus the observations of global misregulation of genes

involved in these pathways underscore the functional importance of *mcircRasGEF1B* during LPS response in TLR4 pathway.

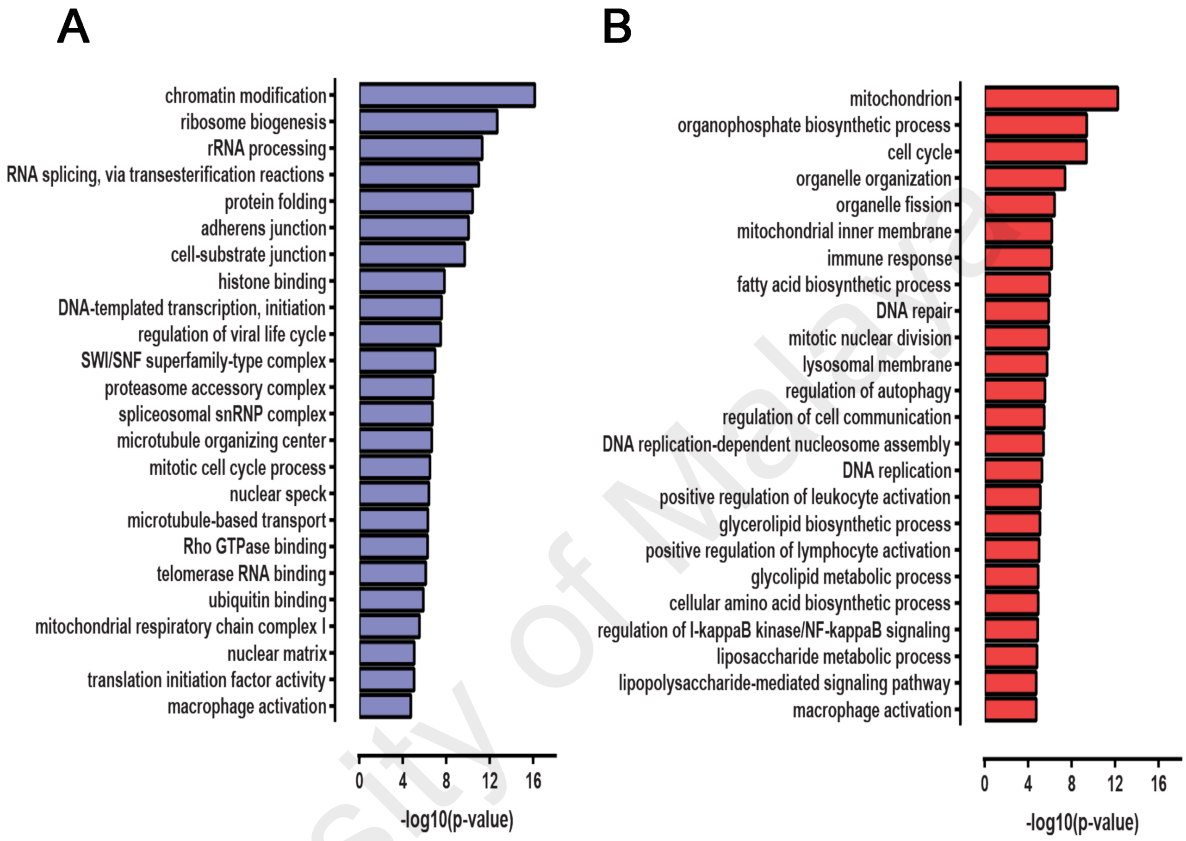

Figure 4.13: Functional categories enriched among differentially expressed LPS-induced genes in ASO II-treated cells relative to control cells. Representative enriched functional categories are shown for (A) downregulated genes; (B) upregulated genes, with the x-axis indicating the statistical significance of the observed enrichment.

CHAPTER 5: DISCUSSION

This study reported a novel LPS-inducible cytoplasmic circular RNA, *mcircRasGEF1B* that modulates the expression of *ICAM-1* in response to LPS stimulation. Several agonists, TRL1/2, TLR3, TLR4, and TLR9, induce the expression of *mcircRasGEF1B* in RAW264.7 cells but not in MEF cells. These treatments induce transcription of *RasGEF1B* gene, which results in both *mlinRasGEF1B*, and *mcircRasGEF1B* expression. Biogenesis study also shows that circRNA are generated co-transcriptionally and circRNAs can function by competing with linear splicing (Ashwal-Fluss et al., 2014). This study also shows the evolutionary conservation of *circRasGEF1B* exons between human and mouse. Furthermore, human and mouse *circRasGEF1B* exhibits similar LPS-induced response properties. Silencing the expression of *mcircRasGEF1B* moderately reduces the mRNA expression and protein levels of *ICAM-1* upon challenging the cells with LPS. Interestingly, *mcircRasGEF1B* is required for maintaining the stability of the mature mRNA of *ICAM-1* in LPS-activated cells. On a broader scale, transcriptomic analysis underscores the importance of *mcircRasGEF1B* in modulating hundreds of gene expression after LPS induction. Taken together, this study highlights a new function of circRNA in TLR4/LPS pathway, which further expands the inventory of non-coding RNAs' role in modulating immune response to protect cells against microbial infections.

The unlikelihood of *mcircRasGEF1B* as miRNA sponges

The discoveries of circRNAs as miRNA sponges provide the first line of consideration in deciphering circRNAs function. In particular, the description of *CDR1-as* and its 63 conserved sites for miR-7 exerts a significant function in mammalian cells (Memczak et al., 2013). Likewise, in this study, it is tempting to speculate that *mcircRasGEF1B* could sequester miRNAs targeting *ICAM-1*. The expression of *ICAM-*

1 was shown to be regulated by several miRNAs, including miR-223 (Tabet et al., 2014), miR-141 (Liu et al., 2015), and miR-296-3p (Liu et al., 2013). However, sequence analysis of *mcircRasGEF1B* does not reveal any enrichment of multiple (≥ 3) binding sites for any known miRNAs within *mcircRasGEF1B*, and more importantly, it harbors no binding sites for miR-223, miR-141 and miR-296-3p (data not shown). Moreover, these observations are consistent with previous reports by Guo et al. and Conn et al. analysis showing that the majority of circRNAs do not act as miRNA sponges (Conn et al., 2015; Guo et al., 2014).

No evidence of *mcircRasGEF1B* translation

After the exclusion of *mcircRasGEF1B* as miRNA sponge, the focus shifts to understand whether majority of the cytosolic circRNAs originates from protein-coding DNA sequences could be bound by ribosomes and translated into polypeptides. Early reports demonstrated *in vitro* translation (Chen & Sarnow, 1995) and protein-coding abilities of artificial circRNA constructs (Abe et al., 2015; Wang & Wang, 2015). However, unlike linear mRNAs, endogenous circRNAs are devoid of 5' cap and 3' poly-A tail, the key structures required for cap-dependent translational initiation. Alternatively, cap-independent translation has been reported for many mRNAs with sequences that could act as internal ribosome entry site (IRES) (Gilbert, 2010). In fact, evidence from *circ-ZNF609* shows that a AUG-containing exon, and an in frame stop codon upon circularization is bound by heavy polysomes. The protein-coding *circ-ZNF609* utilizes cap-independent machinery for protein translation (Legnini et al., 2017). Though *mcircRasGEF1B* shares the same AUG-containing exon 2 as in *mlinRasGEF1B*, there is no in frame stop codon identified after circularization of the exons. Furthermore, sucrose gradient ultracentrifugation showed that *mcircRasGEF1B* is present in free mRNA (light polysome) fractions instead of heavy polysome fractions. Thus, it is unlikely that *mcircRasGEF1B* is being translated.

Relative abundance of *mcircRasGEF1B* in modulating *ICAM-1*

Based on the calculation, it was estimated that for every 2580 molecules of *ICAM-1*, there is 1 molecule of *mcircRasGEF1B*. To possess physiological effects at such a low abundant level, *mcircRasGEF1B* would need to either participate in catalytic process or interact specifically with the target molecules. First, only a small number of mRNA molecules are needed to participate in the catalytic process of translation, resulting in many productions of protein molecules from each mRNA. However, unlike mRNA, *mcircRasGEF1B* is not translated, therefore it rules out this potential effect. Second, some low abundance lncRNA are proposed to interact with target molecules and modulate the output of a single gene (Ulitsky & Bartel, 2013). This underscores the importance of low abundance non-coding RNAs in cellular functions of which circRNAs could potentially behave the same way. It has also been noted that, for the *cis* effect, the abundance of individual circRNAs do not need to be high to exert an effect. For example, low abundance of ElciRNAs is shown to regulate the transcription of more abundance parental genes (Li et al., 2015c). Similarly, despite the low *mcircRasGEF1B*: *ICAM-1* ratio, the cell-type specific and dynamic expression of *mcircRasGEF1B* in macrophages suggest that this small population of *mcircRasGEF1B* might exert its function through direct- or indirect binding to *ICAM-1* mRNAs in cytoplasm.

The role of *mcircRasGEF1B* as a post-transcriptional regulator of *ICAM-1*

The biochemical fractionation analysis of cellular RNAs indicates that *mcircRasGEF1B* is predominantly found in the cytoplasm. This result prompted the possibility that *mcircRasGEF1B* might regulate the upstream signaling cascade of TLR4 pathway. However, activation of NF-κB and IRF3 is normal in *mcircRasGEF1B*-deficient cells upon LPS stimulation. Furthermore, measurements of *ICAM-1* pre- and mature mRNA levels in control and ASO-transfected cells show that LPS-induced transcription of *ICAM-1* pre-mRNA is not affected by *mcircRasGEF1B*. Taken together these results suggest that *mcircRasGEF1B* regulates *ICAM-1* at the post-transcriptional level.

The LPS-induced expression of the mature *ICAM-1* mRNA is reduced in *mcircRasGEF1B*-deficient cells. A reduction of a mature mRNA could be due to less efficient mRNA splicing or a decrease in mRNA stability. The latter possibility was favored for the following reasons. First, mRNA splicing takes place in the nucleus while mRNA degradation occurs both in the cytoplasm and the nucleus. However, *mcircRasGEF1B* is enriched in the cytoplasm. Nonetheless, there is also a possibility that the presence of a small amount of *mcircRasGEF1B* may affect mRNA splicing in the nucleus. Second, if splicing of *ICAM-1* is blocked in *mcircRasGEF1B*-deficient cells, *ICAM-1* pre-mRNA should accumulate over time, which is not the case. Third, treating cells with ActD blocks RNA synthesis but not pre-mRNA splicing. The turnover rate of *ICAM-1* pre-mRNA is comparable between control and *mcircRasGEF1B*–depleted cells when treated with ActD, suggesting that mRNA splicing is unaffected. Finally, a reproducible reduction of the stability of mature mRNA of *ICAM-1* in *mcircRasGEF1B*-deficient cells was observed in this experiment. Thus, this study suggests that *mcircRasGEF1B* positively regulates the expression of *ICAM-1* through modulating the stability of mature mRNA of *ICAM-1*. Given that

mcircRasGEF1B is unlikely to function as a classic miRNA sponge, *mcircRasGEF1B* might exert its effects on *ICAM-1* expression through a novel, previously unreported mechanism, which serves as an exciting subject for future study in non-coding RNA functions.

Significance of *ICAM-1* in diseases

ICAM-1 is an important adhesion molecule that has been studied extensively especially on endothelial cells due to its role in leukocyte recruitment to inflamed sites. In antigen presenting cells including macrophages, *ICAM-1* participates in cell-cell interactions during antigen presentation while in other cell types *ICAM-1* functions in microbial pathogenesis and as a signal transduction molecule (Hubbard & Rothlein, 2000; Staunton et al., 1989). Physiologically, *ICAM-1* is expressed at a low basal level (Mukhopadhyay et al., 2014). However, during inflammatory and immune responses, *ICAM-1* level increases substantially and aberrantly at sites of inflammation contributing to a number of inflammation-related diseases and injuries such as endotoxin-induced airway disease (Kumasaka et al., 1996; Moreland et al., 2002), and asthma, (Mukhopadhyay et al., 2014; Wegner et al., 1990) arthritis, (Seidel et al., 1997), ulcerative colitis (Vainer, 2010), and chronic cholangiopathies (Andrade et al., 2010). In cancer, *ICAM-1* has been mainly implicated in local inflammatory tumor microenvironment, (Liou et al., 2015) tumor progression, and metastasis (Hayes & Seigel, 2009). The molecular mechanisms underlying the transcriptional regulation of *ICAM-1* gene has an important implication in term of inflammatory-related diseases.

Of importance, *mcircRasGEF1B*-mediated regulation of ICAM-1 indicates that *circRasGEF1B* may have functions in innate immune response such as inflammatory-related diseases, autoimmunity and cancer. For example, depletion of *mcircRasGEF1B* in tumor-associated macrophage (TAM) may cause these cells to adopt the pro-

metastasis M2 phenotype as ICAM-1 expression has been reported to suppress the M2 macrophage polarization in a tumor microenvironment (Yang et al., 2015). Although macrophage is used as a model system here, it is tempting to speculate that *mcircRasGEF1B* may also regulate ICAM-1 level in other cell types. In particular, ICAM-1 plays a major role in the recruitment of neutrophils and lymphocytes in many tissues via leukocyte-endothelial cell bridging, thus *mcircRasGEF1B* deficiency may prevent migration of leukocyte cells to inflammatory sites (Basit et al., 2006; Long, 2011). In addition, down-regulation of *mcircRasGEF1B* in cancer cells may also affect the cytotoxic T-lymphocytes (CTL)-mediated cytotoxicity due to engagement of LFA-1 on CTL by ICAM-1 on target cells is essential for T-cell activation and for directing the released of cytolytic granules into the tumor cells (Hamai et al., 2008).

Transcriptome-wide expression changes modulated by *mcircRasGEF1B*

In this study, a broad spectrum of genes involved in the cellular response to LPS activation whose proper expression dynamics is dependent on the LPS-inducible cytoplasmic circular RNA *mcircRasGEF1B,* were identified. The knockdown of *mcircRasGEF1B* and the effects of its depletion on the transcriptome in resting and LPS-stimulated cells were studied. The specificity of LPS transcription response was examined by assessing the control cells with and without LPS stimulation (mock) and confirmed by most immune-related genes such as *IL23α*, *CXCL10*, *CCL5*, *IL6*, *IL1B* and *IFNB1* by qRT-PCR (APPENDIX D).

Among the top 50 up-regulated genes upon knockdown of mcircRasGEF1B in RAW 264.7 cells (APPENDIX E), some of them have been implicated in LPS, NF-κB signaling, and immune responses. For example, TIFAB is a TRAF6 inhibitor that controls the dynamic of TLR pathway activation, notably LPS-, but not TNF-induced TRAF6 dependent NF-κB activation (Varney et al., 2015). It is mainly expressed in the

B cells rather than T cells in the spleen and microinjection of TIFAB in NIH3T3 cells inhibits the entry of the cells into the S phase of cell cycle (Matsumura et al., 2009). Additionally, CD97 inhibits LPS-induced NF-κB pathway through up-regulation of PPART-γ in human primary macrophage (Wang et al., 2016b) while ASB2α regulates the cell motility in immature dendritic cells (Lamsoul et al., 2013). Several genes in the metabolism process were also up-regulated. For example, GCHFR regulates the metabolism of tetrahydrobiopterin, an essential co-factor in nitric oxide synthase(Gesierich et al., 2003; Nandi et al., 2008). Furthermore, ER located DAD1 is a subunit of oligosaccharyltransferase and is required for N-linked glycosylation (Kelleher & Gilmore, 1997; Makishima et al., 1997). Besides, ADC is essential in polyamine biosynthesis and seed development in Arabidopsis (Hanfrey et al., 2001; Urano et al., 2005).

Among the top 50 down-regulated genes upon knockdown of mcircRasGEF1B in RAW 264.7 cells (APPENDIX F) in the context of macrophage activation, loss of MYBPC3 triggers proinflammatory responses in dilated cardiomyopathy and increases M1 macrophages activation in mice (Lynch et al., 2017). In fine-tuning immune responses and cell cycle process, NEK10 mediates G2/M cell cycle arrest and auto-activates MEK after UV irradiation to restore cellular homeostasis (Moniz & Stambolic, 2011). Similarly, upon LPS treatment, CRIP1 alters cytokine IL-2, IL-10 and IL-6 production (Lanningham-Foster et al., 2002). In addition, it has been shown that CXCR2+ neutrophils are recruited by TNFα-activated mesenchymal stromal cells to promote breast cancer metastasis (Yu et al., 2017). From the metabolism perspective, DOC2A is involved in insulin secretion and glucose uptake(Li et al., 2014a). GPD1 is reported to regulate amino acid metabolism during fasting in mice (Sato et al., 2016). Moreover, GPD1 also take part in lipid oxidation in the skeletal muscle during exercise (Sato et al., 2015). Besides, CAR14 is shown to play key roles in intracellular pH

regulation in hippocampal neurons in buffering activity (Svichar et al., 2009).

Overall, transcriptomic analysis showed that the depletion of *mcircRasGEF1B* leads to the misregulation of a plethora of genes involved in macrophage activation , LPS response signaling, cell cycle progression, cell adhesion and metabolic activity. Thus, normal level of *mcircRasGEF1B* is important for the proper progression of macrophage activation and LPS signaling. Further experiments should reveal in detail the precise mechanisms through which *mcircRasGEF1B* exerts its function.

CHAPTER 6: CONCLUSION

CircRNAs is a unique non-coding RNA with prospective biological functions. In this study, thousands of circRNAs have been extracted from published RNA-seq data. Interestingly, one of the circRNAs, *mcircRasGEF1B,* was shown to be induced by LPS, which marks an exciting feature for further study. The general properties of circRNAs: back-splice junction, RNase R resistant, evolutionary conserved, cytoplasmic, and untranslated, were fulfilled by *mcircRasGEF1B*. The highlight is that knockdown of *mcircRasGEF1B* reduces *ICAM-1* transcript and protein levels, through regulating mature *ICAM-1* mRNA stability. Overall, this study demonstrates two key findings. First, *mcircRasGEF1B* functions as a positive post-transcriptional regulator of *ICAM-1* in the TLR4/LPS pathway. Second, functional significance of *mcircRasGEF1B* underscores its important role in immune responses regulation. However, the detail molecular mechanism of the interaction between *mcircRasGEF1B* and mature *ICAM-1* mRNA remains unclear. In addition, the precise mechanism of how *mcircRasGEF1B* exerts its effect requires further validation experiments.

Future research direction should focus on the interaction of *mcircRasGEF1B* and *ICAM-1* mRNA. The low abundance of *mcircRasGEF1B* could potentially bind to *ICAM-1* mRNA for a direct RNA stabilization. Biochemical approach can be employed to answer this question. For example, RNA-immunoprecipitation (RIP) assay with biotinylated control and *mcircRasGEF1B*-specific ASO, which are complement to the back-splice junction of exon 4 and 2. Both ASOs could be used to pull down the *mcircRasGEF1B*. Enrichment of *mcircRasGEF1B* and relative abundance of *ICAM-1* mRNA levels can be measured by qRT-PCR. Additional focus should pinpoint the precise mechanism of *mcircRasGEF1B*'s function. This includes validation of the differentially expressed genes related to LPS, and macrophage activation to discover other key genes involved in the pathway. Last but not least, further efforts can also be

focused to elucidate the functions of *circRasGEF1B* using human macrophages in responses to different external stimuli.

REFERENCES

Abe, N., Matsumoto, K., Nishihara, M., Nakano, Y., Shibata, A., Maruyama, H., . . . Abe, H. (2015). Rolling circle translation of circular RNA in living human cells. *Scientific Reports, 5*, 16435.

Akira, S., & Takeda, K. (2004). Toll-like receptor signalling. *Nature Reviews: Immunology, 4*(7), 499-511.

Akira, S., Uematsu, S., & Takeuchi, O. (2006). Pathogen recognition and innate immunity. *Cell, 124*(4), 783-801.

Alkalay, I., Yaron, A., Hatzubai, A., Orian, A., Ciechanover, A., & Ben-Neriah, Y. (1995). Stimulation-dependent I kappa B alpha phosphorylation marks the NF-kappa B inhibitor for degradation via the ubiquitin-proteasome pathway. *Proceedings of the National Academy of Sciences of the United States of America, 92*(23), 10599-10603.

Anders, S., Pyl, P. T., & Huber, W. (2015). HTSeq--a Python framework to work with high-throughput sequencing data. *Bioinformatics, 31*(2), 166-169.

Anderson, K. V., Jurgens, G., & Nusslein-Volhard, C. (1985). Establishment of dorsal-ventral polarity in the Drosophila embryo: genetic studies on the role of the Toll gene product. *Cell, 42*(3), 779-789.

Andrade, W. A., Silva, A. M., Alves, V. S., Salgado, A. P., Melo, M. B., Andrade, H. M., . . . Gazzinelli, R. T. (2010). Early endosome localization and activity of RasGEF1b, a toll-like receptor-inducible Ras guanine-nucleotide exchange factor. *Genes & Immunity, 11*(6), 447-457.

Arnberg, A. C., Vanommen, G. J. B., Grivell, L. A., Vanbruggen, E. F. J., & Borst, P. (1980). Some yeast mitochondrial Rnas are circular. *Cell, 19*(2), 313-319.

Ashwal-Fluss, R., Meyer, M., Pamudurti, N. R., Ivanov, A., Bartok, O., Hanan, M., . . . Kadener, S. (2014). circRNA biogenesis competes with pre-mRNA splicing. *Molecular Cell, 56*(1), 55-66.

Bahn, J. H., Zhang, Q., Li, F., Chan, T. M., Lin, X., Kim, Y., . . . Xiao, X. (2015). The landscape of microRNA, Piwi-interacting RNA, and circular RNA in human saliva. *Clinical Chemistry, 61*(1), 221-230.

Barrett, S. P., Wang, P. L., & Salzman, J. (2015). Circular RNA biogenesis can proceed through an exon-containing lariat precursor. *Elife, 4*, e07540.

Basit, A., Reutershan, J., Morris, M. A., Solga, M., Rose, C. E., & Ley, K. (2006). ICAM-1 and LFA-1 play critical roles in LPS-induced neutrophil recruitment into the alveolar space. *American Journal of Physiology-Lung Cellular and Molecular Physiology, 291*(2), L200-L207.

Berriz, G. F., Beaver, J. E., Cenik, C., Tasan, M., & Roth, F. P. (2009). Next generation software for functional trend analysis. *Bioinformatics, 25*(22), 3043-3044.

Beutler, B. (2000). Tlr4: central component of the sole mammalian LPS sensor. *Current Opinion in Immunology, 12*(1), 20-26.

Bhatt, D. M., Pandya-Jones, A., Tong, A. J., Barozzi, I., Lissner, M. M., Natoli, G., . . . Smale, S. T. (2012). Transcript dynamics of proinflammatory genes revealed by sequence analysis of subcellular RNA fractions. *Cell, 150*(2), 279-290.

Boesler, C., Kruse, J., Soderbom, F., & Hammann, C. (2011). Sequence and generation of mature ribosomal RNA transcripts in *Dictyostelium discoideum*. *Journal of Biological Chemistry, 286*(20), 17693-17703.

Broadbent, K. M., Broadbent, J. C., Ribacke, U., Wirth, D., Rinn, J. L., & Sabeti, P. C. (2015). Strand-specific RNA sequencing in Plasmodium falciparum malaria identifies developmentally regulated long non-coding RNA and circular RNA. *BMC Genomics, 16*, 454.

Brown, K., Gerstberger, S., Carlson, L., Franzoso, G., & Siebenlist, U. (1995). Control of I kappa B-alpha proteolysis by site-specific, signal-induced phosphorylation. *Science, 267*(5203), 1485-1488.

Burd, C. E., Jeck, W. R., Liu, Y., Sanoff, H. K., Wang, Z., & Sharpless, N. E. (2010). Expression of linear and novel circular forms of an INK4/ARF-associated non-coding RNA correlates with atherosclerosis risk. *PLOS Genetics, 6*(12), e1001233.

Capel, B., Swain, A., Nicolis, S., Hacker, A., Walter, M., Koopman, P., . . . Lovell-Badge, R. (1993). Circular transcripts of the testis-determining gene Sry in adult mouse testis. *Cell, 73*(5), 1019-1030.

Chao, C. W., Chan, D. C., Kuo, A., & Leder, P. (1998). The mouse formin (Fmn) gene: abundant circular RNA transcripts and gene-targeted deletion analysis. *Molecular Medicine, 4*(9), 614-628.

Chen, C. Y., & Sarnow, P. (1995). Initiation of protein synthesis by the eukaryotic translational apparatus on circular RNAs. *Science, 268*(5209), 415-417.

Chen, Z., Hagler, J., Palombella, V. J., Melandri, F., Scherer, D., Ballard, D., & Maniatis, T. (1995). Signal-induced site-specific phosphorylation targets I kappa B alpha to the ubiquitin-proteasome pathway. *Genes & Development, 9*(13), 1586-1597.

Chen, Z. J., Parent, L., & Maniatis, T. (1996). Site-specific phosphorylation of I kappa B alpha by a novel ubiquitination-dependent protein kinase activity. *Cell, 84*(6), 853-862.

Chu, Q., Zhang, X., Zhu, X., Liu, C., Mao, L., Ye, C., . . . Fan, L. (2017). PlantcircBase: A database for Plant circular RNAs. *Molecular Plant, 10*(8), 1126-1128.

Cocquerelle, C., Daubersies, P., Majerus, M. A., Kerckaert, J. P., & Bailleul, B. (1992). Splicing with inverted order of exons occurs proximal to large introns. *EMBO Journal, 11*(3), 1095-1098.

Cocquerelle, C., Mascrez, B., Hetuin, D., & Bailleul, B. (1993). Mis-splicing yields circular RNA molecules. *FASEB Journal, 7*(1), 155-160.

Conn, S. J., Pillman, K. A., Toubia, J., Conn, V. M., Salmanidis, M., Phillips, C. A., . . . Goodall, G. J. (2015). The RNA binding protein quaking regulates formation of circRNAs. *Cell, 160*(6), 1125-1134.

Danan, M., Schwartz, S., Edelheit, S., & Sorek, R. (2012). Transcriptome-wide discovery of circular RNAs in Archaea. *Nucleic Acids Research, 40*(7), 3131-3142.

Dang, Y., Yan, L., Hu, B., Fan, X., Ren, Y., Li, R., . . . Qiao, J. (2016). Tracing the expression of circular RNAs in human pre-implantation embryos. *Genome Biology, 17*(1), 130.

DiDonato, J., Mercurio, F., Rosette, C., Wu-Li, J., Suyang, H., Ghosh, S., & Karin, M. (1996). Mapping of the inducible I kappa B phosphorylation sites that signal its ubiquitination and degradation. *Molecular and Cellular Biology, 16*(4), 1295-1304.

Du, W. W., Yang, W., Chen, Y., Wu, Z. K., Foster, F. S., Yang, Z., . . . Yang, B. B. (2016). Foxo3 circular RNA promotes cardiac senescence by modulating multiple factors associated with stress and senescence responses. *European Heart Journal, 38*(18), 1402-1412.

Dubin, R. A., Kazmi, M. A., & Ostrer, H. (1995). Inverted repeats are necessary for circularization of the mouse testis Sry transcript. *Gene, 167*(1-2), 245-248.

Dudekula, D. B., Panda, A. C., Grammatikakis, I., De, S., Abdelmohsen, K., & Gorospe, M. (2016). CircInteractome: A web tool for exploring circular RNAs and their interacting proteins and microRNAs. *RNA Biology, 13*(1), 34-42.

Fan, X., Zhang, X., Wu, X., Guo, H., Hu, Y., Tang, F., & Huang, Y. (2015). Single-cell RNA-seq transcriptome analysis of linear and circular RNAs in mouse preimplantation embryos. *Genome Biology, 16*, 148.

Gesierich, A., Niroomand, F., & Tiefenbacher, C. P. (2003). Role of human GTP cyclohydrolase I and its regulatory protein in tetrahydrobiopterin metabolism. *Basic Research in Cardiology, 98*(2), 69-75.

Ghosal, S., Das, S., Sen, R., Basak, P., & Chakrabarti, J. (2013). Circ2Traits: a comprehensive database for circular RNA potentially associated with disease and traits. *Frontiers in Genetics, 4*, 283.

Ghosh, S., May, M. J., & Kopp, E. B. (1998). NF-kappa B and Rel proteins: evolutionarily conserved mediators of immune responses. *Annual Review of Immunology, 16*, 225-260.

Gilbert, W. V. (2010). Alternative ways to think about cellular internal ribosome entry. *Journal of Biological Chemistry, 285*(38), 29033-29038.

Gilmore, T. D. (2006). Introduction to NF-kappa B: players, pathways, perspectives. *Oncogene, 25*(51), 6680-6684.

Glazar, P., Papavasileiou, P., & Rajewsky, N. (2014). circBase: a database for circular RNAs. *RNA, 20*(11), 1666-1670.

Gomes, A. Q., Nolasco, S., & Soares, H. (2013). Non-Coding RNAs: Multi-Tasking Molecules in the Cell. *International Journal of Molecular Sciences, 14*(8), 16010-16039.

Gualandi, F., Trabanelli, C., Rimessi, P., Calzolari, E., Toffolatti, L., Patarnello, T., . . . Ferlini, A. (2003). Multiple exon skipping and RNA circularisation contribute to the severe phenotypic expression of exon 5 dystrophin deletion. *Journal of Medical Genetics, 40*(8), e100.

Guo, J. U., Agarwal, V., Guo, H., & Bartel, D. P. (2014). Expanded identification and characterization of mammalian circular RNAs. *Genome Biology, 15*(7), 409.

Hacker, H., Redecke, V., Blagoev, B., Kratchmarova, I., Hsu, L. C., Wang, G. G., . . . Karin, M. (2006). Specificity in Toll-like receptor signalling through distinct effector functions of TRAF3 and TRAF6. *Nature, 439*(7073), 204-207.

Hamai, A., Meslin, F., Benlalam, H., Jalil, A., Mehrpour, M., Faure, F., . . . Chouaib, S. (2008). ICAM-1 has a critical role in the regulation of metastatic melanoma tumor susceptibility to CTL lysis by interfering with PI3K/AKT pathway. *Cancer Research, 68*(23), 9854-9864.

Hanfrey, C., Sommer, S., Mayer, M. J., Burtin, D., & Michael, A. J. (2001). Arabidopsis polyamine biosynthesis: absence of ornithine decarboxylase and the mechanism of arginine decarboxylase activity. *Plant Journal, 27*(6), 551-560.

Hansen, T. B., Jensen, T. I., Clausen, B. H., Bramsen, J. B., Finsen, B., Damgaard, C. K., & Kjems, J. (2013). Natural RNA circles function as efficient microRNA sponges. *Nature, 495*(7441), 384-388.

Hayden, M. S., & Ghosh, S. (2004). Signaling to NF-kappa B. *Genes & Development, 18*(18), 2195-2224.

Hayes, S. H., & Seigel, G. M. (2009). Immunoreactivity of ICAM-1 in human tumors, metastases and normal tissues. *International Journal of Clinical and Experimental Pathology, 2*(6), 553-560.

Hemmi, H., Kaisho, T., Takeuchi, O., Sato, S., Sanjo, H., Hoshino, K., . . . Akira, S. (2002). Small anti-viral compounds activate immune cells via the TLR7 MyD88-dependent signaling pathway. *Nature Immunology, 3*(2), 196-200.

Hewlett, M. J., Pettersson, R. F., & Baltimore, D. (1977). Circular forms of Uukuniemi virion RNA: an electron microscopic study. *Journal of Virology, 21*(3), 1085-1093.

Hsu, M. T., & Coca-Prados, M. (1979). Electron microscopic evidence for the circular form of RNA in the cytoplasm of eukaryotic cells. *Nature, 280*(5720), 339-340.

Hsu, M. T., Kung, H. J., & Davidson, N. (1974). An electron microscope study of Sindbis virus RNA. *Cold Spring Harbor Symposia on Quantitative Biology, 38*, 943-950.

Hubbard, A. K., & Rothlein, R. (2000). Intercellular adhesion molecule-1 (ICAM-1) expression and cell signaling cascades. *Free Radical Biology and Medicine, 28*(9), 1379-1386.

Ivanov, A., Memczak, S., Wyler, E., Torti, F., Porath, H. T., Orejuela, M. R., . . . Rajewsky, N. (2015). Analysis of intron sequences reveals hallmarks of circular RNA biogenesis in animals. *Cell Reports, 10*(2), 170-177.

Iwasaki, Y. W., Siomi, M. C., & Siomi, H. (2015). PIWI-Interacting RNA: Its Biogenesis and Functions. *Annual Review of Biochemistry, 84*, 405-433.

Jeck, W. R., & Sharpless, N. E. (2014). Detecting and characterizing circular RNAs. *Nature Biotechnology, 32*(5), 453-461.

Jeck, W. R., Sorrentino, J. A., Wang, K., Slevin, M. K., Burd, C. E., Liu, J., . . . Sharpless, N. E. (2013). Circular RNAs are abundant, conserved, and associated with ALU repeats. *RNA, 19*(2), 141-157.

Jiang, J., & Struhl, G. (1998). Regulation of the hedgehog and wingless signalling pathways by the F-box/WD40-repeat protein Slimb. *Nature, 391*(6666), 493-496.

Jiang, Q., Wang, Y., Hao, Y., Juan, L., Teng, M., Zhang, X., . . . Liu, Y. (2009). miR2Disease: a manually curated database for microRNA deregulation in human disease. *Nucleic Acids Research, 37*(Database issue), D98-104.

Kawai, T., & Akira, S. (2007). Signaling to NF-kappa B by Toll-like receptors. *Trends in Molecular Medicine, 13*(11), 460-469.

Kelleher, D. J., & Gilmore, R. (1997). DAD1, the defender against apoptotic cell death, is a subunit of the mammalian oligosaccharyltransferase. *Proceedings of the National Academy of Sciences of the United States of America, 94*(10), 4994-4999.

Kim, D., Pertea, G., Trapnell, C., Pimentel, H., Kelley, R., & Salzberg, S. L. (2013). TopHat2: accurate alignment of transcriptomes in the presence of insertions, deletions and gene fusions. *Genome Biology, 14*(4), R36.

Kolakofsky, D. (1976). Isolation and characterization of Sendai virus DI-RNAs. *Cell, 8*(4), 547-555.

Kos, A., Dijkema, R., Arnberg, A. C., van der Meide, P. H., & Schellekens, H. (1986). The hepatitis delta (delta) virus possesses a circular RNA. *Nature, 323*(6088), 558-560.

Kramer, M. C., Liang, D., Tatomer, D. C., Gold, B., March, Z. M., Cherry, S., & Wilusz, J. E. (2015). Combinatorial control of Drosophila circular RNA expression by intronic repeats, hnRNPs, and SR proteins. *Genes & Development, 29*(20), 2168-2182.

Kumasaka, T., Quinlan, W. M., Doyle, N. A., Condon, T. P., Sligh, J., Takei, F., . . . Doerschuk, C. M. (1996). Role of the intercellular adhesion molecule-1(ICAM-1) in endotoxin-induced pneumonia evaluated using ICAM-1 antisense oligonucleotides, anti-ICAM-1 monoclonal antibodies, and ICAM-1 mutant mice. *The Journal of Clinical Investigation, 97*(10), 2362-2369.

Kung, H. J., Bailey, J. M., Davidson, N., Vogt, P. K., Nicolson, M. O., & McAllister, R. M. (1975). Electron microscope studies of tumor virus RNA. *Cold Spring Harbor Symposia on Quantitative Biology, 39 Pt 2*, 827-834.

Lam, M. T., Li, W., Rosenfeld, M. G., & Glass, C. K. (2014). Enhancer RNAs and regulated transcriptional programs. *Trends in Biochemical Sciences, 39*(4), 170-182.

Lamsoul, I., Metais, A., Gouot, E., Heuze, M. L., Lennon-Dumenil, A. M., Moog-Lutz, C., & Lutz, P. G. (2013). ASB2alpha regulates migration of immature dendritic cells. *Blood, 122*(4), 533-541.

Lander, E. S., Linton, L. M., Birren, B., Nusbaum, C., Zody, M. C., Baldwin, J., . . . International Human Genome Sequencing, C. (2001). Initial sequencing and analysis of the human genome. *Nature, 409*(6822), 860-921.

Langmead, B., Trapnell, C., Pop, M., & Salzberg, S. L. (2009). Ultrafast and memory-efficient alignment of short DNA sequences to the human genome. *Genome Biology, 10*(3), R25.

Lanningham-Foster, L., Green, C. L., Langkamp-Henken, B., Davis, B. A., Nguyen, K. T., Bender, B. S., & Cousins, R. J. (2002). Overexpression of CRIP in transgenic mice alters cytokine patterns and the immune response. *American Journal of Physiology: Endocrinology and Metabolism, 282*(6), E1197-1203.

Lasda, E., & Parker, R. (2014). Circular RNAs: diversity of form and function. *RNA, 20*(12), 1829-1842.

Legnini, I., Di Timoteo, G., Rossi, F., Morlando, M., Briganti, F., Sthandier, O., . . . Bozzoni, I. (2017). Circ-ZNF609 is a circular RNA that can be translated and functions in myogenesis. *Molecular Cell, 66*(1), 22-37 e29.

Lemaitre, B., Nicolas, E., Michaut, L., Reichhart, J. M., & Hoffmann, J. A. (1996). The dorsoventral regulatory gene cassette spatzle/Toll/cactus controls the potent antifungal response in Drosophila adults. *Cell, 86*(6), 973-983.

Li, F., Zhang, L., Li, W., Deng, J., Zheng, J., An, M., . . . Zhou, Y. (2015a). Circular RNA ITCH has inhibitory effect on ESCC by suppressing the Wnt/beta-catenin pathway. *Oncotarget, 6*(8), 6001-6013.

Li, J., Cantley, J., Burchfield, J. G., Meoli, C. C., Stockli, J., Whitworth, P. T., . . . James, D. E. (2014a). DOC2 isoforms play dual roles in insulin secretion and insulin-stimulated glucose uptake. *Diabetologia, 57*(10), 2173-2182.

Li, J. H., Liu, S., Zhou, H., Qu, L. H., & Yang, J. H. (2014b). starBase v2.0: decoding miRNA-ceRNA, miRNA-ncRNA and protein-RNA interaction networks from large-scale CLIP-Seq data. *Nucleic Acids Research, 42*(Database issue), D92-97.

Li, Y., Zheng, Q. P., Bao, C. Y., Li, S. Y., Guo, W. J., Zhao, J., . . . Huang, S. L. (2015b). Circular RNA is enriched and stable in exosomes: a promising biomarker for cancer diagnosis. *Cell Research, 25*(8), 981-984.

Li, Z., Huang, C., Bao, C., Chen, L., Lin, M., Wang, X., . . . Shan, G. (2015c). Exon-intron circular RNAs regulate transcription in the nucleus. *Nature Structural & Molecular Biology, 22*(3), 256-264.

Liang, D., & Wilusz, J. E. (2014). Short intronic repeat sequences facilitate circular RNA production. *Genes & Development, 28*(20), 2233-2247.

Liou, G. Y., Doppler, H., Necela, B., Edenfield, B., Zhang, L., Dawson, D. W., & Storz, P. (2015). Mutant KRAS-induced expression of ICAM-1 in pancreatic acinar cells causes attraction of macrophages to expedite the formation of precancerous lesions. *Cancer Discovery, 5*(1), 52-63.

Liu, J., Guan, X., & Ma, X. (2005). Interferon regulatory factor 1 is an essential and direct transcriptional activator for interferon {gamma}-induced RANTES/CCl5 expression in macrophages. *Journal of Biological Chemistry, 280*(26), 24347-24355.

Liu, R. R., Li, J., Gong, J. Y., Kuang, F., Liu, J. Y., Zhang, Y. S., . . . Chen, L. H. (2015). MicroRNA-141 regulates the expression level of ICAM-1 on endothelium to decrease myocardial ischemia-reperfusion injury. *American Journal of Physiology: Heart and Circulatory Physiology, 309*(8), H1303-1313.

Liu, X., Chen, Q., Yan, J., Wang, Y., Zhu, C., Chen, C., . . . Yu, J. (2013). MiRNA-296-3p-ICAM-1 axis promotes metastasis of prostate cancer by possible enhancing survival of natural killer cell-resistant circulating tumour cells. *Cell Death & Disease, 4*, e928.

Liu, Y. C., Li, J. R., Sun, C. H., Andrews, E., Chao, R. F., Lin, F. M., . . . Huang, H. D. (2016). CircNet: a database of circular RNAs derived from transcriptome sequencing data. *Nucleic Acids Research, 44*(D1), D209-215.

Long, E. O. (2011). ICAM-1: getting a grip on leukocyte adhesion. *Journal of Immunology, 186*(9), 5021-5023.

Love, M. I., Huber, W., & Anders, S. (2014). Moderated estimation of fold change and dispersion for RNA-seq data with DESeq2. *Genome Biology, 15*(12), 550.

Lu, T., Cui, L., Zhou, Y., Zhu, C., Fan, D., Gong, H., . . . Han, B. (2015). Transcriptome-wide investigation of circular RNAs in rice. *RNA, 21*(12), 2076-2087.

Lynch, T. L. t., Ismahil, M. A., Jegga, A. G., Zilliox, M. J., Troidl, C., Prabhu, S. D., & Sadayappan, S. (2017). Cardiac inflammation in genetic dilated cardiomyopathy caused by MYBPC3 mutation. *Journal of Molecular and Cellular Cardiology, 102*, 83-93.

Makishima, T., Nakashima, T., Nagata-Kuno, K., Fukushima, K., Iida, H., Sakaguchi, M., . . . Nishimoto, T. (1997). The highly conserved DAD1 protein involved in apoptosis is required for N-linked glycosylation. *Genes to Cells, 2*(2), 129-141.

Margottin, F., Bour, S. P., Durand, H., Selig, L., Benichou, S., Richard, V., . . . Benarous, R. (1998). A novel human WD protein, h-beta TrCP, that interacts with HIV-1 Vpu connects CD4 to the ER degradation pathway through an F-box motif. *Molecular Cell, 1*(4), 565-574.

Matsumoto, Y., Fishel, R., & Wickner, R. B. (1990). Circular single-stranded RNA replicon in Saccharomyces cerevisiae. *Proceedings of the National Academy of Sciences of the United States of America, 87*(19), 7628-7632.

Matsumura, T., Kawamura-Tsuzuku, J., Yamamoto, T., Semba, K., & Inoue, J. (2009). TRAF-interacting protein with a forkhead-associated domain B (TIFAB) is a

negative regulator of the TRAF6-induced cellular functions. *Journal of Biochemistry, 146*(3), 375-381.

Medzhitov, R., & Horng, T. (2009). Transcriptional control of the inflammatory response. *Nature Reviews: Immunology, 9*(10), 692-703.

Memczak, S., Jens, M., Elefsinioti, A., Torti, F., Krueger, J., Rybak, A., . . . Rajewsky, N. (2013). Circular RNAs are a large class of animal RNAs with regulatory potency. *Nature, 495*(7441), 333-338.

Memczak, S., Papavasileiou, P., Peters, O., & Rajewsky, N. (2015). Identification and characterization of circular RNAs as a new class of putative biomarkers in human blood. *PLOS ONE, 10*(10), e0141214.

Moniz, L. S., & Stambolic, V. (2011). Nek10 mediates G2/M cell cycle arrest and MEK autoactivation in response to UV irradiation. *Molecular and Cellular Biology, 31*(1), 30-42.

Moreland, J. G., Fuhrman, R. M., Pruessner, J. A., & Schwartz, D. A. (2002). CD11b and intercellular adhesion molecule-1 are involved in pulmonary neutrophil recruitment in lipopolysaccharide-induced airway disease. *American Journal of Respiratory Cell and Molecular Biology, 27*(4), 474-480.

Morris, K. V., & Mattick, J. S. (2014). The rise of regulatory RNA. *Nature Review: Genetics, 15*(6), 423-437.

Mukhopadhyay, S., Malik, P., Arora, S. K., & Mukherjee, T. K. (2014). Intercellular adhesion molecule-1 as a drug target in asthma and rhinitis. *Respirology, 19*(4), 508-513.

Nandi, M., Kelly, P., Vallance, P., & Leiper, J. (2008). Over-expression of GTP-cyclohydrolase 1 feedback regulatory protein attenuates LPS and cytokine-stimulated nitric oxide production. *Vascular Medicine, 13*(1), 29-36.

Nigro, J. M., Cho, K. R., Fearon, E. R., Kern, S. E., Ruppert, J. M., Oliner, J. D., . . . Vogelstein, B. (1991). Scrambled exons. *Cell, 64*(3), 607-613.

Oganesyan, G., Saha, S. K., Guo, B., He, J. Q., Shahangian, A., Zarnegar, B., . . . Cheng, G. (2006). Critical role of TRAF3 in the Toll-like receptor-dependent and -independent antiviral response. *Nature, 439*(7073), 208-211.

Peng, L., Chen, G., Zhu, Z., Shen, Z., Du, C., Zang, R., . . . Tang, W. (2017). Circular RNA ZNF609 functions as a competitive endogenous RNA to regulate AKT3 expression by sponging miR-150-5p in Hirschsprung's disease. *Oncotarget, 8*(1), 808-818.

Poltorak, A., He, X., Smirnova, I., Liu, M. Y., Van Huffel, C., Du, X., . . . Beutler, B. (1998). Defective LPS signaling in C3H/HeJ and C57BL/10ScCr mice: mutations in Tlr4 gene. *Science, 282*(5396), 2085-2088.

Qin, H., Wilson, C. A., Lee, S. J., Zhao, X., & Benveniste, E. N. (2005). LPS induces CD40 gene expression through the activation of NF-kappa B and STAT-1alpha in macrophages and microglia. *Blood, 106*(9), 3114-3122.

Qin, M., Liu, G., Huo, X., Tao, X., Sun, X., Ge, Z., . . . Qin, W. (2016). Hsa_circ_0001649: A circular RNA and potential novel biomarker for hepatocellular carcinoma. *Cancer Biomarkers, 16*(1), 161-169.

Raetz, C. R., & Whitfield, C. (2002). Lipopolysaccharide endotoxins. *Annual Review of Biochemistry, 71*, 635-700.

Rybak-Wolf, A., Stottmeister, C., Glazar, P., Jens, M., Pino, N., Giusti, S., . . . Rajewsky, N. (2015). Circular RNAs in the mammalian brain are highly abundant, conserved, and dynamically expressed. *Molecular Cell, 58*(5), 870-885.

Salzman, J., Chen, R. E., Olsen, M. N., Wang, P. L., & Brown, P. O. (2013). Cell-type specific features of circular RNA expression. *PLOS Genetics, 9*(9), e1003777.

Salzman, J., Gawad, C., Wang, P. L., Lacayo, N., & Brown, P. O. (2012). Circular RNAs are the predominant transcript isoform from hundreds of human genes in diverse cell types. *PLOS ONE, 7*(2), e30733.

Sanger, H. L., Klotz, G., Riesner, D., Gross, H. J., & Kleinschmidt, A. K. (1976). Viroids are single-stranded covalently closed circular RNA molecules existing as highly base-paired rod-like structures. *Proceedings of the National Academy of Sciences of the United States of America, 73*(11), 3852-3856.

Sato, T., Morita, A., Mori, N., & Miura, S. (2015). Glycerol 3-phosphate dehydrogenase 1 deficiency enhances exercise capacity due to increased lipid oxidation during strenuous exercise. *Biochemical and Biophysical Research Communications, 457*(4), 653-658.

Sato, T., Yoshida, Y., Morita, A., Mori, N., & Miura, S. (2016). Glycerol-3-phosphate dehydrogenase 1 deficiency induces compensatory amino acid metabolism during fasting in mice. *Metabolism: Clinical and Experimental, 65*(11), 1646-1656.

Schwanhausser, B., Busse, D., Li, N., Dittmar, G., Schuchhardt, J., Wolf, J., . . . Selbach, M. (2011). Global quantification of mammalian gene expression control. *Nature, 473*(7347), 337-342.

Seidel, M. F., Keck, R., & Vetter, H. (1997). ICAM-1/LFA-1 expression in acute osteodestructive joint lesions in collagen-induced arthritis in rats. *The Journal of Histochemistry and Cytochemistry : Official Journal of the Histochemistry Society, 45*(9), 1247-1253.

Spencer, E., Jiang, J., & Chen, Z. J. (1999). Signal-induced ubiquitination of I kappa B alpha by the F-box protein Slimb/beta-TrCP. *Genes & Development, 13*(3), 284-294.

Staunton, D. E., Merluzzi, V. J., Rothlein, R., Barton, R., Marlin, S. D., & Springer, T. A. (1989). A cell adhesion molecule, ICAM-1, is the major surface receptor for rhinoviruses. *Cell, 56*(5), 849-853.

Suzuki, H., Zuo, Y., Wang, J., Zhang, M. Q., Malhotra, A., & Mayeda, A. (2006). Characterization of RNase R-digested cellular RNA source that consists of lariat

and circular RNAs from pre-mRNA splicing. *Nucleic Acids Research, 34*(8), e63.

Svichar, N., Waheed, A., Sly, W. S., Hennings, J. C., Hubner, C. A., & Chesler, M. (2009). Carbonic anhydrases CA4 and CA14 both enhance AE3-mediated Cl--HCO3- exchange in hippocampal neurons. *Journal of Neuroscience, 29*(10), 3252-3258.

Tabak, H. F., Van der Horst, G., Smit, J., Winter, A. J., Mul, Y., & Groot Koerkamp, M. J. (1988). Discrimination between RNA circles, interlocked RNA circles and lariats using two-dimensional polyacrylamide gel electrophoresis. *Nucleic Acids Research, 16*(14A), 6597-6605.

Tabet, F., Vickers, K. C., Cuesta Torres, L. F., Wiese, C. B., Shoucri, B. M., Lambert, G., . . . Rye, K. A. (2014). HDL-transferred microRNA-223 regulates ICAM-1 expression in endothelial cells. *Nature Communications, 5*, 3292.

Takeda, K., & Akira, S. (2004). TLR signaling pathways. *Seminars in Immunology, 16*(1), 3-9.

Tang, C. M., Zhang, M., Huang, L., Hu, Z. Q., Zhu, J. N., Xiao, Z., . . . Shan, Z. X. (2017). CircRNA_000203 enhances the expression of fibrosis-associated genes by derepressing targets of miR-26b-5p, Col1a2 and CTGF, in cardiac fibroblasts. *Scientific Reports, 7*, 40342.

Tollervey, D., & Kiss, T. (1997). Function and synthesis of small nucleolar RNAs. *Current Opinion in Cell Biology, 9*(3), 337-342.

Toshchakov, V., Jones, B. W., Perera, P. Y., Thomas, K., Cody, M. J., Zhang, S., . . . Vogel, S. N. (2002). TLR4, but not TLR2, mediates IFN-beta-induced STAT1alpha/beta-dependent gene expression in macrophages. *Nature Immunology, 3*(4), 392-398.

Trapnell, C., Roberts, A., Goff, L., Pertea, G., Kim, D., Kelley, D. R., . . . Pachter, L. (2012). Differential gene and transcript expression analysis of RNA-seq experiments with TopHat and Cufflinks. *Nature Protocols, 7*(3), 562-578.

Turner, M., Galloway, A., & Vigorito, E. (2014). Noncoding RNA and its associated proteins as regulatory elements of the immune system. *Nature Immunology, 15*(6), 484-491.

Ulitsky, I., & Bartel, D. P. (2013). lincRNAs: genomics, evolution, and mechanisms. *Cell, 154*(1), 26-46.

Urano, K., Hobo, T., & Shinozaki, K. (2005). Arabidopsis ADC genes involved in polyamine biosynthesis are essential for seed development. *FEBS Letters, 579*(6), 1557-1564.

Vainer, B. (2010). Intercellular adhesion molecule-1 (ICAM-1) in ulcerative colitis: presence, visualization, and significance. *APMIS. Supplementum*(129), 1-43.

Vanderveen, R., Arnberg, A. C., Vanderhorst, G., Bonen, L., Tabak, H. F., & Grivell, L. A. (1986). Excised group-Ii introns in yeast mitochondria are lariats and can be formed by self-splicing *in vitro*. *Cell, 44*(2), 225-234.

Varney, M. E., Niederkorn, M., Konno, H., Matsumura, T., Gohda, J., Yoshida, N., . . . Starczynowski, D. T. (2015). Loss of Tifab, a del(5q) MDS gene, alters hematopoiesis through derepression of Toll-like receptor-TRAF6 signaling. *Journal of Experimental Medicine, 212*(11), 1967-1985.

Veno, M. T., Hansen, T. B., Veno, S. T., Clausen, B. H., Grebing, M., Finsen, B., . . . Kjems, J. (2015). Spatio-temporal regulation of circular RNA expression during porcine embryonic brain development. *Genome Biology, 16*, 245.

Waelchli, R., Bollbuck, B., Bruns, C., Buhl, T., Eder, J., Feifel, R., . . . Schlapbach, A. (2006). Design and preparation of 2-benzamido-pyrimidines as inhibitors of IKK. *Bioorganic and Medicinal Chemistry Letters, 16*(1), 108-112.

Wang, K., Long, B., Liu, F., Wang, J. X., Liu, C. Y., Zhao, B., . . . Li, P. F. (2016a). A circular RNA protects the heart from pathological hypertrophy and heart failure by targeting miR-223. *European Heart Journal, 37*(33), 2602-2611.

Wang, S., Sun, Z., Zhao, W., Wang, Z., Wu, M., Pan, Y., . . . Zhu, J. (2016b). CD97/ADGRE5 inhibits LPS induced NF-kappa B activation through PPAR-gamma upregulation in macrophages. *Mediators of Inflammation, 2016*, 1605948.

Wang, Y., & Wang, Z. (2015). Efficient backsplicing produces translatable circular mRNAs. *RNA, 21*(2), 172-179.

Wang, Y. H., Yu, X. H., Luo, S. S., & Han, H. (2015). Comprehensive circular RNA profiling reveals that circular RNA100783 is involved in chronic CD28-associated CD8(+)T cell ageing. *Immunity & Ageing, 12*, 17.

Wegner, C. D., Gundel, R. H., Reilly, P., Haynes, N., Letts, L. G., & Rothlein, R. (1990). Intercellular adhesion molecule-1 (ICAM-1) in the pathogenesis of asthma. *Science, 247*(4941), 456-459.

Westholm, J. O., Miura, P., Olson, S., Shenker, S., Joseph, B., Sanfilippo, P., . . . Lai, E. C. (2014). Genome-wide analysis of drosophila circular RNAs reveals their structural and sequence properties and age-dependent neural accumulation. *Cell Reports, 9*(5), 1966-1980.

Winston, J. T., Strack, P., Beer-Romero, P., Chu, C. Y., Elledge, S. J., & Harper, J. W. (1999). The SCFbeta-TRCP-ubiquitin ligase complex associates specifically with phosphorylated destruction motifs in I kappa B alpha and beta-catenin and stimulates I kappa B alpha ubiquitination *in vitro*. *Genes & Development, 13*(3), 270-283.

Wu, Y., Zhang, Y., Zhang, Y., & Wang, J. J. (2017). CircRNA hsa_circ_0005105 upregulates NAMPT expression and promotes chondrocyte extracellular matrix degradation by sponging miR-26a. *Cell Biology International, 41*(12), 1283-1289.

Xu, A. N., Chen, X. H., Tan, Y. H., Qi, X. L., Xu, Z. F., Zhang, L. L., . . . Wang, H. W. (2013). Identification of a novel circularized transcript of the AML1 gene. *BMB Reports, 46*(3), 163-168.

Yang, M., Liu, J., Piao, C., Shao, J., & Du, J. (2015). ICAM-1 suppresses tumor metastasis by inhibiting macrophage M2 polarization through blockade of efferocytosis. *Cell Death & Disease, 6*, e1780.

Yaron, A., Hatzubai, A., Davis, M., Lavon, I., Amit, S., Manning, A. M., . . . Ben-Neriah, Y. (1998). Identification of the receptor component of the I kappa B alpha-ubiquitin ligase. *Nature, 396*(6711), 590-594.

You, X., Vlatkovic, I., Babic, A., Will, T., Epstein, I., Tushev, G., . . . Chen, W. (2015). Neural circular RNAs are derived from synaptic genes and regulated by development and plasticity. *Nature Neuroscience, 18*(4), 603-610.

Yu, P. F., Huang, Y., Han, Y. Y., Lin, L. Y., Sun, W. H., Rabson, A. B., . . . Shi, Y. F. (2017). TNFalpha-activated mesenchymal stromal cells promote breast cancer metastasis by recruiting CXCR2(+) neutrophils. *Oncogene, 36*(4), 482-490.

Zaphiropoulos, P. G. (1996). Circular RNAs from transcripts of the rat cytochrome P450 2C24 gene: correlation with exon skipping. *Proceedings of the National Academy of Sciences of the United States of America, 93*(13), 6536-6541.

Zaphiropoulos, P. G. (1997). Exon skipping and circular RNA formation in transcripts of the human cytochrome P-450 2C18 gene in epidermis and of the rat androgen binding protein gene in testis. *Molecular and Cellular Biology, 17*(6), 2985-2993.

Zhang, X. O., Dong, R., Zhang, Y., Zhang, J. L., Luo, Z., Zhang, J., . . . Yang, L. (2016). Diverse alternative back-splicing and alternative splicing landscape of circular RNAs. *Genome Research, 26*(9), 1277-1287.

Zhang, X. O., Wang, H. B., Zhang, Y., Lu, X., Chen, L. L., & Yang, L. (2014). Complementary sequence-mediated exon circularization. *Cell, 159*(1), 134-147.

Zhao, Z., Li, X., Gao, C., Jian, D., Hao, P., Rao, L., & Li, M. (2017). Peripheral blood circular RNA hsa_circ_0124644 can be used as a diagnostic biomarker of coronary artery disease. *Scientific Reports, 7*, 39918.

Zheng, Q., Bao, C., Guo, W., Li, S., Chen, J., Chen, B., . . . Huang, S. (2016). Circular RNA profiling reveals an abundant circHIPK3 that regulates cell growth by sponging multiple miRNAs. *Nature Communications, 7*, 11215.

Zhuang, J. C., & Wogan, G. N. (1997). Growth and viability of macrophages continuously stimulated to produce nitric oxide. *Proceedings of the National Academy of Sciences of the United States of America, 94*(22), 11875-11880.

LIST OF PUBLICATIONS AND PAPERS PRESENTED

1. **Ng, W. L**., Marinov, G. K., Liau, E. S., Lam, Y. L., Lim, Y. Y., & Ea, C. K. (2016). Inducible RasGEF1B circular RNA is a positive regulator of ICAM-1 in the TLR4/LPS pathway. *RNA Biology, 13*(9), 861-871.

2. **Ng, W. L**., Marinov, G. K., Chin, Y. M., Lim, Y. Y., & Ea, C. K. (2017). Transcriptomic analysis of RasGEF1B circular RNA in the TLR4/LPS pathway. *Scientific Reports 7* (1), 12227.

3. **Ng, W. L**., & Ea, C. K. " Circular RNAs (circRNAs) in Epstein-Barr Virus". The 4th NPC research day. 31 March 2015, Kuala Lumpur, Malaysia.